PD ISO/TR 10828:2015

BSI Standards Publication

Worm gears — Worm profiles and gear mesh geometry

bsi.

...making excellence a habit.™

National foreword

This Published Document is the UK implementation of ISO/TR 10828:2015. It supersedes BS ISO TR 10828:1997 which is withdrawn.

The UK participation in its preparation was entrusted to Technical Committee MCE/5/-/7, Worm Gears.

A list of organizations represented on this committee can be obtained on request to its secretary.

This publication does not purport to include all the necessary provisions of a contract. Users are responsible for its correct application.

ISBN 978 0 580 85447 7

ICS 21.200

Compliance with a British Standard cannot confer immunity from legal obligations.

This Published Document was published under the authority of the Standards Policy and Strategy Committee on 30 September 2015.

Amendments issued since publication

Date	Text affected

PD ISO/TR 10828:2015

TECHNICAL REPORT

ISO/TR 10828

Second edition
2015-08-15

Worm gears — Worm profiles and gear mesh geometry

Engrenages à vis cylindriques — Géométrique des profils de vis et des engrènements

Reference number
ISO/TR 10828:2015(E)

COPYRIGHT PROTECTED DOCUMENT

ISO copyright office
Ch. de Blandonnet 8 • CP 401
CH-1214 Vernier, Geneva, Switzerland
Tel. +41 22 749 01 11
Fax +41 22 749 09 47
copyright@iso.org
www.iso.org

Contents

Page

Foreword

ISO (the International Organization for Standardization) is a worldwide federation of national standards bodies (ISO member bodies). The work of preparing International Standards is normally carried out through ISO technical committees. Each member body interested in a subject for which a technical committee has been established has the right to be represented on that committee. International organizations, governmental and non-governmental, in liaison with ISO, also take part in the work. ISO collaborates closely with the International Electrotechnical Commission (IEC) on all matters of electrotechnical standardization.

The procedures used to develop this document and those intended for its further maintenance are described in the ISO/IEC Directives, Part 1. In particular the different approval criteria needed for the different types of ISO documents should be noted. This document was drafted in accordance with the editorial rules of the ISO/IEC Directives, Part 2 (see www.iso.org/directives).

Attention is drawn to the possibility that some of the elements of this document may be the subject of patent rights. ISO shall not be held responsible for identifying any or all such patent rights. Details of any patent rights identified during the development of the document will be in the Introduction and/or on the ISO list of patent declarations received (see www.iso.org/patents).

Any trade name used in this document is information given for the convenience of users and does not constitute an endorsement.

For an explanation on the meaning of ISO specific terms and expressions related to conformity assessment, as well as information about ISO's adherence to the WTO principles in the Technical Barriers to Trade (TBT) see the following URL: Foreword - Supplementary information

The committee responsible for this document is ISO/TC 60, *Gears*, Subcommittee SC 1, *Nomenclature and wormgearing*.

This second edition cancels and replaces the first edition (ISO/TR 10828:1997), which has been technically revised.

This edition includes the formulation for the geometrical dimensions of the worm and worm wheel, and that for the determination of gear mesh geometry (path of contact, zone and lines of contact) with the details to determine the non-dimensional parameters used to apply load capacity calculations (radius of curvature, sliding velocities).

Introduction

Thread forms of the worms of worm gear pairs are commonly related to the following machining processes:

— the type of machining process (turning, milling, grinding);

— the shapes of edges or surfaces of the cutting tools used;

— the tool position relative to an axial plane of the worm;

— where relevant, the diameters of disc type tools (grinding wheel diameter).

This Technical Report introduces all the aspects concerning the gear mesh geometry to define conjugate worm wheel, path of contact, lines of contact and other associated geometrical characteristics.

Worm gears — Worm profiles and gear mesh geometry

1 Scope

In this Technical Report, thread profiles of the five most common types of worms at the date of publication are described and formulae of their axial profiles are given.

The five worm types covered in this technical report are designated by the letters A, C, I, K and N.

The formulae to calculate the path of contact, the conjugate profile of the worm wheel, the lines of contact, the radius of curvature and the velocities at points of contact are provided. At the end the application of those formulae to calculate parameters used in load capacity calculations are provided.

2 Normative references

The following documents, in whole or in part, are normatively referenced in this document and are indispensable for its application. For dated references, only the edition cited applies. For undated references, the latest edition of the referenced document (including any amendments) applies.

ISO 1122-2, *Vocabulary — Worm gears*

ISO 701, *International gear notations — Symbols for geometrical data*

ISO/TR 14521, *Worm gears — Load capacity of worm gears*

3 Symbols and abbreviated terms

For the purposes of this document, Tables 1 to 3 give the symbols the indices and the description.

Table 1 — Symbols for worm gears from Clause 4 of this document

Symbols	Description	Units	Figures	Formula number
A	distance from the worm axis to virtual point of the cutter (see ref.[1])	mm	Fig. A.4	
a	centre distance	mm	Fig. 3	41/42
a_0	refers to the worm/tool centre distance (length of the common perpendicular to the worm/tool axes)	mm	Fig. 18	54
a_1 to a_4	coefficient for A, I and N profile			
b_1	facewidth of worm	mm		24
b_{2H}	effective wheel facewidth	mm	Fig. 4	39
b_{2R}	wheel rim width	mm	Fig. 4	
c_1,c_2	tip clearance	mm		46/47

Symbols	Description	Units	Figures	Formula number
d_{a1}	worm tip diameter	mm		14
d_{a2}	worm wheel throat diameter	mm		35
d_{b1}	base diameter of involute helicoid (for I profile)	mm		22
d_{e2}	worm wheel outside diameter	mm		36
d_{f1}	worm root diameter	mm		15
d_{f2}	worm wheel root diameter	mm		34
d_{m1}	worm reference diameter	mm	Fig. 1/3	10
d_{m2}	worm wheel reference diameter	mm	Fig 2/3	25
d_{w1}	worm pitch diameter	mm		43
d_{w2}	worm wheel pitch diameter	mm	Fig 5	44
$e_{mx\,1}$	worm reference tooth space width in axial section	mm	Fig. 1	17
e_{n1}	worm normal tooth space width in normal section	mm		19
e_{m2}	worm wheel tooth space width in mid-plane section	mm		28
h_1	worm tooth depth	mm		11
h_2	worm wheel tooth depth	mm		32
h_{am1}	worm tooth reference addendum in axial section	mm	Fig. 3	12
h_{am2}	worm wheel tooth reference addendum in mid-plane section	mm	Fig. 3	30
h^*_{am1}	worm tooth reference addendum coefficient in axial section	-		
h^*_{am2}	worm wheel tooth reference addendum coefficient in mid-plane section	-		
h_{e2}	worm wheel tooth external addendum	mm		33
h_{fm1}	worm tooth reference dedendum in axial section	mm		13
h_{fm2}	worm wheel tooth reference dedendum in mid-plane section	mm		31
h^*_{fm1}	worm tooth reference dedendum coefficient in axial section	-		
h^*_{fm2}	worm wheel tooth reference dedendum coefficient in mid-plane section	-		
j_x	axial backlash	mm		
m_n	normal module	mm		9
m_{x1}	axial module	mm		2/G.1
p_{bn1}	normal pitch on base cylinder	mm		23
p_{n1}	normal pitch	mm		8
p_{t2}	transverse pitch	mm		26
p_{x1}	axial pitch	mm	Fig. 1	1
p_{z1}	lead (of worm)	mm		3
p_{zu1}	unit lead (lead of worm per radian)	mm/rd		4
q_1	diameter quotient	mm		5
r_{g2}	worm wheel throat form radius	mm		40

Symbols	Description	Units	Figures	Formula number
r_{b1}	base radius for involute profile	mm	Fig. A.4 and A.5	
r'_{b1}	base radius of a notional base circle	mm	Fig. A.4 and A.5	
r_t	radius at cusp	mm	Fig. 29	
s_{m2}	tooth thickness at the reference diameter of the worm wheel	mm	Fig. 2	27
s_K	rim thickness	mm	Fig. 12	
s_{mx1}	worm thread thickness in axial section	mm	Fig. 1	16
s^*_{mx1}	worm thread thickness in axial section coefficient	-		
s_{n1}	normal worm thread thickness in normal section	mm		18
u	gear ratio			45
x_2	worm wheel profile shift coefficient	-		29
z_1	number of threads in worm	-		
z_2	number of teeth in worm wheel	-		
α_{0n}	tool normal pressure angle	°		
α_{0t}	tool transverse pressure angle for A and I profiles	°	Fig. 7	
α_n	normal pressure angle	°		20
β_{m1}	reference helix angle of worm	°		7
γ_{m1}	reference lead angle of worm	°		6
γ_{b1}	base lead angle of worm thread (for I profile)	°	Fig. A.1	21
γ'_{b1}	base lead angle of the notional base helix	°	Fig. A.4 and A.5	
ρ_{Gm}	Radius of curvature of grinding wheel (C profile)			

In calculation, when a radius is derived, the symbol d for diameter shall be replaced by r for radius.

Table 2 — Subscripts for worm gears

Symbols	Description
0	cutting tool
1	worm
2	Wheel
G	grinding wheel

Table 3 — Coordinate of remarkable points

Symbols	Description
$x_G(y_G)$, y_G, $\alpha_G(y_G)$	Coordinates of a point on the tool flank when the origin is at the point of intersection of the tool axis and the tool median plane, with the x-axis as the tool spindle axis and the

	abscissa on the trace of the median plane;
$x_x(y_r),\ y_x(y_r),\ \alpha_x(y_r)$	Coordinates of axial profile and axial pressure angle for A, I, N worm profiles
$x_x(y_G),\ y_x(y_G),\ \alpha_x(y_G)$	Coordinates of axial profile and axial pressure angle for K and C worm profiles
$x_D(y_{p,}D),\ y_D(y_{p,}D),\ \alpha_D(y_{p,}D)$	Coordinates of worm profile and pressure angle of worm profile in an offset plane
$x_D^{'}(y_{p,}D),\ y_D(y_{p,}D),\ \alpha_D(y_{p,}D)$	Coordinates of worm profile and pressure angle of worm profile in an offset plane with origin on pitch axis
$x_{lD}(y_p, D),\ y_{lD}(y_p, D)$	Coordinates of path of contact in an offset plane with origin on pitch axis
$xR_D(y_p, D),\ yR_D(y_p, D)$	Coordinates of conjugate worm wheel profile of the worm in an offset plane with origin on worm wheel axis
$xT_D(r_{t2D}, D),\ yT_D(r_{t2D}, D)$	Coordinates of trochoid profile of the worm wheel profile in an offset plane with origin on worm wheel axis
$x_D(ycusp, D)$, $y_D(ycusp, D)$	Coordinates of cusp point in an offset plane with origin on pitch axis
$C_{eq1D}(y_p, D)$	Curvature for the worm at a point in an offset plane
$C_{eq2D}(y_p, D)$	Curvature for the worm wheel at a point in an offset plane
$R_{eqD}(y_p, D)$	Equivalent radius of curvature in an offset plane
$r_{e2D}(D)$	outside radius of the worm wheel in the offset plane D
r_{t2D}	root radius of the worm wheel in the offset plane D
$\overrightarrow{M_1(y_p, D)}$	Coordinate of a point of contact for the worm (Eq 118)
$M_2(y_p, D)$	Coordinate of a point of contact for the worm wheel (Eq 119)
$\overrightarrow{TN1_{cont}(y_p, D)}$	Tangent unit vector to a line of contact (Eq 128)
$\overrightarrow{\text{Normal}Nxy(y_p, D)}$	Normal unit vector to the lines of contact (Eq 114)
$\overrightarrow{\text{NORMAL}(y_p, D)}$	Normal unit vector to the lines of contact (Eq 116)
$\text{Req}(y_p, D)$	Radius of curvature along the line the contact (Eq 135)
$\overrightarrow{V_1}(y_p, D)$	Velocity of a point of the thread of the worm (Eq 138)
$\overrightarrow{V_2}(y_p, D)$	Velocity of a point of the tooth flank of the worm (Eq 140)
$V_{cDn}(y_p, D)$	Velocity at the contact point along the path of contact (Eq 150)
$V_{SUMn}(y_p, D)$	Sum of velocities at the point of contact (Eq 153) for method B in ISO/TR 14521

4 Formulae for calculation of dimensions

4.1 Parameters for a cylindrical worm

4.1.1 Axial pitch

$$p_{x1} = \pi \cdot m_{x1} \tag{1}$$

4.1.2 Axial module

$$m_{x1} = \frac{p_{x1}}{\pi} \tag{2}$$

4.1.3 Lead

$$p_{z1} = z_1 \cdot p_{x1} \tag{3}$$

4.1.4 Unit lead

$$p_{zu1} = \frac{p_{z1}}{2 \cdot \pi} \tag{4}$$

4.1.5 Diameter quotient

$$q_1 = \frac{d_{m1}}{m_{x1}} \tag{5}$$

4.1.6 Reference lead angle

$$\tan \gamma_{m1} = \frac{m_{x1} \cdot z_1}{d_{m1}} = \frac{z_1}{q_1} \tag{6}$$

4.1.7 Reference helix angle

$$\beta_{m1} = 90° - \gamma_{m1} \tag{7}$$

4.1.8 Normal pitch on reference cylinder

$$p_{n1} = p_{x1} \cdot \cos \gamma_{m1} \tag{8}$$

4.1.9 Normal module

$$m_n = m_{x1} \cdot \cos \gamma_{m1} \tag{9}$$

4.1.10 Reference diameter

$$d_{m1} = q_1 \cdot m_{x1} \tag{10}$$

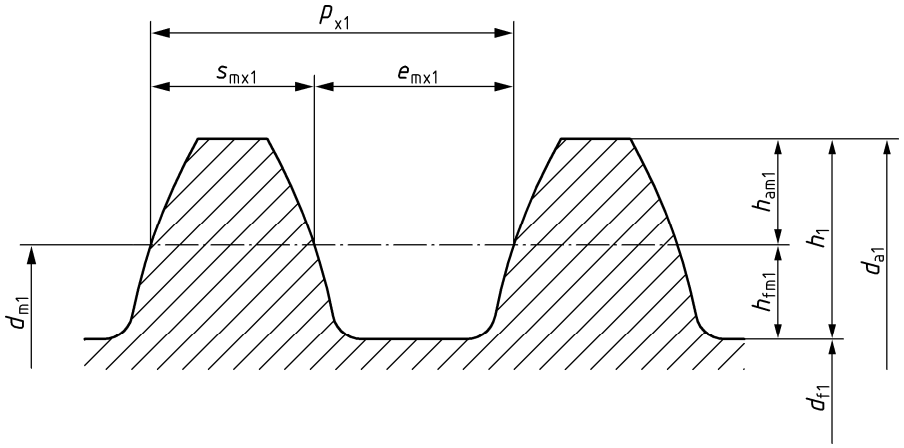

Figure 1 — Axial parameters for worm

4.1.11 Reference tooth depth

$$h_1 = h_{am1} + h_{fm1} = \frac{1}{2} \cdot \left(d_{a1} - d_{f1}\right) \tag{11}$$

4.1.12 Reference addendum

$$h_{am1} = h^*_{am1} \cdot m_{x1} = \frac{1}{2} \cdot (d_{a1} - d_{m1}) \tag{12}$$

where h^*_{am1} is the addendum coefficient; normally h^*_{am1} = 1

4.1.13 Reference dedendum

$$h_{fm1} = h^*_{fm1} \cdot m_{x1} = \frac{1}{2} \cdot (d_{m1} - d_{f1}) \tag{13}$$

where h^*_{fm1} = dedendum coefficient; generally 1,1< h^*_{fm1} <1,3, the recommended value is 1,2

4.1.14 Tip diameter

$$d_{a1} = d_{m1} + 2 \cdot h_{am1} \tag{14}$$

4.1.15 Root diameter

$$d_{f1} = d_{m1} - 2 \cdot h_{fm1} \tag{15}$$

4.1.16 Thread thickness coefficient s^*_{mx1}

A recommended value is s^*_{mx1} = 0,5

In general practice, this coefficient is very often less than 0,5 when there is a wish to increase the worm wheel thread thickness to extend durability against wear of worm wheel.

See Figure 1.

4.1.17 Reference thread thickness in the axial section

$$s_{mx1} = \overset{*}{s}_{mx1} \cdot p_{x1} \tag{16}$$

4.1.18 Reference space width in the axial section

$$e_{mx1} = p_{x1} - s_{mx1} \tag{17}$$

4.1.19 Normal thread thickness

$$s_{n1} = s_{mx1} \cdot \cos \gamma_{m1} \tag{18}$$

4.1.20 Normal space width

$$e_{n1} = e_{mx1} \cdot \cos \gamma_{m1} \tag{19}$$

4.1.21 Profile flank form

It is specified by a letter:

A is the envelope of straight line in the axial section;

N is the envelope of straight line in the normal section of the space width;

I is the involute helicoid (the envelope of straight line in a plane tangent to the base cylinder);

K is a milled helicoid by double cone form;

C is a milled helicoid by circular convex form.

4.1.22 Normal pressure angle

For type-A

$$\tan \alpha_n = \tan \alpha_{0t} \cdot \cos \gamma_{ml} \tag{20}$$

For other type

$\alpha_n = \alpha_{0n}$

where α_{0n} is defined in 6.3, 6.4 and 6.5 for I and N and in 6.6 and 6.7 for K and C.

4.1.23 Base lead angle for I profile

$$\cos \gamma_{bl} = \cos \gamma_{ml} \cdot \cos \alpha_{0n} \tag{21}$$

4.1.24 Base diameter for I profile

$$d_{b1} = d_{m1} \cdot \frac{\tan \gamma_{m1}}{\tan \gamma_{b1}} = \frac{m_{x1} \cdot z_1}{\tan \gamma_{b1}} \tag{22}$$

NOTE For I profile if the root diameter is less than the base diameter attention should be taken in order that the diameter of start of active profile (SAP) is greater than d_{b1}.

4.1.25 Normal pitch on base cylinder

$$p_{bn1} = p_{x1} \cdot \cos\gamma_{b1} \tag{23}$$

4.1.26 Worm face width

$$b_1 \geq \sqrt{(d_{e2})^2 - (2 \cdot a - d_{a1})^2} \tag{24}$$

4.2 Parameters for a worm wheel

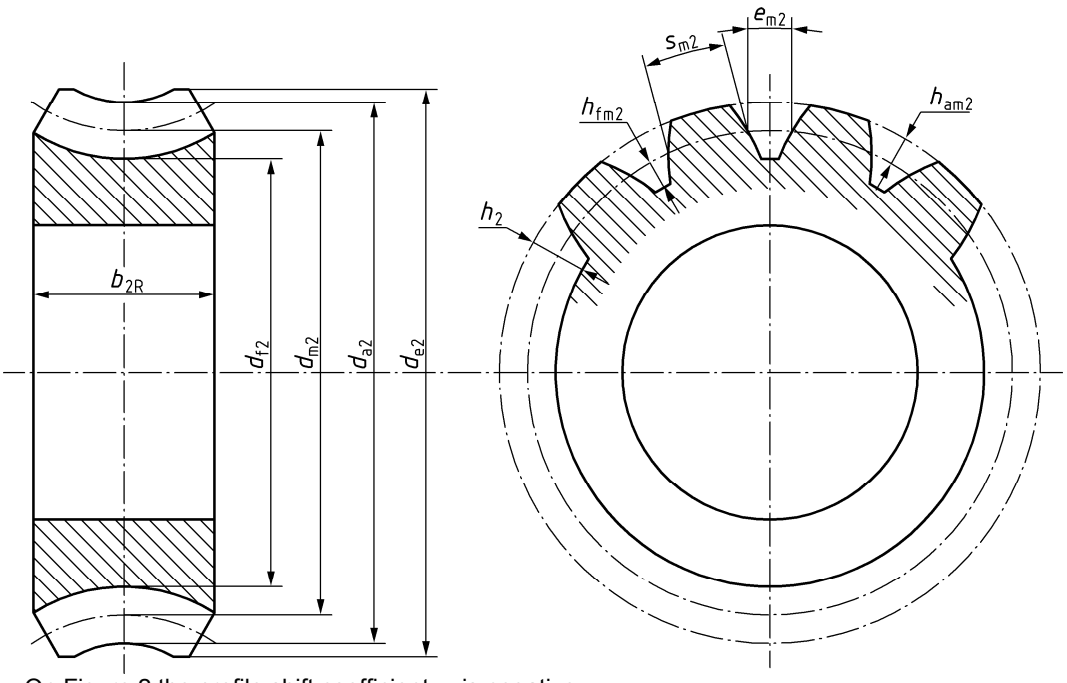

NOTE On Figure 2 the profile shift coefficient x_2 is negative.

Figure 2 — Parameters for worm wheel

4.2.1 Reference diameter

$$d_{m2} = d_{w2} + 2 \cdot x_2 \cdot m_{x1} \text{ or } \qquad d_{m2} = 2 \cdot a - d_{m1} \tag{25}$$

4.2.2 Transverse pitch

$$p_{t2} = p_{x1} \tag{26}$$

4.2.3 Transverse tooth thickness at reference diameter

This value can be calculated only for a worm wheel without profile shift as follows:

$$s_{m2} = e_{mx1} - j_x \tag{27}$$

where j_x = axial backlash.

See Figure 2.

4.2.4 Space width at reference diameter

This value can be calculated only for a worm wheel without profile shift as follows:

$$e_{m2} = p_{x1} - s_{m2} \tag{28}$$

4.2.5 Profile shift coefficient

$$x_2 = \frac{2 \cdot a - d_{m1} - m_{x1} \cdot z_2}{2 \cdot m_{x1}} \tag{29}$$

4.2.6 Addendum

$$h_{am2} = m_{x1} \cdot h^*_{am2} = \frac{1}{2} \cdot (d_{a2} - d_{m2}) \tag{30}$$

where h^*_{am2} is the addendum coefficient; h^*_{am2} = 1 (normally).

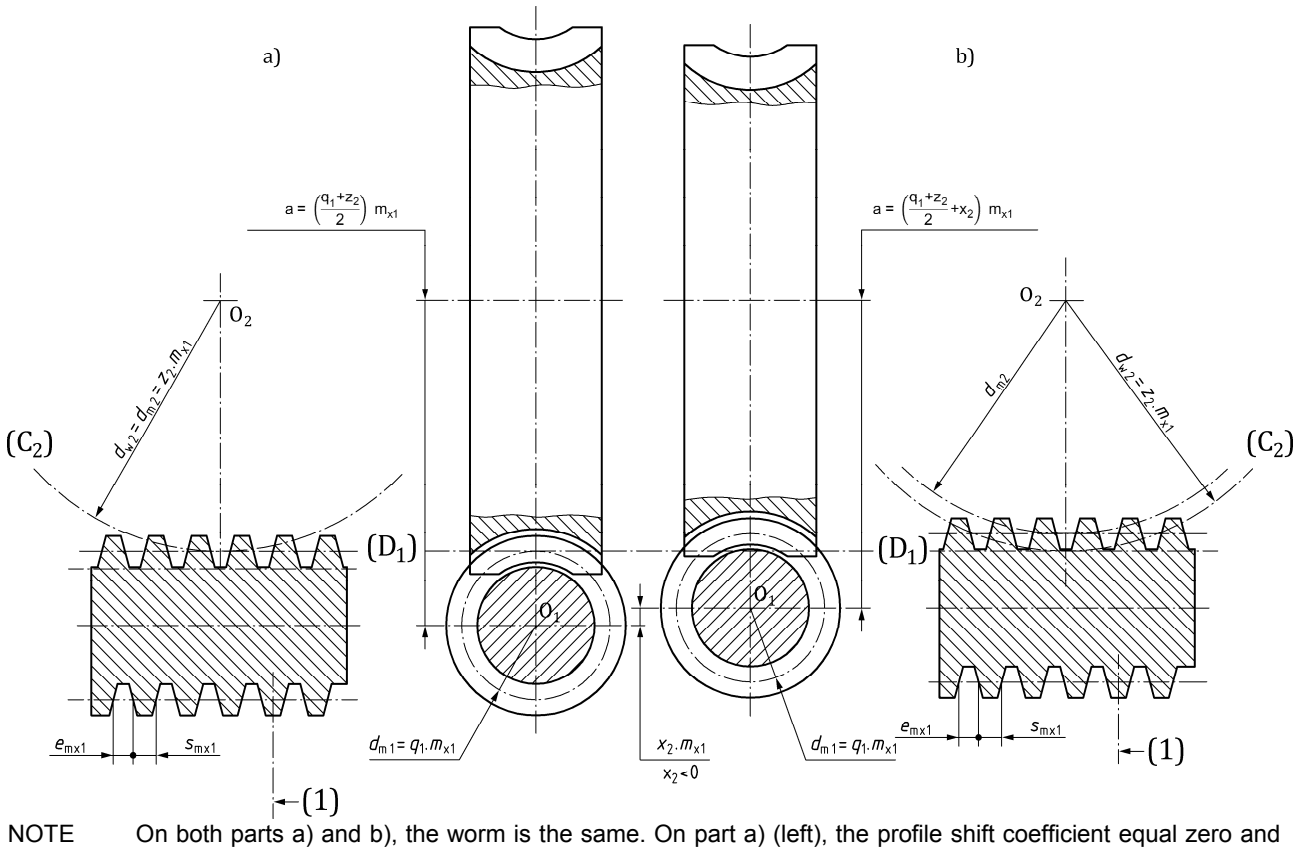

NOTE On both parts a) and b), the worm is the same. On part a) (left), the profile shift coefficient equal zero and on part b) (right) the profile shift coefficient is negative.

Key
1 symmetrical axis of the thread

Figure 3 — Pitch and reference diameters for worm gear set

4.2.7 Dedendum

$$h_{fm2} = m_{x1} \cdot h^{*}_{fm2} = \frac{1}{2} \cdot (d_{m2} - d_{f2}) \quad (31)$$

where h^{*}_{fm2} is the dedendum coefficient; generally 1,1 < h^{*}_{fm2} < 1,3, the recommended value is 1,2.

4.2.8 Tooth depth

$$h_2 = h_{am2} + h_{fm2} \quad (32)$$

4.2.9 Outside addendum

$$h_{e2} = \frac{1}{2} \cdot (d_{e2} - d_{a2}) \quad (33)$$

Generally: $0{,}4 \le \frac{h_{e2}}{m_{x1}} \le 1{,}5$ Normally h_{e2}/m_{x1} = 0,5

4.2.10 Root diameter

$$d_{f2} = d_{m2} - 2h_{fm2} \quad (34)$$

4.2.11 Throat diameter

$$d_{a2} = d_{m2} + 2h_{am2} \quad (35)$$

4.2.12 Outside diameter

$$d_{e2} = d_{a2} + 2 \cdot h_{e2} \quad (36)$$

NOTE For min/max values see 4.2.9.

4.2.13 Minimum and maximum outside diameter

Generally

$$d_{e2min} = d_{a2} + 0{,}8 \cdot m_{x1} \quad (37)$$

$$d_{e2max} = d_{a2} + 3 \cdot m_{x1} \quad (38)$$

4.2.14 Worm wheel face width

$$b_{2H} \le \sqrt{(2 \cdot a - d_{f2})^2 - (2 \cdot a - d_{e2})^2} \quad (39)$$

See Figure 4.

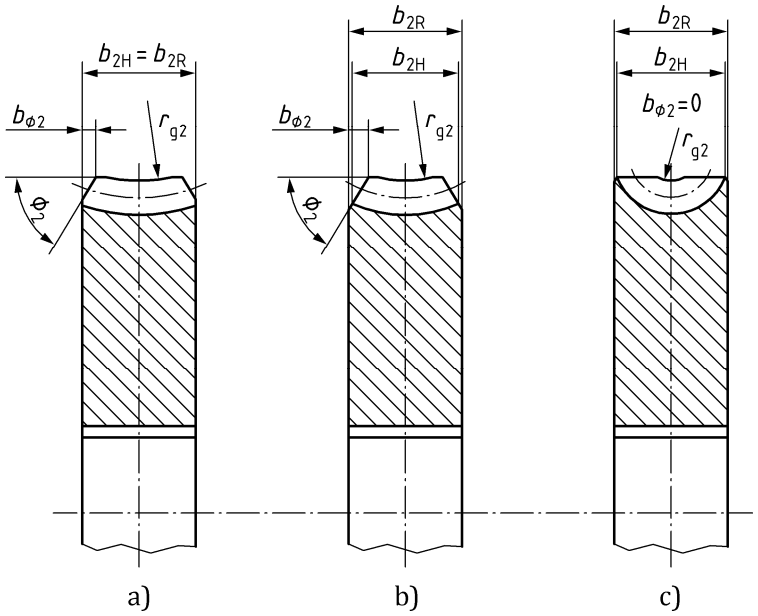

NOTE Case c) represents the geometrical conditions where b_{2H} reaches its maximum value.

Figure 4 — Worm wheel face width

4.2.15 Throat form radius

$$r_{g2} \geq a - \frac{d_{a2}}{2} \tag{40}$$

4.3 Meshing parameters

4.3.1 Centre distance

$$a = 0{,}5 \cdot \left(d_{m1} + d_{m2}\right) = 0{,}5 \cdot \left(d_{w1} + d_{w2}\right) \tag{41}$$

or

$$a = m_{x1} \cdot \left[0{,}5 \cdot \left(q_1 + z_2\right) + x_2\right] \tag{42}$$

See Figure 3.

4.3.2 Pitch diameter of worm wheel

$$d_{w2} = z_2 \cdot m_{x1} \tag{43}$$

4.3.3 Pitch diameter of worm

$$d_{w1} = 2 \cdot a - d_{w2} \tag{44}$$

4.3.4 Worm gear ratio

$$u = \frac{z_2}{z_1} \tag{45}$$

4.3.5 Contact ratio

The calculation of the contact ratio is defined in 10.6.

4.3.6 Tip clearance

$$c_1 = a - 0{,}5 \cdot \left(d_{a2} + d_{f1}\right) \tag{46}$$

$$c_2 = a - 0{,}5 \cdot \left(d_{a1} + d_{f2}\right) \tag{47}$$

5 Generalities on worm profiles

5.1 Definitions

Type A straight sided axial profile;

Type C concave axial profile formed by machining with a convex circular profile disc type cutter or grinding wheel;

Type I involute helicoid, straight generatrix in base tangent planes;

Type N straight profiles in normal plane of thread space helix;

Type K milled helicoid generated by biconical grinding wheel or milling cutter, convex profiles in axial planes.

5.2 Conventions relative to the formulae of this document

5.2.1 The worm threads are right-handed.

The formulae in this Technical Report define the coordinates of the left flank of the axial profile of worm, i.e. in the plane XOY of Figure 5.

To obtain the right flanks, it is necessary to draw a symmetric profile to the left flank relative to a perpendicular axis to the worm axis.

5.2.2 The worm and wheel pairs operate as speed reducing gears with directions of rotation as shown in Figure 5, thus the worm thread left flanks contact the wheel teeth. These are the flanks studied in this report.

5.2.3 The worm wheel is above the worm.

5.2.4 With the origin O, the reference axes X Y Z, are mutually perpendicular (see Figure 5):

— OX the worm axis coincides with the X axis;

— OY the common perpendicular to the worm and wheel axes coincides with the Y axis;

— OZ to complete the direct coordinate system.

A point is defined by its x, y, z coordinates. The following subscripts are used:

— x refers to the X-Y axial plane;

— D refers to an offset plane;

— n refers to the normal plane;

— t for any point refers to a transverse plane.

5.2.5 If the worm is driving, the worm gear set is a reducer. If the worm wheel is driving the worm gear set is an increaser.

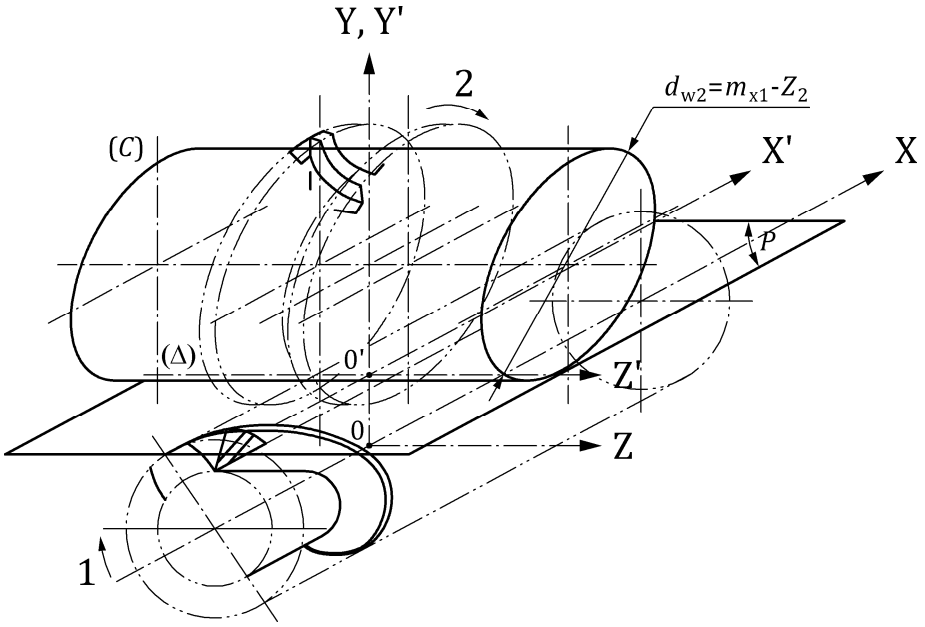

Key

1 direction of rotation of the worm
2 direction of rotation of the worm wheel
(Δ) pitch line
(C) pitch cylinder of the worm wheel – diameter d_{w2}
P pitch plane of the worm – distance from the axis of the worm equal to $d_{w1}/2$

NOTE For the clarity of drawing only one thread for worm is represented.

Figure 5 — Conventions used in formulae

6 Definition of profiles

6.1 Introduction

There are 2 types of worm profiles:

— profiles A, I, N are generated by a helical movement of a straight line in the space. The formulae of the axial profile are a direct function according to the radius of the worm. In that case gear mesh in an

offset plane uses two parameters: y_r which is the radius of the worm and D which is the distance of the offset plane

— profiles K and C are generated by a helical movement of a grinding wheel with a certain profile (see Figures 18) in the space. The generated flanks on the worm are the envelope of the grinding wheel. Each point of the worm profile is generated by a point of the grinding wheel. The formulae of the axial profile IS NOT a direct function according to the radius of the grinding wheel profile. In that case gear mesh in an offset plane uses two parameters: y_r which is the radius of the grinding wheel and D which is the distance of the offset plane. In those cases the calculations are more complex.

6.2 Type A

6.2.1 Geometrical definition

The thread flanks of type A are generated as envelopes of straight lines in axial planes which are inclined at a constant angle: $\frac{\pi}{2} - \alpha_{0t}$ to the axis (see Figure 6). This line as it is moved with simultaneous rotation about and translation along the axis X, defines the worm thread flank (Figure 6). The form of which is commonly described as an Archimedean helix.

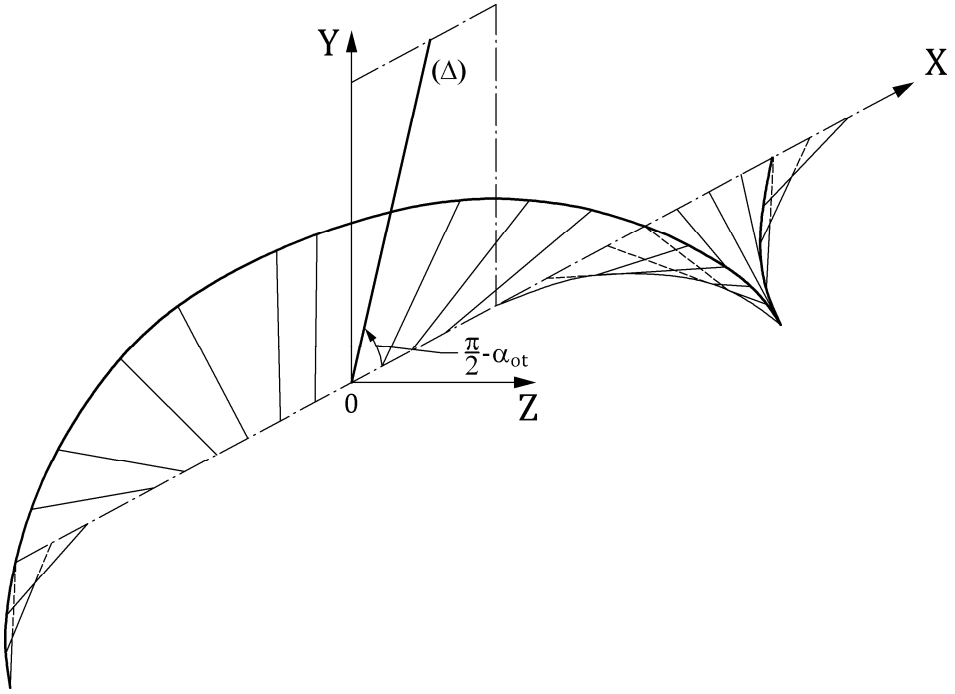

Figure 6 — Profile A: Theoretical Generation

6.2.2 Machining methods

The straight generatrix is always crossing the worm axis; the flank of thread in an axial plane is always a straight line; so machining methods should ensure to generate this straight axial flank.

The threads may be cut on a lathe with a tool having straight edges, the cutting plane of which lies in an axial plane of the worm (Figure 7 a)).

Both flanks of a thread space may be machined simultaneously by using a tool of trapezoidal form.

Another method which is an inversion of the process of cutting a helical gear with a rack cutter, involves the use of an involute shaper to produce the desired rectilinear rack profile in an axial plane of the worm. The cutting face must lie in that axial plane (Figure 7 b)).

It is also necessary that the pitch circle of the shaper should roll without slip on the datum line of the rack profile. This coincides with a straight line generatrix of the worm pitch cylinder.

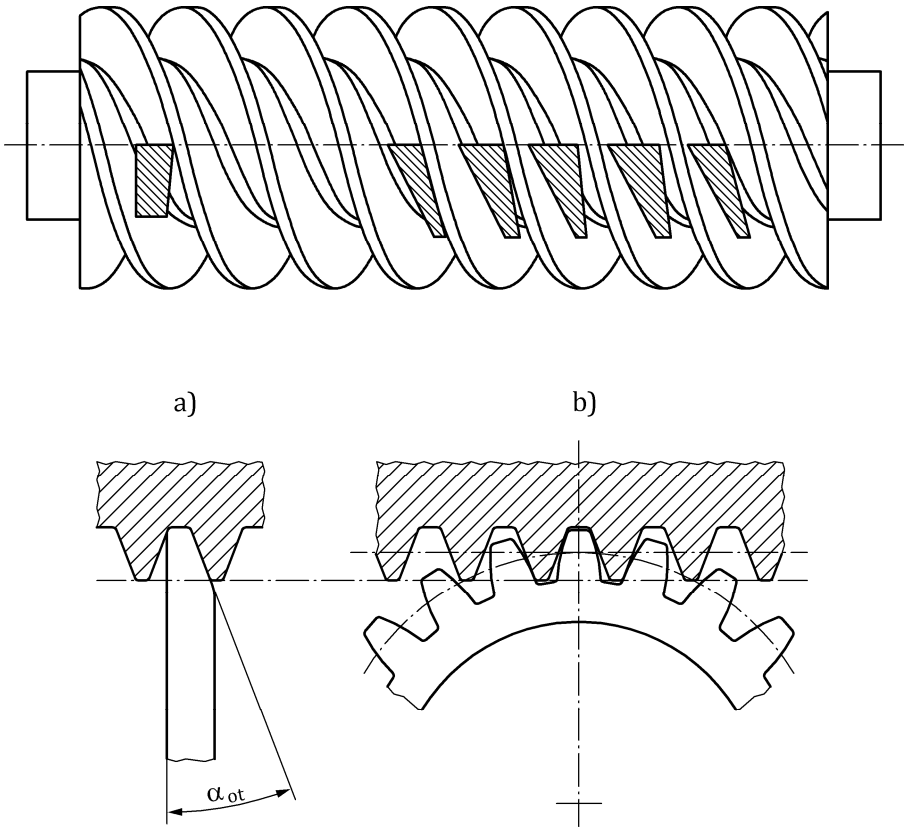

Figure 7 — Profile A - Machining Methods

Type A profile is a straight line in an axial plane.

The development of the formulae for the axial profile of type A worm is in Annex A, A.2.

6.3 Type I

6.3.1 Geometrical definition

A flank of a type I worm is an involute helicoidal surface. The form of which may be generated by a base tangent (Δ) to a helix (H), which moves along this - the base helix lying on the base cylinder of the worm, which is concentric with the worm axis (Figure 8).

A transverse profile (in a normal plane to the worm axis) of a flank is an involute to a circle.

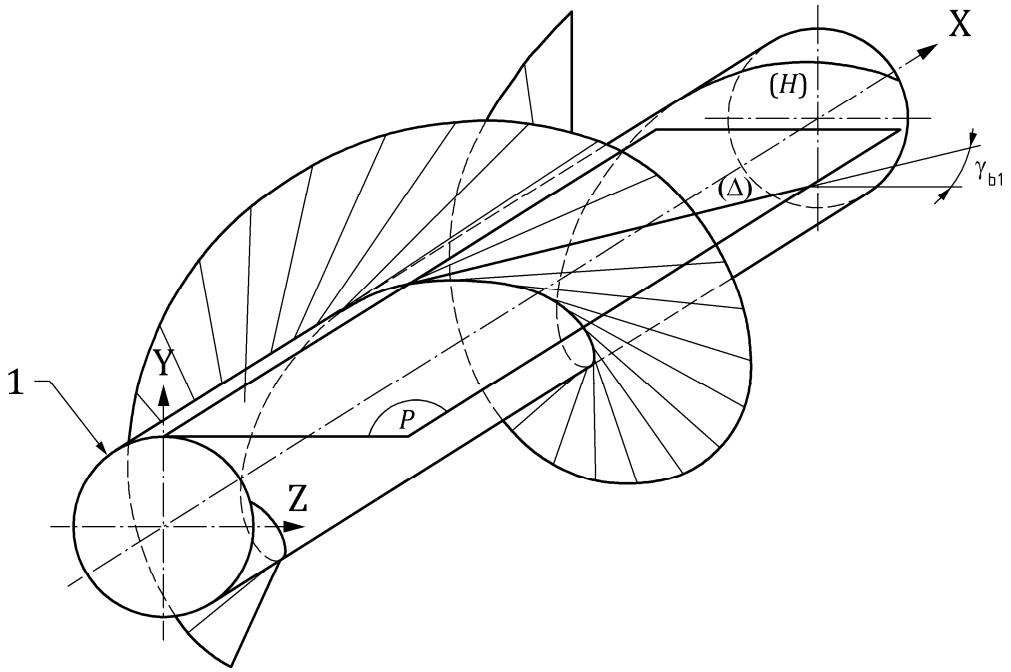

Key

1 base cylinder of the worm

Figure 8 — Profile I - Theoretical generation

6.3.2 Machining methods

The straight generatrix is always tangential to the base helix in a plane which is tangential to the base cylinder, so the flank of the worm is a straight line in an offset plane which is tangential to the base cylinder. Machining methods should ensure this straight offset profile.

The involute helicoidal flanks of the threads can be generated by turning on a lathe using a knife tool with its straight edge aligned with the base tangent generatrix in a plane tangential to the base cylinder.

In order to machine both flanks of a thread simultaneously, it is necessary to set one left hand tool in one plane and one right hand tool in another plane as described after (Figure 9).

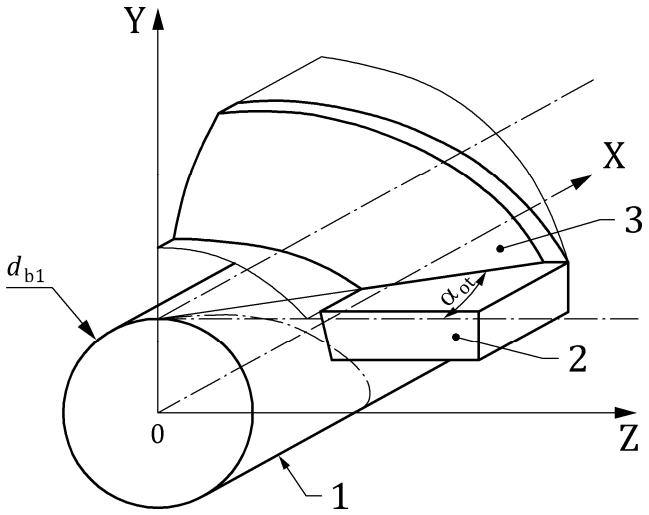

Key

1 base cylinder
2 cutting tool
3 generatrix

NOTE $\alpha_{0t} = \gamma_{b1}$

Figure 9 — Profile I - Machining method with a lathe

The worm flanks can be machined by milling or grinding using the plane side face of a disc type milling cutter or grinding wheel. The cutting face has to be aligned either

— with its axis parallel to the X-Z plane and the base tangent generatrix of the flank in the cutting face (Figure 10), or

— with the reference helix of the worm and in a plane perpendicular to the reference helix set to the normal pressure angle α_{0n} (Figure 11).

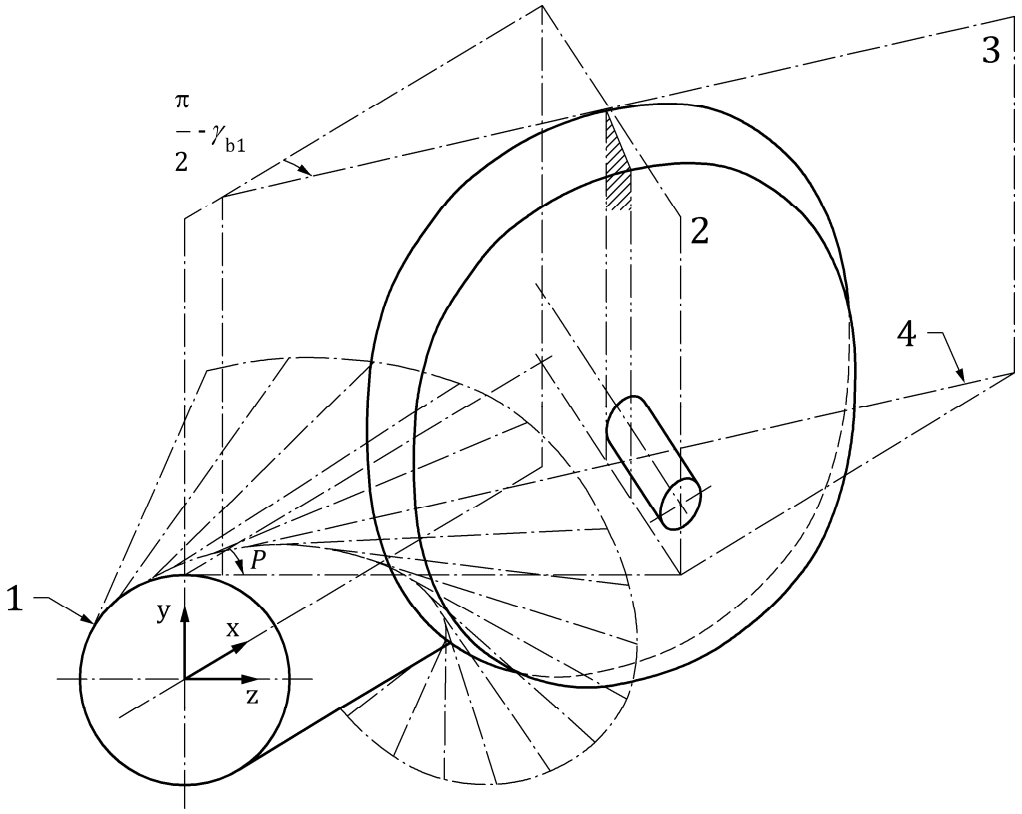

Key

1 base cylinder
2 grinding wheel (with flat active face)
3 action plane of the grinding wheel
4 generatrix
P plane tangent to the base circle containing the generatrix

Figure 10 — Profile I - Machining method by grinding (solution 1)

The latter method of alignment has the advantage that the cutting face extends to near the thread root whereas in order to do so by the previous method it will be necessary raise the cutter/grinding-wheel spindle so that the cutter/wheel periphery is tangential to the point of intersection of the base tangent generatrix with the root cylinder of the worm.

Both methods require that the mounting of the worm in the milling/grinding machine must be reversed between machining right and left flanks.

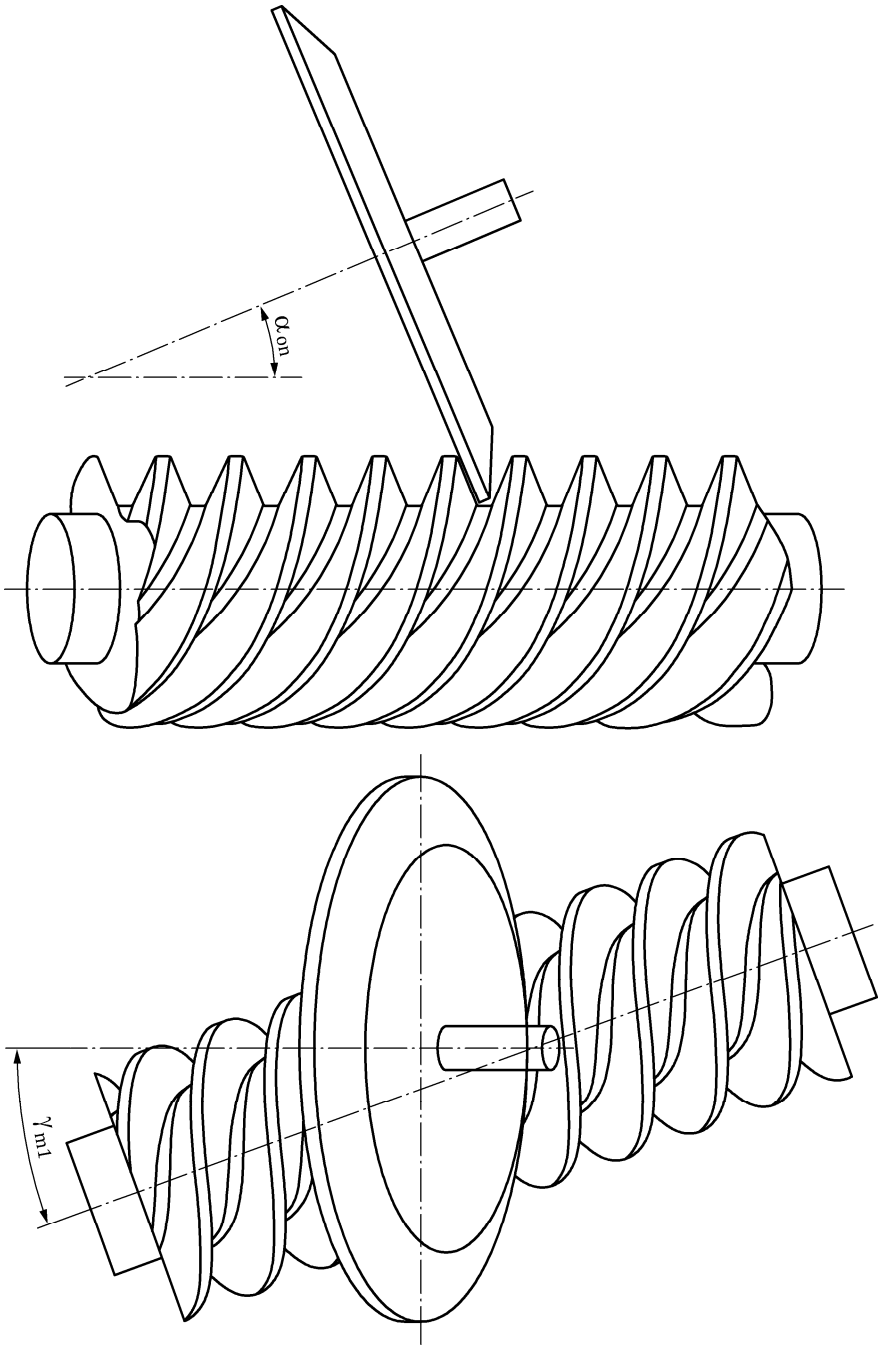

Figure 11 — Profile I - Machining method by grinding (solution 2)

Type I profile is slightly convex in an axial plane.

The development of the formulae for the axial profile of type I worm is in Annex A, A.3.

6.4 Type N

6.4.1 Geometrical definition

Each flank of a type N worm is formed by a straight line generatrix (Δ) which lies in a plane normal to the reference helix (H_1); crossing (M) which is a common point of intersection of a vector radius, the generatrix (Δ) and the reference helix H. The angle α between (Δ) and the radius vector at M point is constant.

The flank envelope is formed by the generatrix (Δ), due to the helicoidal movement of the vector radius carrying the point M which describes the reference helix (Figure 12).

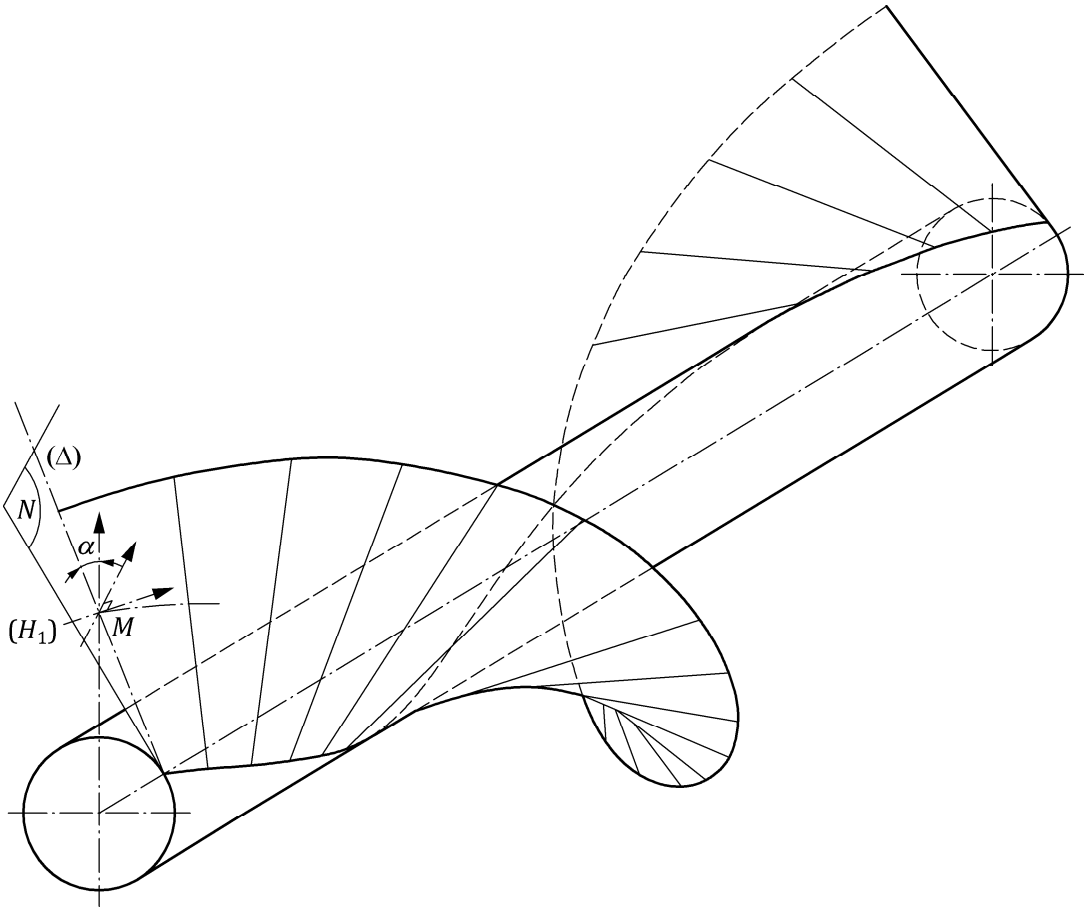

Figure 12 — Profile N - Theoretical generation

6.4.2 Machining methods

The threads may be cut in a lathe with a tool having trapezoidal form having edges in the cutting plane which match the profile of the thread space in a plane normal to the reference helix of the thread space.

This is equivalent to placing the tool as for A type threads, then to rotate it around an axis matching its symmetrical axis up to an angle equal to the reference lead angle γ_{m1} (Figure 13).

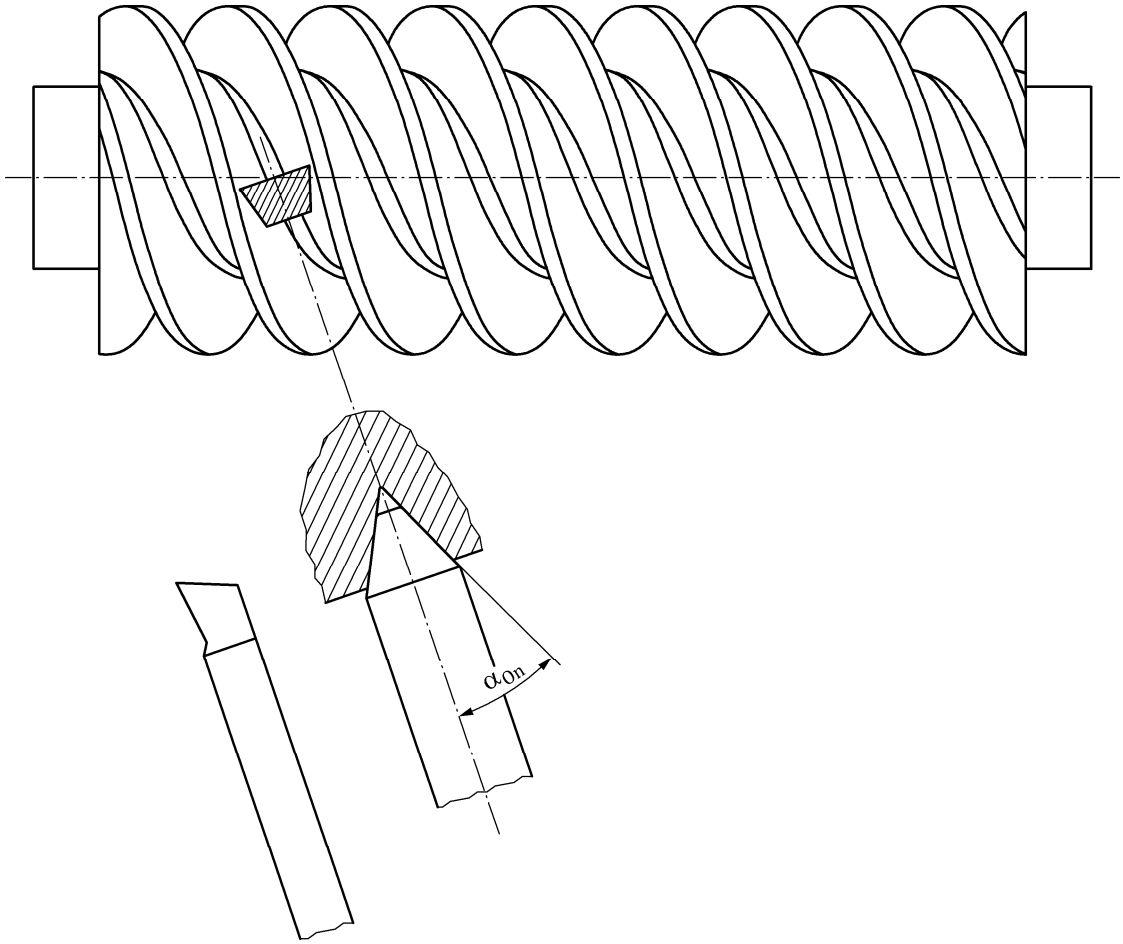

Figure 13 — Profile N - Machining methods

Type N profiles are slightly concave in an axial plane.

The development of the formulae for the axial profile of type N worm is in Annex A, A.4.

6.5 General formulae for A, I and N profiles

6.5.1 General formula of axial profile for A, I, N profiles

The general formula of the axial profile of the worm for A, I, N profiles can be given by a single formula as follows, with x_x as the axial abscissa of the axial profile point function of the radius of the circle y_r at this point:

$$x_x(y_r) = a_1 \cdot \arctan\left(\frac{\sqrt{y_r^2 - a_2^2}}{a_2}\right) + a_3 \cdot \sqrt{y_r^2 - a_2^2} + a_4 \tag{48}$$

$$y_x(y_r) = y_r \tag{49}$$

The values for the coefficients are given in Table 4.

Table 4 — Coefficients a_1 to a_4 for A, I and N profiles

Coefficient	Profile		
	A Profile	I Profile	N Profile
a_1	$a_{1A} = 0$	$a_{1I} = -p_{zu1}$	$a_{1N} = p_{zu1}$
a_2	$a_{2A} = 0$	$a_{2I} = r_{bI}$	$a_{2N} = \frac{A \cdot \sin(\gamma_{m1}) \cdot \tan(\alpha_{0n})}{\sqrt{1 + (\sin(\gamma_{m1}) \cdot \tan(\alpha_{0n}))^2}}$ $A = r_{mI} - \frac{s_{mx1} \cdot \cos(\gamma_{m1})}{2 \cdot \tan(\alpha_{0n})}$
a_3	$a_{3A} = \frac{\tan(\alpha_{0n})}{\cos(\gamma_{m1})}$	$a_{3I} = \tan(\gamma_{b1})$	$a_{3N} = \frac{a_{2N}}{A \cdot \tan(\gamma_{m1})}$
a_4	0	0	0

In Formula (48), a_4 coefficient allows to translate the axial profile and to set up it at the correct position needed in the calculation.

To set up axial profile at the pitch point in the mid plane the a_4 coefficient has to be determined by the application of the general formula for the pitch radius r_{w1}

$$a_4 = -x_x(r_{w1}) = -a_1 \cdot \arctan\left(\frac{\sqrt{r_{w1}^2 - a_2^2}}{a_2}\right) - a_3 \cdot \sqrt{r_{w1}^2 - a_2^2} \tag{50}$$

In complement to the coordinate of the axial point it possible to define at this point the axial pressure angle at the y_r circle which is defined by the derivate of x_x function according to y_r:

$$dx_x(y_r) = \left(\frac{a_1 \cdot a_2}{y_r} + a_3 \cdot y_r\right) \cdot \frac{1}{\sqrt{y_r^2 - a_2^2}} \tag{51}$$

$$dy_x(y_r) = 1 \tag{52}$$

$$\tan\alpha_x(y_r) = \frac{dx_x(y_r)}{dy_x(y_r)} \tag{53}$$

6.6 Type K

6.6.1 Geometrical definition and method

Unlike those of types A, I and N, the thread flanks of type K worms do not have straight line generatrices. The thread spaces of type K worms are generated with a biconical grinding wheel or disc type milling cutter having straight cone generatrices (Figure 14).

The common perpendicular to the tool spindle and worm axes lies in the line (Δ) of intersection of the median plane (M) of the tool and a transverse plane of the worm (R). The angle between the two planes is equal to the worm reference lead angle of the worm γ_{m1}.The straight generatrix of each tool cone and the median plane of the tool forms an angle equal to the normal pressure angle α_{0n} of the tool.

The worm is turned uniformly with simultaneous axial translation of threads so that a point on the common perpendicular, distant r_1 (r_1: reference radius of worm) from the worm axis, describes the reference helix.

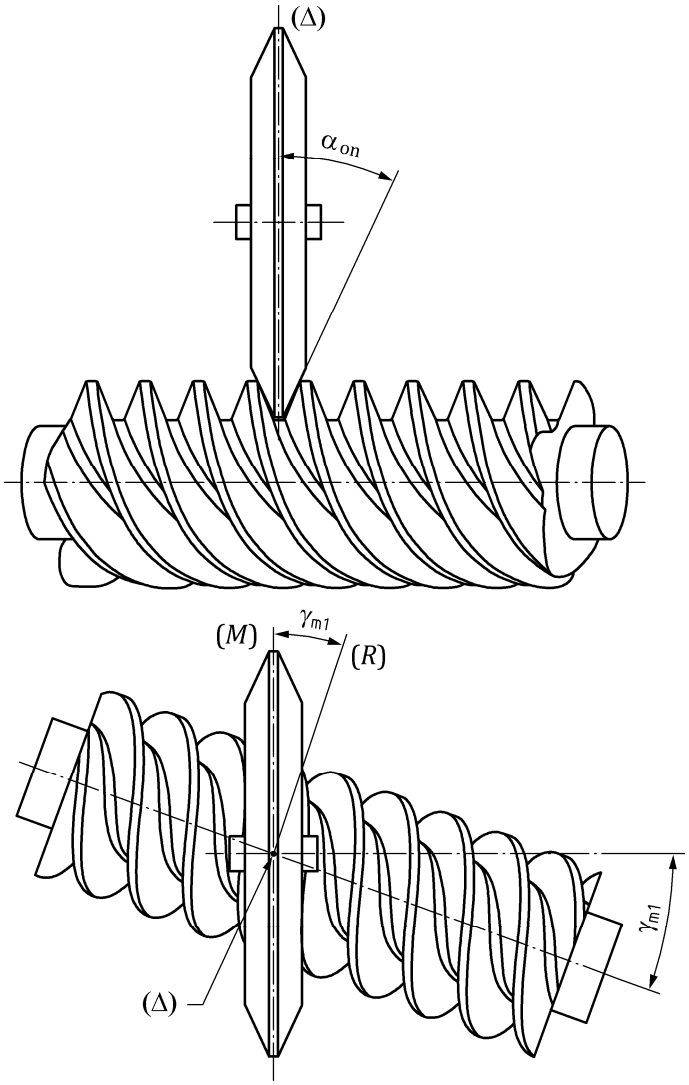

Figure 14 — Profile K - Machining method

The helicoidal flanks of the worm are generated by the conical sides of the tool and the profile form is influenced by the change of helix angle with change of thread height and points on the tool flanks which contact the worm threads lie on a curve and not on any one cone generatrix (Figure 15).

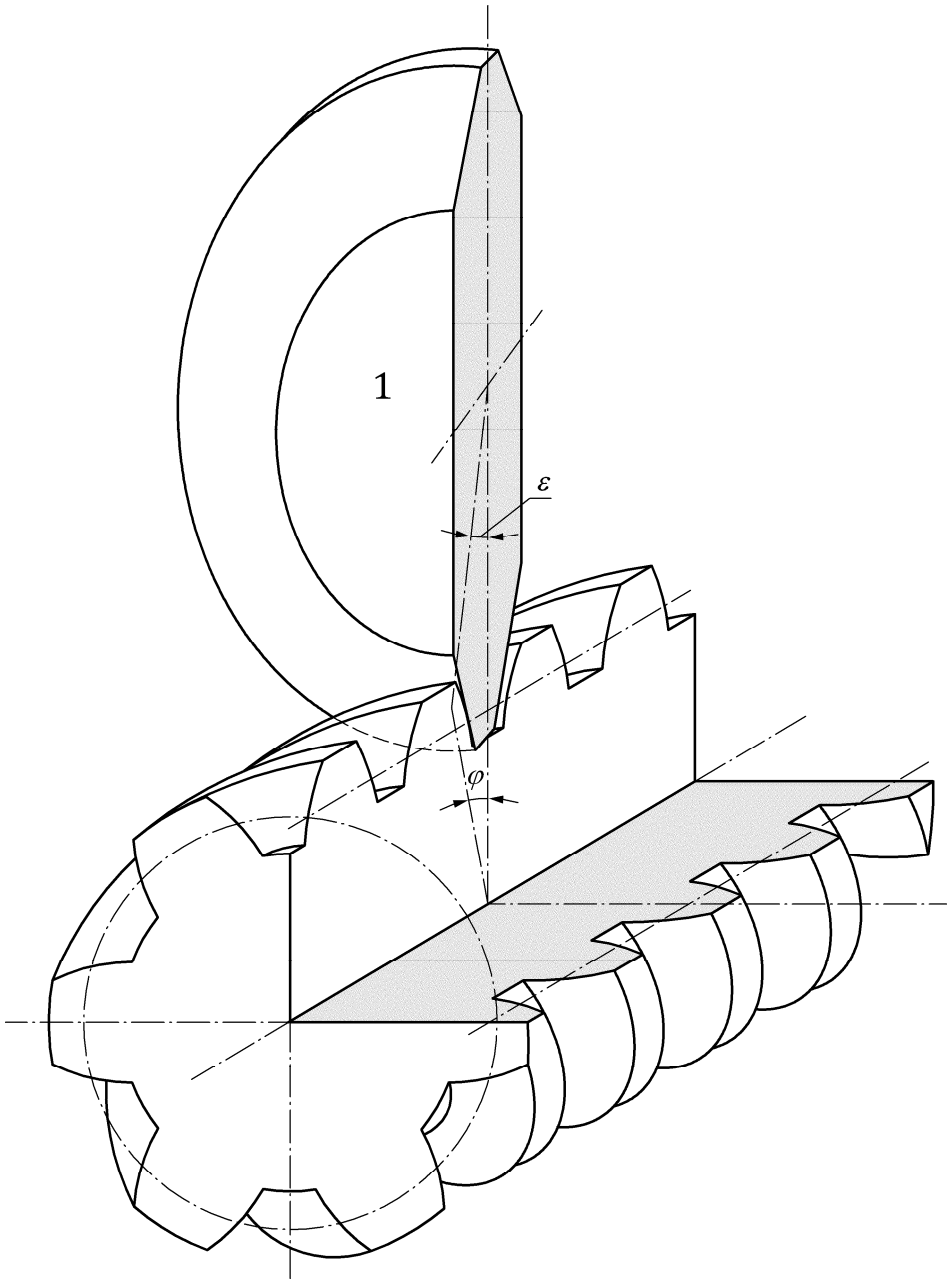

Key

1 grinding wheel

Figure 15 — Profile K - System of coordinates

Like type I profile, profile K is convex in axial planes.

The development of the formulae for the axial profile of grinding wheel for type K worm is in Annex B, B.1.

6.7 Type C

6.7.1 Geometrical definition

Unlike those of types A, I and N, the thread flanks of type C worms do not have straight line genatrices.

Like type K worms, the thread spaces of type C worms are generated with a grinding wheel or disc type milling cutter. In order to produce the concave thread profiles of type C worms, the tool has a cutting profile consisting of convex circular arcs. Figure 16 shows a tool and worm with the system of coordinates for the worm (x, y, z) and for the tool (x_G, y_G, z_G).

The length of the line of centres a_0 (the common perpendicular to the worm and tool axes x_G and x) varies with the tool diameter. The angle between the projections of these axes (x, x_G) onto a plane perpendicular to the line of centres is usually equal to the reference lead angle of worm γ_{m1}. Figure 17 shows partially the tool. The 4 tool dimensions which determine the thread form of the worm are: the profile radius ρ_{Gm}, the mean radius R_{Gm} of the tool profile, the tool pressure angle α_{0n} and the tool thickness (equal to 2 times x_{Gm}).

The process of generating the worm C profiles is the same as for type K (see 6.6).

The thread flank profile form varies a little with a change of tool diameter.

However in contrast to type K thread profiles, type C thread profiles can be adjusted to compensate change of tool diameter by modifying the radius ρ_{Gm} and the angle α_{0n} of the tool.

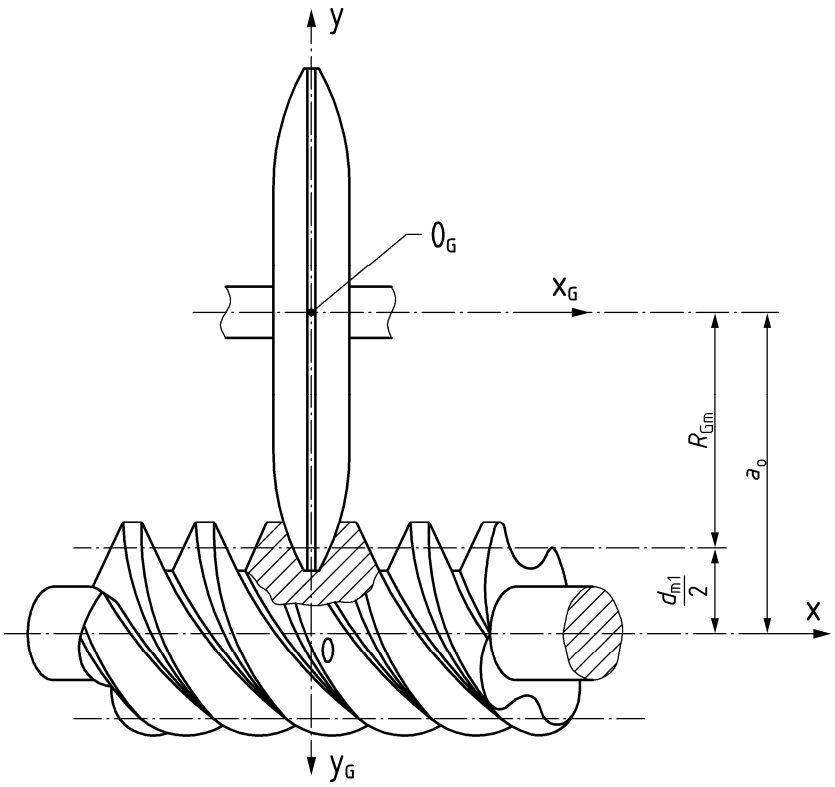

Figure 16 — Profile C - System of coordinate

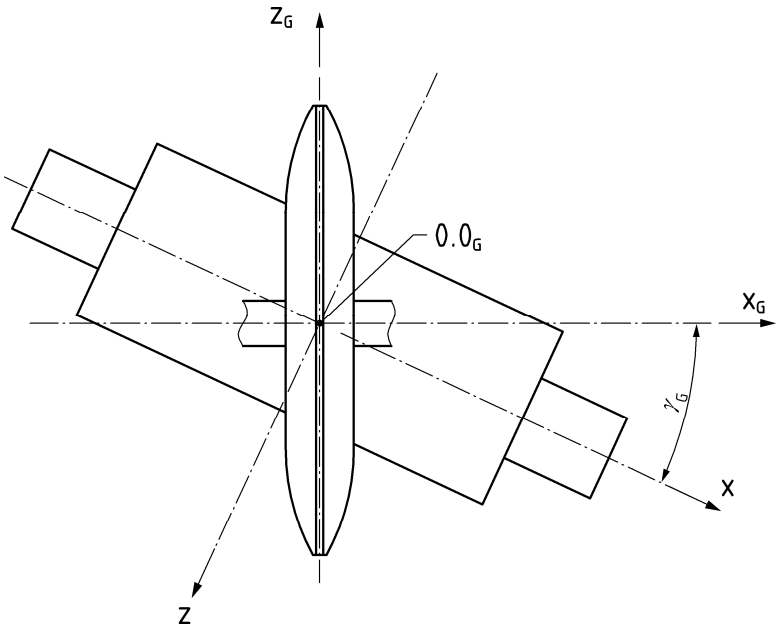

Key

$\gamma_G = \gamma_{m1}$

Figure 17 a) — System of coordinate

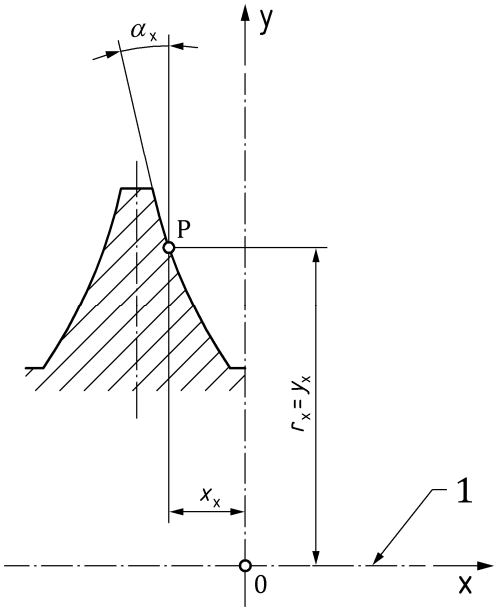

Key

1 worm axis

Figure 17 b) — Axial section of the worm

Figure 17 — Profile C

Type C profile is concave in an axial plane.

The development of the formulae for the axial profile of grinding wheel for type C worm is in Annex B, B.2.

6.7.2 General formula for C and K profiles

For C and K profiles the parameter of the profile is the Y-circle radius y_G at a point on the profile of the grinding wheel which generates a point of the profile of the worm which has to be projected along its own helix in the axial plane of worm to obtain the axial profile point.

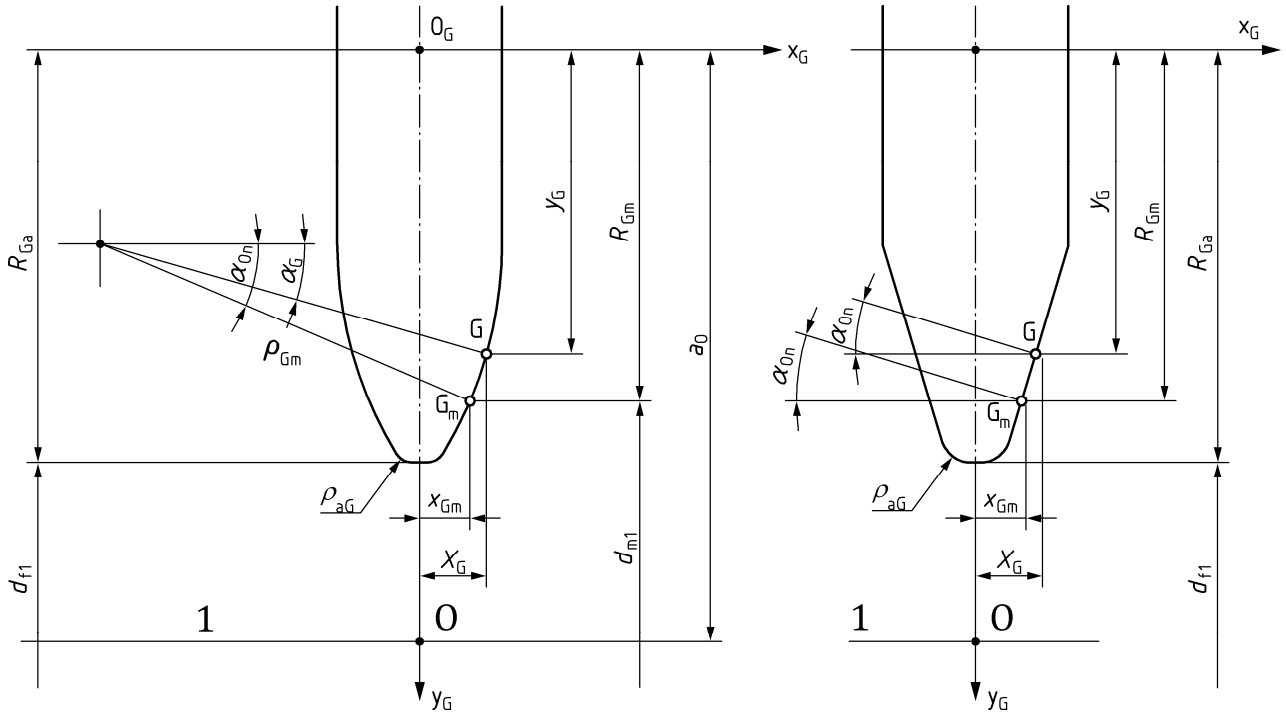

a) C Profile b) K Profile

Key

1 worm axis

Figure 18 — Parameter of grinding wheel

Table 5 — Parameters for profile grinding wheel

	K Profile	C Profile
Pressure angle at a point of axial profile of the grinding wheel	$\alpha_G(y_G) = \alpha_{0n}$	$\alpha_G(y_G) = \arcsin\left(\sin(\alpha_{0n}) - \frac{R_{Gm} - y_G}{\rho_{Gm}}\right)$
Abscissa at a point of axial profile of the grinding wheel	$x_G(y_G) = x_{Gm} - \tan(\alpha_{0n}) \cdot (y_G - R_{Ga})$	$x_G(y_G) = x_{Gm} + \rho_{Gm} \cdot (\cos(\alpha_G(y_G)) - \cos(\alpha_{0n}))$
Radius at a point of axial profile of the grinding wheel	y_G	y_G
		ρ_{Gm}: Radius of curvature of the grinding wheel

With:

Centre distance for grinding:

$$a_{0n} = R_{Ga} + \frac{d_{f1}}{2} \tag{54}$$

with R_{Ga} as the outside radius of the grinding wheel

Nominal radius of the grinding wheel:

$$R_{Gm} = a_{0n} - \frac{d_{m1}}{2} \tag{55}$$

$$x_{Gm} = \frac{(\pi \cdot m_{x1} - s_{mx1}) \cdot \cos(\gamma_{m1})}{2} \tag{56}$$

6.7.2.1 Formula for the point generated on the worm

The following formula shows the mesh condition of point G on the tool with a worm surface:

$$(c_1 \cdot \sin(\varepsilon_G(y_G)) + c_2(y_G)) + c_2(y_G) \cdot \cos(\varepsilon_G(y_G)) - c_3(y_G)) = 0 \tag{57}$$

where $\varepsilon_G(y_G)$is rotation angle of the tool:

$$c_1 = a_0 \cdot \cos(\gamma_{m1}) + p_{zu1} \cdot \sin(\gamma_{m1}) \tag{58}$$

$$c_2(y_G) = \sin(\gamma_{m1}) \cdot \left(x_G(y_G) - \frac{y_G}{\tan(\alpha_G(y_G))} \right) \tag{59}$$

$$c_3(y_G) = \left(-\frac{1}{\tan(\alpha_G(y_G))} \right) \cdot (a_0 \cdot \sin(\gamma_{m1}) - p_{zu1} \cdot \cos(\gamma_{m1})) \tag{60}$$

NOTE By default the inclination of the grinding wheel is equal to the lead angle.

From these formulae $\varepsilon_G(y_G)$ is calculated as follows:

$$\varepsilon_G(y_G) = \arcsin\left(\frac{c_3(y_G)}{\sqrt{c_1^2 + c_2(y_G)^2}} \right) - \arctan\left(\frac{c_2(y_G)}{c_1} \right) \tag{61}$$

Then the point on the worm surface generated by the point G is shown by the following formulae:

$$xc_{uw}(y_G) = x_G(y_G) \cdot \cos(\gamma_{m1}) - y_G \cdot \sin(\varepsilon_G(y_G)) \cdot \sin(\gamma_{m1}) \tag{62}$$

$$yc_{uw}(y_G) = a_0 - y_G \cdot \cos(\varepsilon_G(y_G)) \tag{63}$$

$$zc_{uw}(y_G) = -x_G(y_G) \cdot \sin(\gamma_{m1}) - y_G \cdot \cos(\gamma_{m1}) \cdot \sin(\varepsilon_G(y_G)) \tag{64}$$

6.7.2.2 Point of the worm surface in the axial plane

$$\phi_x(y_G) = \arctan\left(\frac{zc_{uw}(y_G)}{yc_{uw}(y_G)}\right) \tag{65}$$

$$x_x(y_G) = xc_{uw}(y_G) - p_{zu1} \cdot \phi_x(y_G) \tag{66}$$

$$y_x(y_G) = \frac{yc_{uw}(y_G)}{\cos(\phi_x(y_G))} \tag{67}$$

6.7.2.3 Pressure angle of the C/K profiles

6.7.2.3.1 First derivative of $c_2(y_G)$ et $c_3(y_G)$

$$\mathrm{d}c_2(y_G) = \left(\mathrm{d}x_G(y_G) + \frac{1}{\mathrm{d}x_G(y_G)} - \frac{y_G}{\mathrm{d}x_G(y_G)^2} \cdot \mathrm{d}2x_G(y_G)\right) \cdot \sin(\gamma_{m1}) \tag{68}$$

$$\mathrm{d}c_3(y_G) = \left(\frac{-a_0 \cdot \sin(\gamma_{m1}) + p_{zu1} \cdot \cos(\gamma_{m1})}{\mathrm{d}x_G(y_G)^2} \cdot \mathrm{d}2x_G(y_G)\right) \tag{69}$$

6.7.2.3.2 First derivative of $\varepsilon_G(y_G)$

$$\mathrm{d}\varepsilon_G(y_G) = \frac{\mathrm{d}c_3(y_G)}{\left(c_1^2 + c_2(y_G)^2 - c_3(y_G)^2\right)^{\frac{1}{2}}} - \frac{c_3(y_G) \cdot c_2(y_G) \cdot \mathrm{d}c_2(y_G)}{\left(c_1^2 + c_2(y_G)^2\right) \cdot \left(c_1^2 + c_2(y_G)^2 - c_3(y_G)^2\right)^{\frac{1}{2}}} - \frac{\mathrm{d}c_2(y_G) \cdot c_1}{c_1^2 + c_2(y_G)^2} \tag{70}$$

6.7.2.3.3 First derivative of point generated by the grinding wheel

$$\mathrm{d}xc_{uw}(y_G) = \mathrm{d}x_G(y_G) \cdot \cos(\gamma_{m1}) - \left(\sin(\varepsilon_G(y_G)) + y_G \cdot \cos(\varepsilon_G(y_G)) \cdot \mathrm{d}\varepsilon_G(y_G)\right) \cdot \sin(\gamma_{m1}) \tag{71}$$

$$\mathrm{d}yc_{uw}(y_G) = -\cos(\varepsilon_G(y_G)) + y_G \cdot \sin(\varepsilon_G(y_G)) \cdot \mathrm{d}\varepsilon_G(y_G) \tag{72}$$

$$\mathrm{d}zc_{uw}(y_G) = -\left(\mathrm{d}x_G(y_G) \cdot \sin(\gamma_{m1})\right) - \left[\sin(\varepsilon_G(y_G)) + y_G \cdot \cos(\varepsilon_G(y_G)) \cdot \left(\mathrm{d}\varepsilon_G(y_G)\right)\right] \cdot \cos(\gamma_{m1}) \tag{73}$$

6.7.2.3.4 First derivative of point generated by the grinding wheel projected in the axial plane of the worm

$$\mathrm{d}\phi_x(y_G) = \frac{\mathrm{d}zc_{uw}(y_G) \cdot yc_{uw}(y_G) - zc_{uw}(y_G) \cdot \mathrm{d}yc_{uw}(y_G)}{yc_{uw}(y_G)^2 + zc_{uw}(y_G)^2} \tag{74}$$

$$\mathrm{d}x_x(y_G) = \mathrm{d}xc_{uw}(y_G) - p_{zu1} \cdot \mathrm{d}\phi_x(y_G) \tag{75}$$

$$\mathrm{d}y_x(y_G) = \frac{\mathrm{d}yc_{uw}(y_G)}{\cos(\phi_x(y_G))} + \frac{yc_{uw}(y_G)}{\cos(\phi_x(y_G))^2} \cdot \sin(\phi_x(y_G)) \cdot \mathrm{d}\phi_x(y_G) \tag{76}$$

6.7.2.3.5 Pressure angle of the C/K profiles in axial plane

$$\tan\alpha_x(y_G) = \frac{\mathrm{d}x_x(y_G)}{\mathrm{d}y_x(y_G)} \tag{77}$$

6.7.2.3.6 Derivative of pressure angle of the C/K profiles

$$\mathrm{d}\tan\alpha_{\mathrm{x}}(y_{\mathrm{G}}) = \frac{\mathrm{d}2x_{\mathrm{x}}(y_{\mathrm{G}})}{\mathrm{d}y_{x}(y_{\mathrm{G}})} - \frac{\mathrm{d}x_{\mathrm{x}}(y_{\mathrm{G}})\cdot \mathrm{d}2x_{\mathrm{x}}(y_{\mathrm{G}})}{\mathrm{d}y_{\mathrm{x}}(y_{\mathrm{G}})^{2}} \tag{78}$$

For the calculation of second derivative of x_{x}, y_{x} see Annex A for A, I, N profiles and Annex B for C and K profiles.

NOTE The previous formulae apply to any profile of disc type tool.

6.7.3 General formula of the axial profile

In the following of document the axial profile of the worm is considered with general formulae $x_{\mathrm{x}}(y_{\mathrm{p}})$, $y_{\mathrm{x}}(y_{\mathrm{p}})$, $\tan\alpha_{\mathrm{x}}(y_{\mathrm{p}})$ as a function of a parameter y_{p}, with

— $y_{\mathrm{p}} = y_{\mathrm{r}}$, radius of the worm for A, I, N profiles, and

— and $y_{\mathrm{p}} = y_{\mathrm{G}}$ for radius of the worm for C and K profiles.

6.8 Algorithm to initialize the calculation

The first step is to initialize the calculation by the input of geometric parameters:

— of the worm: z_1, γ_{m1}, m_{x1}, α_{n}, profile type, d_{f1}, d_1, c_1^*, s_{mx1}^* and only for K profile R_{Ga} and C profile R_{Ga}, ρ_{Gm};

— of the worm wheel: $z_2, b_{2\mathrm{H}}, x_2, c_1^*, c_2^*, d_{\mathrm{e2}}$.

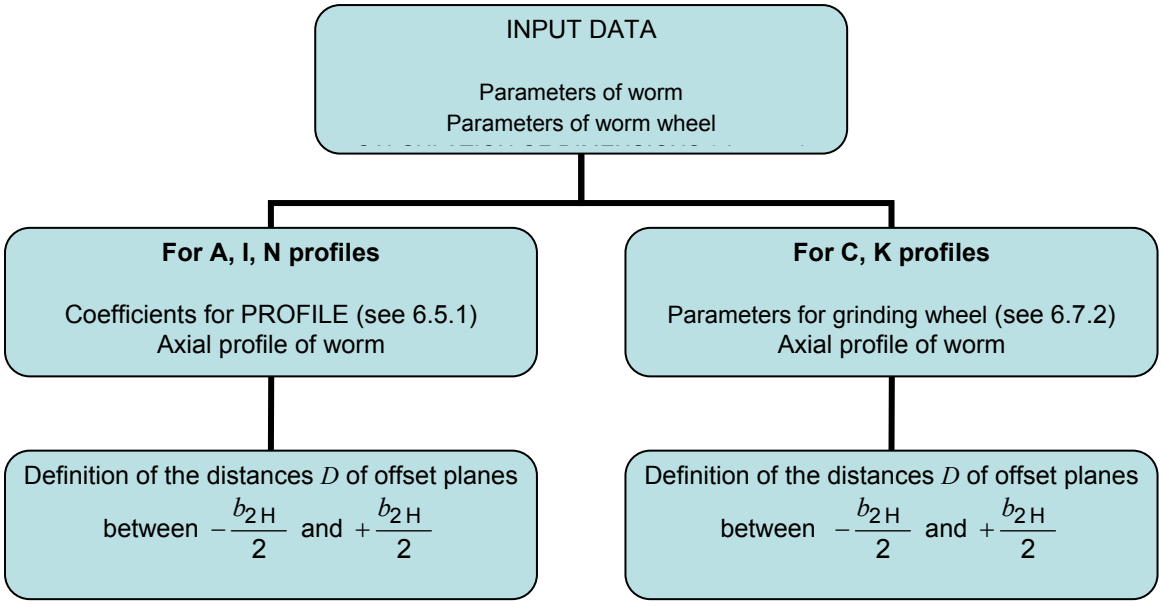

Note The worm gear mesh is split in an odd number of offset planes, N_{plane}, equally spaced by a value of $b_{2\mathrm{H}}/(N_{\mathrm{plane}} - 1)$. The Offset planes are noted D_{i} .

The algorithm has to be continued in 10.4.1.

7 Section planes

7.1 Introduction

The section planes are defined in Figure 19.

7.2 Axial plane

The axial plane is the plane containing the worm axis and the X and Y axes of the coordinate system (see plane X, Figure 19).

7.3 Offset plane

An offset plane is parallel to the X-Y plane at an offset D (Z axis) (see plane D, Figure 19).

A point in the offset plane is determined by the point of intersection with that plane of the helix through a reference point x, y, in X-Y plane.

7.4 Transverse plane

A transverse plane is a plane which is perpendicular to the axis of the worm (see plane R, Figure 19).

7.5 Normal plane

A normal plane is defined as a plane which is perpendicular to the reference helix crossing the symmetric axes of the complete axial profile (left and right flank) (see plane N, Figure 19).

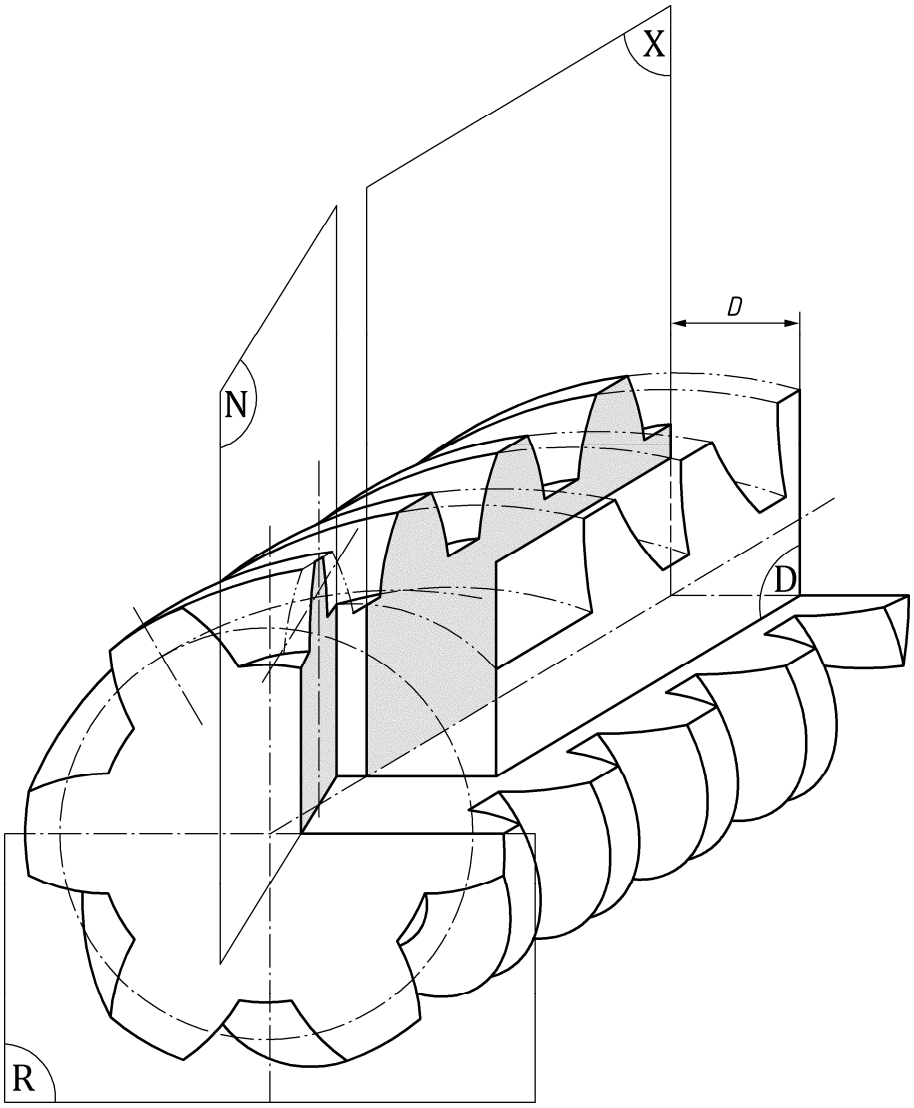

Figure 19 — Section planes

7.6 Point of the worm surface in an offset plane: offset profile of worm

By definition the worm wheel is conjugate to the worm. The profile of the worm is defined in an axial plane, and it is projected in offset planes (Figure 20) in order to study the gear mesh of the worm gear set.

The distance between the axial plane of the worm and an offset plane is defined by distance D. D can be positive or negative along Z axis.

The coordinates of point (M_d) in an offset plane and on the helix curve, which pass the point (M_x) in the plane, are shown as follows:

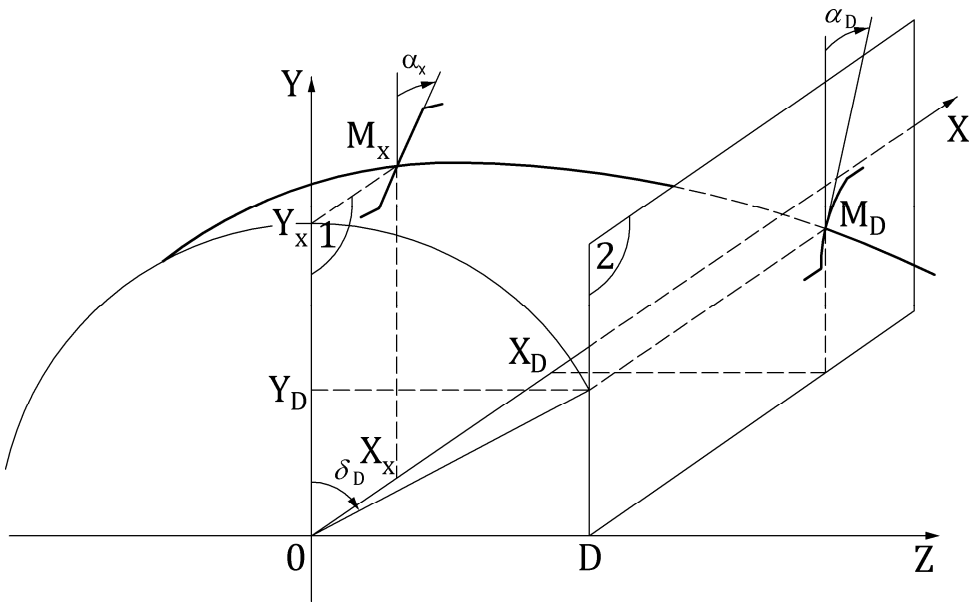

Key

1 axial plane (O, X, Y)
2 offset plane

Figure 20 — Relationship between axial profile and the profile in an offset plane

For a given axial point of worm surface, the corresponding point x_D and y_D on the same helix in an offset plane D, is obtained with the angle δ_D in the transverse plane (Y,Z).

$$\delta_D(y_p, D) = \arcsin\left(\frac{D}{y_x(y_p)}\right) \tag{79}$$

$$x_D(y_p, D) = x_x(y_p) + p_{zu1} \cdot \delta_D(y_p, D) \tag{80}$$

$$y_D(y_p, D) = y_x(y_p) \cdot \cos(\delta_D(y_p, D)) \tag{81}$$

First derivatives of rack Profile formula:

With the derivatives according to y_p:

$$\mathrm{d}\delta_D(y_p, D) = \frac{-D}{y_x(y_p)} \cdot \frac{\mathrm{d}y_x(y_p)}{\sqrt{y_x(y_p)^2 - D^2}} \tag{82}$$

$$\mathrm{d}x_D(y_p, D) = \mathrm{d}x_x(y_p) + p_{zu1} \cdot \mathrm{d}\delta_D(y_p, D) \tag{83}$$

$$\mathrm{d}y_D(y_p, D) = \mathrm{d}y_x(y_p) \cdot \cos(\delta_D(y_p, D)) - y_x(y_p) \cdot \sin(\delta_D(y_p, D)) \cdot \mathrm{d}\delta_D(y_p, D) \tag{84}$$

And it results the pressure angle of the axial projected point is:

$$\tan\alpha_{\mathrm{D}}\left(y_{\mathrm{p}},D\right)=\frac{\mathrm{d}\,x_{\mathrm{D}}\left(y_{\mathrm{p}},D\right)}{\mathrm{d}\,y_{\mathrm{D}}\left(y_{\mathrm{p}},D\right)} \tag{85}$$

8 Pitch surfaces

To study worm gear geometry the first step is to define the main parameters of the worm gear set (see Clause 4), and to select the type of the worm profile:

— For the worm:

  — number of threads on worm;

  — diameter quotient;

  — axial module;

  — normal pressure angle;

  — thread thickness;

  — rotational speed of the worm (rpm);

  — worm profile;

  — outside diameter of the grinding wheel for K and C profile;

  — radius of curvature of the grinding wheel for C profile.

— For the worm wheel:

  — number of teeth on worm wheel;

  — profile shift coefficient;

  — face width of worm wheel;

  — outside addendum coefficient;

  — bottom clearance coefficient;

— In complement addendum and dedendum coefficients can be defined if they are not equal to proposed values of Clause 4.

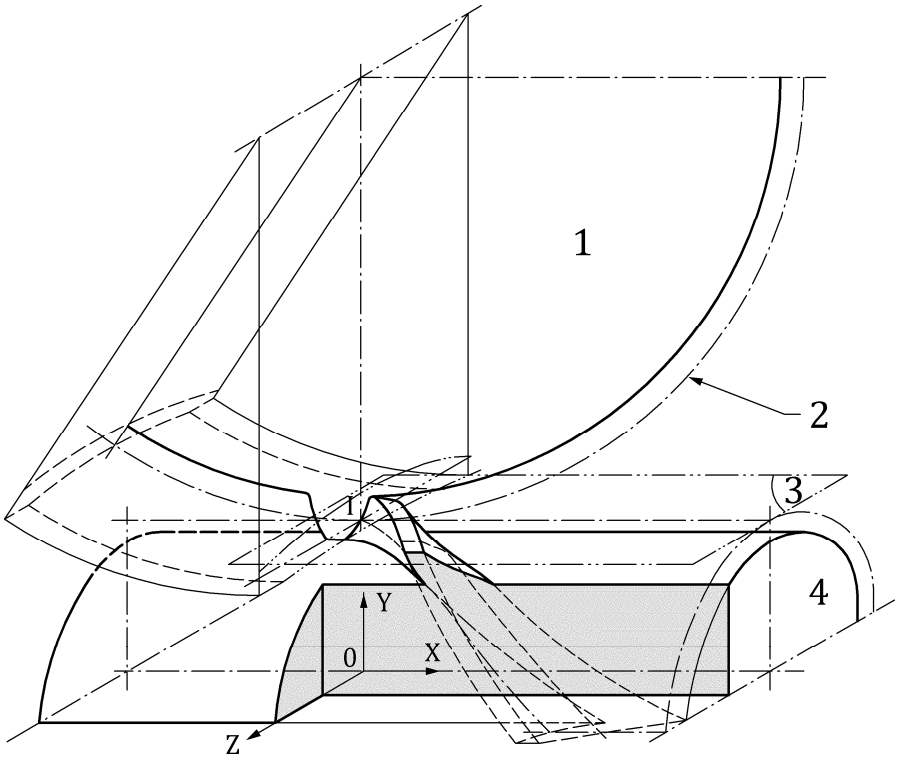

Key

1 worm wheel
2 pitch circle in the offset plane
3 pitch plane
4 worm

NOTE Definition of axes (by default a right hand driving worm is considered).

Figure 21 — Definition of pitch surfaces

The axis to study the gear mesh (Figure 21) are (0, X, Y, Z), with OX as the axis of the worm, OY along the centre line in the mid plane of the worm wheel. The Z axis is used to define the distance D of each offset plane according to the mid plane.

Right hand worm threads are considered, as the worm is driving and the worm wheel driven.

The pitch surface of the worm is a plane parallel to the axis of the worm and the axis of the wheel with a distance to the axis of the worm equal to the half of pitch diameter $d_{w1}/2$ (see 4.3.3).

The pitch cylinder of the worm wheel is defined with the pitch diameter d_{w2} (see 4.3.2).

The pitch cylinder of the wheel is rolling without sliding on the pitch plane of the worm.

The common tangent between the 2 pitch surfaces is called pitch axis; it is also the instantaneous axis of rotation.

9 Conjugate worm wheel profile

9.1 Introduction

For all the calculations in Clauses 9 to 15 the origin of the abscissa of the profile in an offset plane D has to be defined on the pitch line (see Clause 8) with the following transformation:

$$r_{wD} = \sqrt{D^2 + \left(\frac{d_{w1}}{2}\right)^2} \tag{86}$$

$$\delta_{DI}(D) = \delta_D(r_{wD}, D) = \arcsin\left(\frac{D}{y_x(r_{wD})}\right) \tag{87}$$

$$\Delta x_D(D) = x_x(r_{wD}) + p_{zu1} \cdot \delta_{DI}(D) \tag{88}$$

As the projection of the axial plane in an offset plane is done along the helix, consequently each offset profile, obtained with formulae 70 to 81, has to be translated by a value $\Delta x_D(D)$ in order that each offset profile crosses the pitch axis (see end of Clause 8). This is necessary for the following calculations to determine the values defined in Clauses 9 and 10.

This translation is given by:

$$x'_D(y_P, D) = x_D(y_P, D) - \Delta x_D(D) \tag{89}$$

9.2 Path of contact

The path of contact in an offset plane is the line along which the contact point between the flank of the worm and the conjugate flank of the worm wheel is moving during the gear mesh. The coordinate of the path of contact is defined in Figure 22 and the followings formulae:

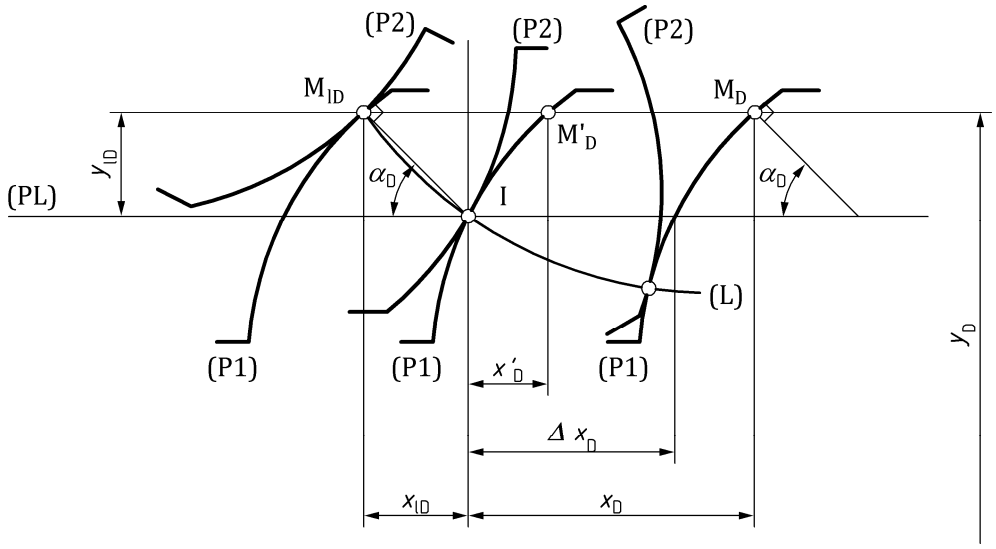

Key

(P1) profile of worm wheel
(P2) profile of worm
(L) path of contact
(PL) pitch line of worm

Figure 22 — Path of contact in offset plane D

$$y_{lD}\left(y_{\mathrm{p}},D\right)=y_{\mathrm{D}}\left(y_{\mathrm{p}},D\right)-\frac{d_{\mathrm{w1}}}{2} \tag{90}$$

$$x_{lD}\left(y_{\mathrm{p}},D\right)=-\frac{y_{lD}\left(y_{\mathrm{p}},D\right)}{\tan\alpha_{\mathrm{D}}\left(y_{\mathrm{p}},D\right)} \tag{91}$$

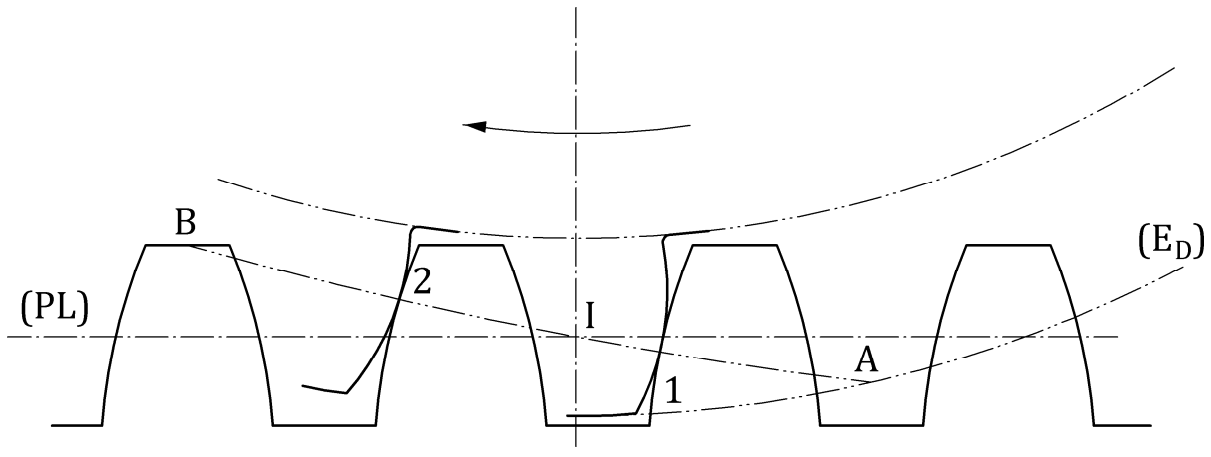

Key

1 point of contact n°1
2 point of contact n°2
(ED) external diameter
(PL) pitch line

Figure 23 — Path of contact

When there is no singularity (see 9.6) in the gear mesh the active path of contact is limited:

— on one side by the outside diameter of the worm wheel to define the start of active profile (SAP), point A on Figure 23;

— on the other side by the active tip diameter of the worm (often equal to the outside diameter of the worm except if there is chamfering), point B on Figure 23.

For the calculation of point A and B see 10.3.

9.3 Worm wheel profile conjugate with worm profile

The worm wheel profile conjugate with the worm profile in an offset plane D is obtained in Figure 24 and the following formulae. Each point of the worm wheel profile is obtained from a point of the path of contact. The kinematic conditions of rolling without sliding of pitch surfaces allow projecting those points in circular coordinates of the wheel defined according to the centreline crossing the pitch point of the offset plane.

Circular coordinates:

$$r_{M2D}\left(y_p, D\right) = \sqrt{\left(r_{w2} - y_{ID}\left(y_p, D\right)\right)^2 + x_{ID}\left(y_p, D\right)^2} \tag{92}$$

$$\varepsilon_D\left(y_p, D\right) = \frac{\left(x'_D\left(y_p, D\right) - x'_D\left(r_{wD}, D\right)\right) - x_{ID}\left(y_p, D\right)}{r_{w2}} \tag{93}$$

$$\theta_D\left(y_p, D\right) = \varepsilon_D\left(y_p, D\right) + \arctan\left(\frac{x_{ID}\left(y_p, D\right)}{r_{w2} - y_{ID}\left(y_p, D\right)}\right) \tag{94}$$

Cartesian coordinates with origin at the pitch point:

$$xR_D\left(y_p, D\right) = r_{M2D}\left(y_p, D\right) \cdot \sin\left(\theta_D\left(y_p, D\right)\right) \tag{95}$$

$$yR_D\left(y_p, D\right) = r_{w_2} - r_{M2D}\left(y_p, D\right) \cdot \cos\left(\theta_D\left(y_p, D\right)\right) \tag{96}$$

The angular origin of the conjugate profile with worm is on axis O_{2l} crossing the pitch point (see Figure 24).

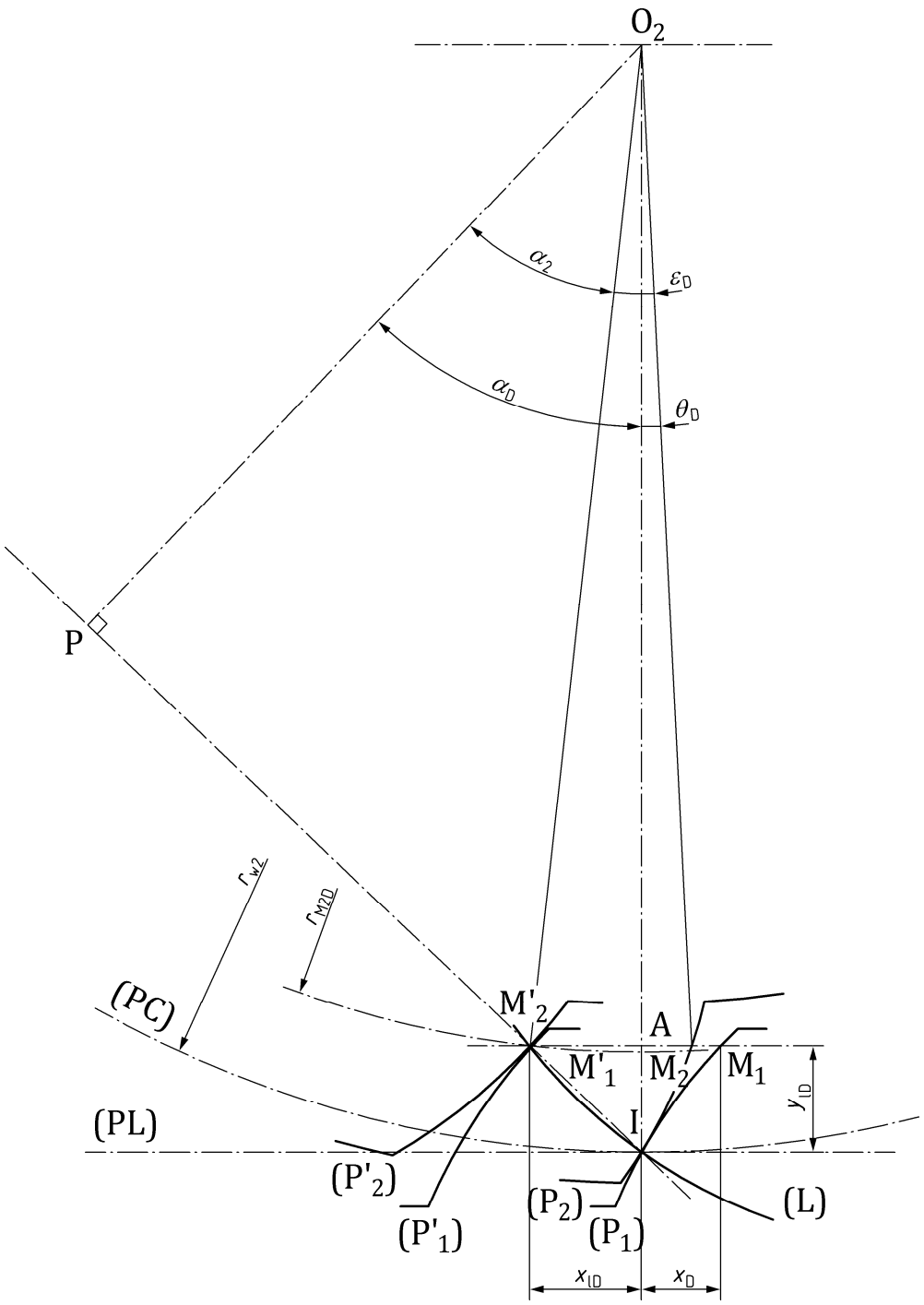

Key

(PC) pitch circle of the worm wheel
(PL) pitch line of worm
(L) path of contact

Figure 24 — Determination of the worm wheel profile conjugate with the worm profile in an offset plane

The outside radius of the worm wheel in the OFF SET plane D is given by:

$$r_{e2D}(D) = \min\left[a - \sqrt{\left(\frac{d_{f1}}{2} + c_1\right)^2 - D^2},\ 0{,}5 \cdot d_{e2} \right] \tag{97}$$

In certain cases it is interesting to determine the point of the worm (for A, I, N profiles) or of the grinding wheel (for C and K profile) which has generated the point of the worm wheel in an offset plane r_{Wheel}. The algorithm is given in Annex C.

9.4 Trochoid (or fillet) at root of the worm wheel

The tip corner of the cutting tool, which generates the worm wheel, generates a fillet or trochoid at the root of the worm wheel tooth. The tip corner is defined in each offset plane by the coordinates (x_{a0D}, y_{a0D}) obtained by increasing the outside diameter of the worm by the value of the clearance at the root of the worm wheel teeth; this corresponds to the outside radius of the cutting tool r_{a0}. The principle for the profile of the worm in an offset plane D is obtained in Figure 25 and the following formulae. Here again the kinematic conditions of rolling without sliding of pitch surfaces allow for the projection of those points in circular coordinates of the wheel defined according to the centreline crossing the tip corner of the offset plane.

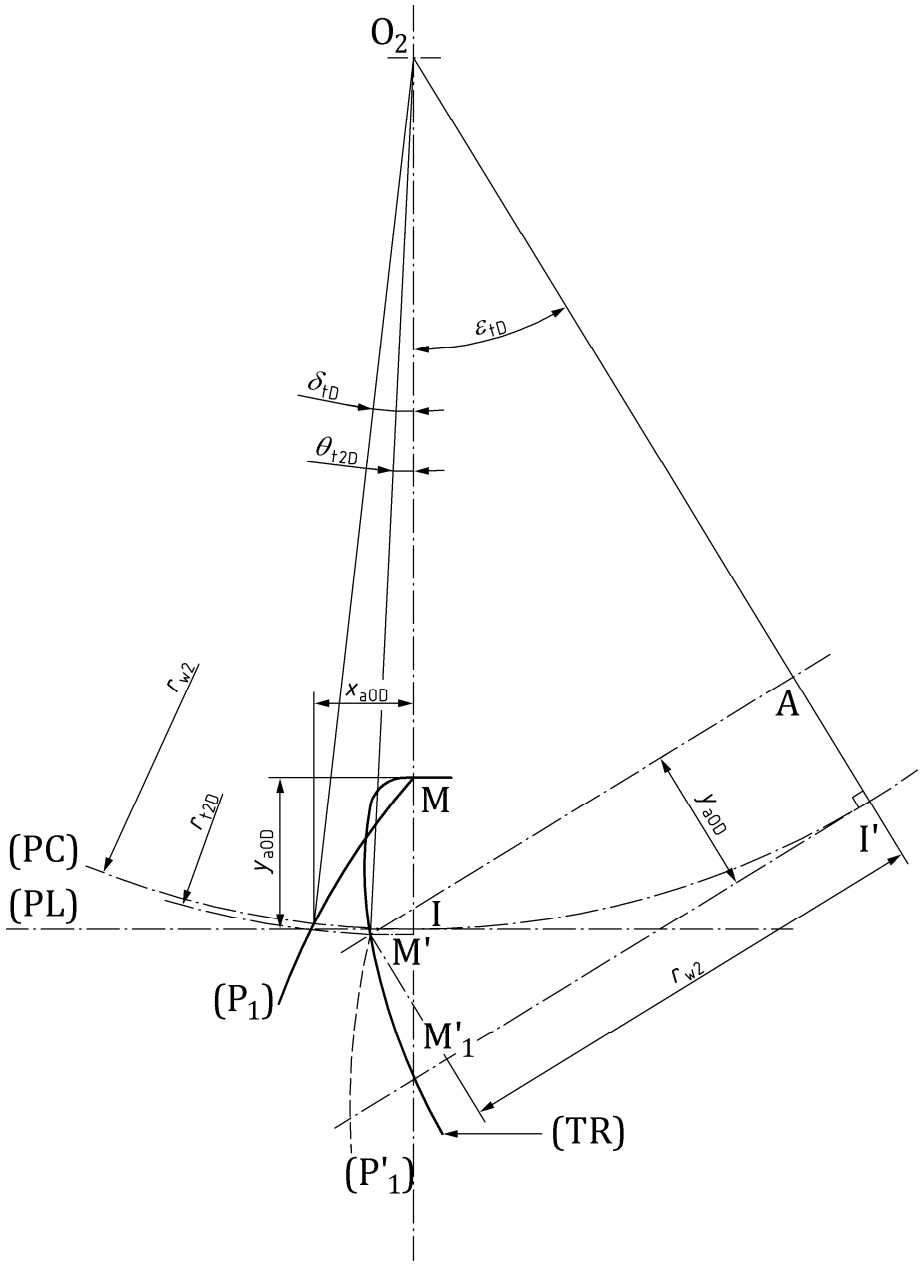

Key

(PC) pitch circle of the worm wheel
(PL) pitch line of worm
(P_1) (P'_1) offset profile of equivalent cutting tool
(TR) trochoid generated by tip corner of cutting tool

Figure 25 — Trochoid (or fillet) of the worm wheel teeth

Circular coordinates (r_{t2D}, θ_{t2D}): in the formulae the radius circle of the point of the fillet r_{t2D} is the parameter.

r_{t2D} has to be greater than the root radius of the worm wheel r_{f2D} given by:

$$r_{f2D} = a_w - \sqrt{r_{a0}^2 - D^2} \tag{98}$$

and:

$$\theta_{t2D} = \frac{x'_D(r_{a0}, D) - x'_D(r_{wD}, D)}{r_{w2}} - \arctan\left[\frac{\sqrt{r_{t2D}^2 - (r_{w2} - y_{ID}(r_{a0}, D))^2}}{r_{w2} - y_{ID}(r_{a0}, D)}\right] + \frac{\sqrt{r_{t2D}^2 - (r_{w2} - y_{ID}(r_{a0}, D))^2}}{r_{w2}} \quad (99)$$

Cartesian coordinates:

$$xT_D(r_{t2D}, D) = r_{t2D} \cdot \sin(\theta_{t2D}(r_{t2D}, D)) \quad (100)$$

$$yT_D(r_{t2D}, D) = r_{w2} - r_{t2D} \cdot \cos(\theta_{t2D}(r_{t2D}, D)) \quad (101)$$

The relations are obtained directly as a function of a radius of the circle crossing the point of the trochoid. In Formula (100 and 101) θ_{t2D} is determined with the same origin axis O_2I as the conjugate profile of the worm wheel (see 9.3).

This allows to calculate, for each offset plane, the form radius of the worm wheel r_{fnD} which corresponds to the intersection of the trochoid and conjugate profile. This value is obtained when $\theta_{t2D} = \theta_D$ for $r_{t2D} = r_{M2D}$ (see Formulae (92), (94) and (99).

9.5 Equivalent radius of curvature in an offset plane

To determine the equivalent radius of curvature the following process is used:

1) calculation of the radius of curvature of the worm at the point of contact. This calculation is made on the basis of analytical formula of the worm profile in each off set plane;

2) calculation of the radius of curvature of the conjugate profile of the worm wheel by using the EULER SAVARY method;

3) from those 2 values it is possible to calculate an equivalent radius of curvature.

9.5.1 Curvature for the worm at a point in an offset plane

It is given by the following formula resulting of general mathematical formulae for a curve in 2 dimensions:

$$C_{eq1D}(y_p, D) = \frac{\cos(\delta_D(y_p, D)) \cdot \frac{d\tan\alpha_D(y_G, D)}{d y_x(y_G)}}{\left[1 + \left(\frac{d x_D(y_p, D)}{d y_D(y_p, D)}\right)^2\right]^{\frac{3}{2}}} = \frac{1}{\rho_1(y_p, D)} \quad (102)$$

9.5.2 Curvature for the worm wheel at a point in an offset plane

To determine the radius of curvature of the worm wheel, we are using EULER-SAVARY geometric construction (see Figure 26).

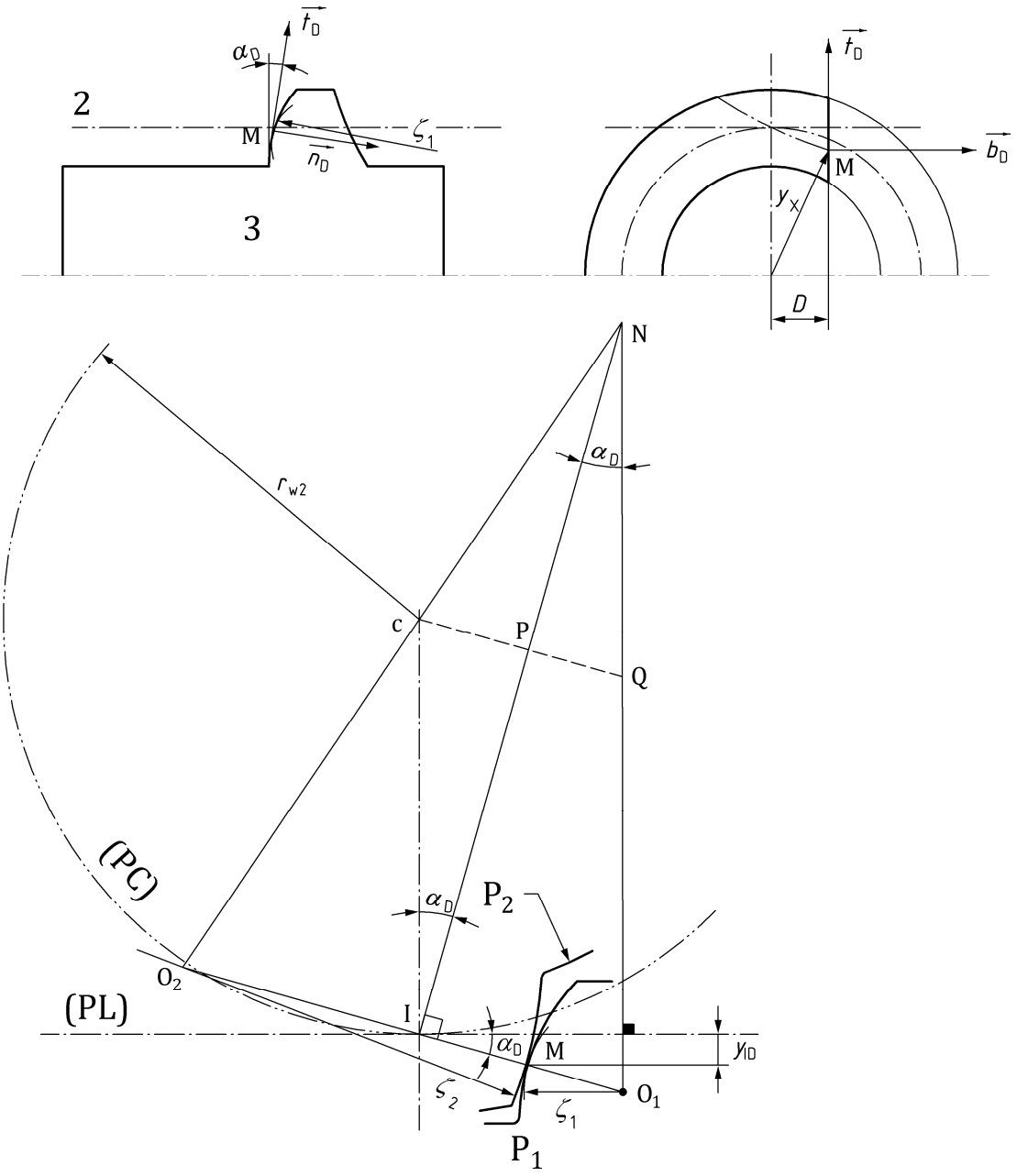

Key

(P1) offset profile of worm
(P2) worm wheel profile conjugate to the offset profile of worm
(PC) pitch circle of the worm wheel
(PL) pitch line of worm

Figure 26 — Radius of curvature in an offset plane

In an offset plane, at a point M of path of contact, the centre of curvature of the worm wheel profile resulting from the enveloping curve (envelope) of the worm profile, is the same as the centre of curvature 0_2 of the trajectory of the centre of curvature 0_1 of the worm profile.

$$C_{\mathrm{eq2D}}\left(y_{\mathrm{p}},D\right)=\frac{1-C_{\mathrm{eq1D}}\left(y_{\mathrm{p}},D\right)\cdot\left(\frac{y_{\mathrm{lD}}\left(y_{\mathrm{p}},D\right)}{\sin\alpha_{D}\left(y_{p},D\right)}+r_{\mathrm{w2}}\cdot\sin\alpha_{\mathrm{D}}\left(y_{\mathrm{p}},D\right)\right)}{r_{\mathrm{w2}}\cdot\sin\alpha_{\mathrm{D}}\left(y_{\mathrm{p}},D\right)-\frac{y_{\mathrm{lD}}\left(y_{\mathrm{p}},D\right)}{\sin\alpha_{\mathrm{D}}\left(y_{\mathrm{p}},D\right)}\cdot\left(1-\frac{y_{\mathrm{lD}}\left(y_{\mathrm{p}},D\right)\cdot C_{\mathrm{eq1D}}\left(y_{\mathrm{p}},D\right)}{\sin\alpha_{\mathrm{D}}\left(y_{\mathrm{p}},D\right)}\right)}=\frac{1}{\rho_{2}\left(y_{\mathrm{p}},D\right)} \tag{103}$$

With:

$$\sin\alpha_{\mathrm{D}}\left(y_{\mathrm{p}},D\right)=\sin\left(\arctan\left(\tan\alpha_{\mathrm{D}}\left(y_{\mathrm{p}},D\right)\right)\right) \tag{104}$$

9.5.3 Equivalent radius of curvature in an offset plane

It is given by:

$$R_{\mathrm{eqD}}\left(y_{\mathrm{p}},D\right)=\frac{1}{C_{\mathrm{eq1D}}\left(y_{\mathrm{p}},D\right)+C_{\mathrm{eq2D}}\left(y_{\mathrm{p}},D\right)} \tag{105}$$

9.6 Singularities of worm gear mesh

9.6.1 Point of zero pressure angle

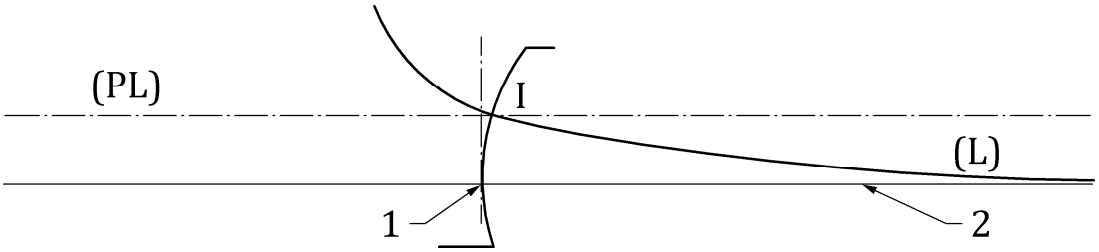

Key

(PL)	pitch line of worm
I	pitch point
(L)	path of contact
1	point of zero pressure angle
2	asymptote

Figure 27 — Point of zero pressure angle

It can be observed on Figure 27 that the presence of a point of an offset profile with zero pressure angle gives a very flat path of contact. It is said that there is an asymptotic direction above the point of zero pressure angle.

The calculation of the point of the worm in the offset plane with pressure angle equal to zero is only valid if $D > 0$.

It is based on the calculation of the point where $\tan\alpha_{\mathrm{D}}\left(ynul,D\right)=0$ in each off set plane.

The algorithm is given in the table:

A, I, N Profiles	C and K profiles
$\text{ZERO}(D) :=$ $y\min \leftarrow \max(D, a_2)$ $y\max \leftarrow r_{a1}$ $\text{ynul} \leftarrow 0{,}5 \cdot (y\min + y\max)$ DO while $\lvert\tan\alpha_D(\text{ynul}, D)\rvert > 0{,}0000001$ $y\min \leftarrow \text{ynul}$ if $\tan\alpha_D(\text{ynul}, D) < 0$ $y\max \leftarrow \text{ynul}$ if $\tan\alpha_D(\text{ynul}, D) > 0$ $\text{ynul} \leftarrow 0{,}5 \cdot (y\min + y\max)$ END DO return ynul	$\text{ZERO}(D) :=$ $y\min \leftarrow R\text{grindw}(R_{Gm}, m_{x1}, r_{a1})$ $y\max \leftarrow R\text{grindw}(R_{Gm}, m_{x1}, D)$ $\text{ynul} \leftarrow 0{,}5 \cdot (y\min + y\max)$ DO while $\lvert\tan\alpha_D(\text{ynul}, D)\rvert > 0{,}0000001$ $y\min \leftarrow \text{ynul}$ if $\tan\alpha_D(\text{ynul}, D) > 0$ $y\max \leftarrow \text{ynul}$ if $\tan\alpha_D(\text{ynul}, D) < 0$ $\text{ynul} \leftarrow 0{,}5 \cdot (y\min + y\max)$ END DO return ynul

The coordinate of the point of zero pressure angle is obtained by calculation $x'_D(ynul, D)$ and $y_D(ynul, D)$ (Formulae (80) and (81)).

For the different offset planes (with D > 0) the points of zero pressure angle give the line of zero pressure angle.

For profile I the line of zero pressure angle is an horizontal line tangent to the cylinder base.

9.6.2 Loss of contact

The zero pressure angle gives a very flat path of contact which can give a limitation of the gear mesh (Figure 28).

This phenomenon can only appear for offset planes with D > 0 – This can be a limitation of the active face width of worm wheel.

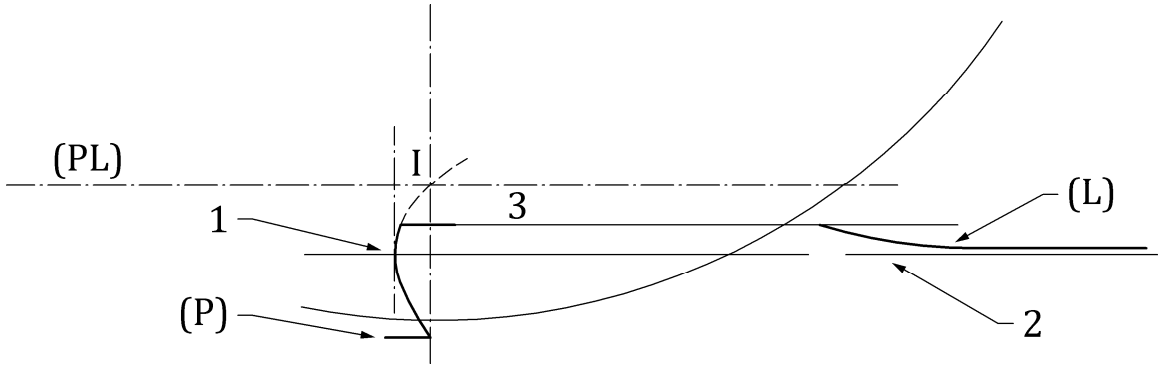

Key

(PL) pitch line of the worm
(L) path of contact
I pitch point
(P) offset profile of worm
3 tip circle
1 point of zero pressure angle
2 asymptote to the path of contact

Figure 28 — Limitation of gear mesh by the point of zero pressure angle

This phenomenon can appear for offset planes with D > 0 and closed to the border of face width of the worm wheel.

The process to detect such case is as follow:

— Determine the point of path of contact for y_p = r_{a1} (point B on Figure 28) with Formula (91), $x_{laD} = x_{lD}(r_{a1}, D)$

— Calculate the radius $r_{a2D} = \sqrt{(x_{lD}(r_{a1}, D))^2 + \left(r_{w2}^2 - y_{lD}(r_{a1}, D)\right)^2}$

— If $r_{a2D} > r_{e2D}$ there is no point of contact with the worm in the offset plane as in Figure 28 otherwise the start of active profile (point A) exists as in Figure 23.

9.6.3 Cusp

In certain circumstances it can appear a limitation of conjugate action due to the fact that the path of contact presents a cusp as shown in the following Figure 29.

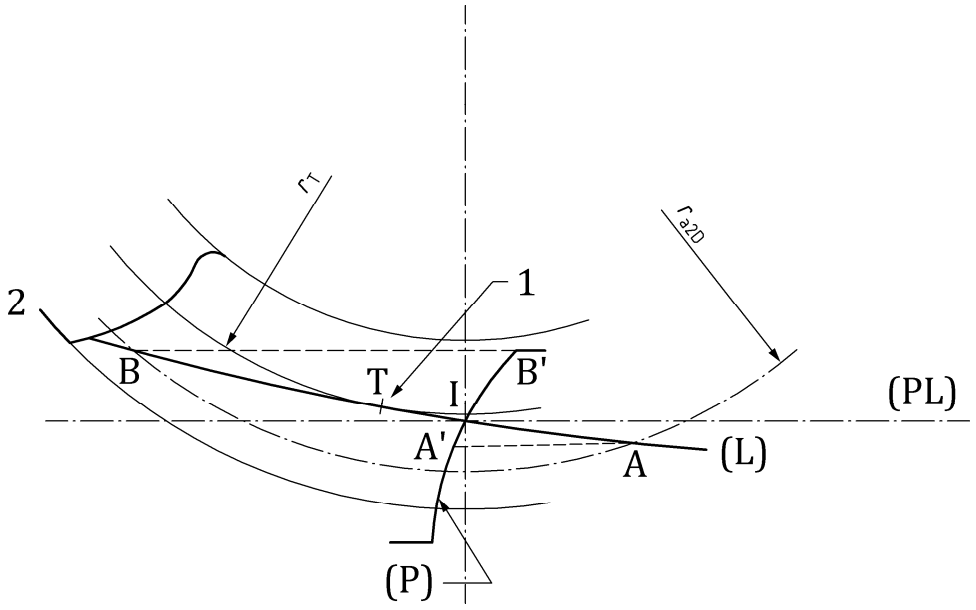

Key

1 point of tangency: cusp
2 worm wheel profile
(PL) pitch line of worm
(L) path of contact
I pitch point
(P) offset profile of worm (rack profile)

Figure 29 — Cusp effect

This effect can appear when the path of contact is flat – C profile is more sensitive to this effect than other profile types. It produces a limitation of the contact ratio because the path of contact is limited to the points between A and T. The potential of contact between T and B is lost.

Calculation of the cusp point of the worm wheel in the offset plane is valid for all the face width of the worm wheel. It is based on the calculation of the minimum value of the radius of the conjugate worm wheel in each off set plane.

To obtain this minimum value we determined when the derivative of $R_{M2D}(y_p, D)$ according to y_p is equal to zero.

$$\begin{aligned} \mathrm{d}\,R_{M2D}(y_p, D) = {} & \frac{1}{R_{M2D}(y_p, D)} \cdot \\ & \left[-\left(a_w - y_D(y_p, D)\right) \cdot \mathrm{d}\,y_D(y_p, D)\right] \\ & + \left(\frac{y_D(y_p, D) - r_{w1}}{\tan\alpha_D(y_p, D)}\right) \cdot \frac{1}{\tan\alpha_D(y_p, D)^2} \cdot \left[\mathrm{d}\,y_D(y_p, D) \cdot \tan\alpha_D(y_p, D) - \left(y_D(y_p, D) - r_{w1}\right) \cdot \left(1 + \tan\alpha_D(y_p, D)\right)\right] \end{aligned} \tag{106}$$

The algorithm is:

A, I, N Profiles	C and K profiles
$\mathrm{ZERO}(D) :=$ $y\min \leftarrow r_{w1}$ $y\max \leftarrow 6 r_{a1}$ $y\mathrm{cusp} \leftarrow 0{,}5 \cdot (y\min + y\max)$ DO while $\lvert \mathrm{d}\,R_{M2D}(y\mathrm{cusp}, D) \rvert > 0{,}0000001$ $y\min \leftarrow y\mathrm{cusp}$ if $\mathrm{d}\,R_{M2D}(y\mathrm{cusp}, D) < 0$ $y\max \leftarrow y\mathrm{cusp}$ if $\mathrm{d}\,R_{M2D}(y\mathrm{cusp}, D) > 0$ $y\mathrm{cusp} \leftarrow 0{,}5 \cdot (y\min + y\max)$ END DO return $y\mathrm{cusp}$	$\mathrm{ZERO}(D) :=$ $y\min \leftarrow R\mathrm{grindw}(R_w, m_{x1}, r_{w1})$ $y\max \leftarrow R\mathrm{grindw}(R_w, m_{x1}, r_{a1} + 5R_w)$ $y\mathrm{cusp} \leftarrow 0{,}5 \cdot (y\min + y\max)$ DO while $\lvert \mathrm{d}\,R_{M2D}(y\mathrm{cusp}, D) \rvert > 0{,}0000001$ $y\min \leftarrow y\mathrm{cusp}$ if $\mathrm{d}\,R_{M2D}(y\mathrm{cusp}, D) > 0$ $y\max \leftarrow y\mathrm{cusp}$ if $\mathrm{d}\,R_{M2D}(y\mathrm{cusp}, D) < 0$ $y\mathrm{cusp} \leftarrow 0{,}5 \cdot (y\min + y\max)$ END DO return $y\mathrm{cusp}$

The coordinate of the cusp is obtained by calculation $x_D(y\mathrm{cusp}, D)$ and $y_D(y\mathrm{cusp}, D)$ (Formulae (80) and (81)).

For the different offset planes the cusps give the line of cusp points (see Figure 30). This line has to be outside of the zone of contact otherwise it limits the maximum potential contact and reduces the load capacity.

At each point of cusp the equivalent radius of curvature is equal to zero the other reason to avoid this line in the zone of contact.

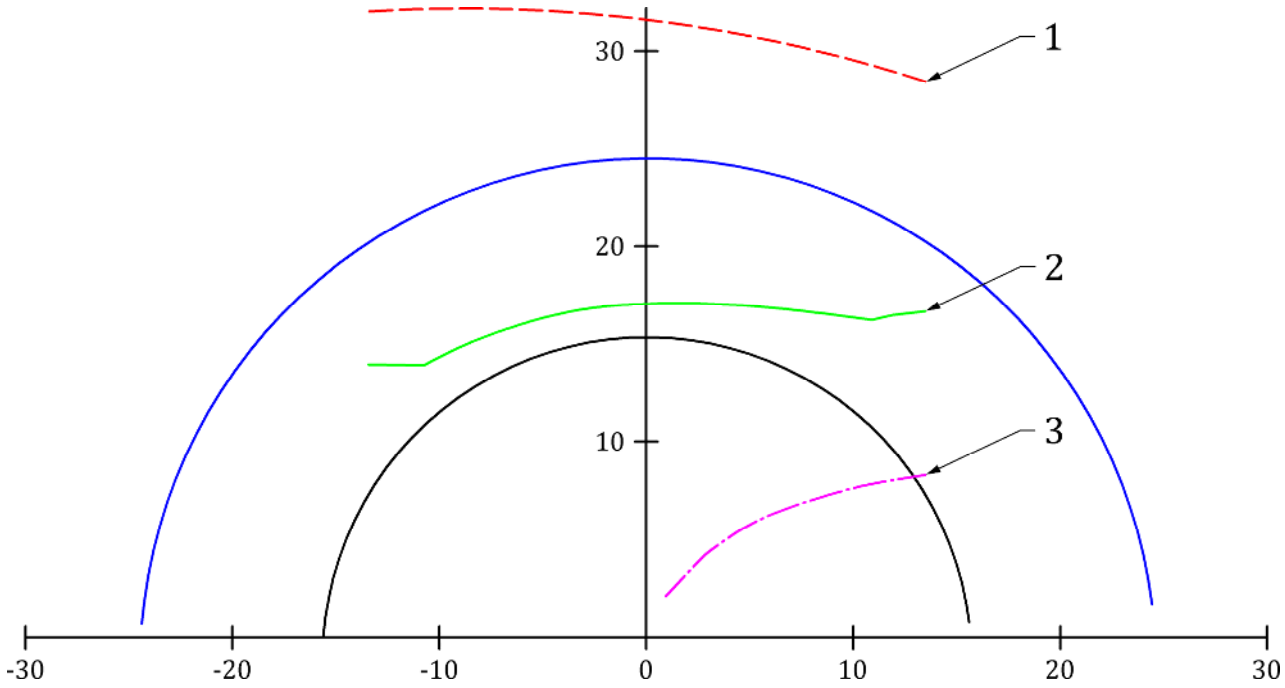

Key

1 line of cusp point
2 line of start of active profile points or start of zone of contact
3 line of zero pressure angle point

In BLACK it is the ROOT CYLINDER of the WORM.

In BLUE it is the OUTSIDE CYLINDER of the WORM.

In GREEN (continuous line) it is the limit given by the ROOT ACTIVE radius on the WORM. Normally the lines of contact are between that line and the outside circle of the worm in BLUE.

In RED (dashed line) it is the limit given by the CUSP. If this line is CROSSING the outside cylinder of the worm, there is a LIMITATION of gear mesh. For the point of contact closed to CUSP LINE the radius of curvature is closed to ZERO.

In MAGENTA (dashed dot line) it is the limit given by the ZERO PRESSURE ANGLE - When this line is near ROOT ACTIVE lines there is a LIMITATION of gear mesh.

Figure 30 — Cusp line, zero pressure angle line, active root line for worm

10 Geometry of contact

10.1 General

In fact the development of the formulae for the profile of the worm is function of 2 parameters y_p and D.

With the partial derivative according to these 2 parameters of the vector which define the coordinate vector of a point of the worm we are able to obtain 2 vectors of the tangential plane to the worm.

$$\overrightarrow{P(y_p, D)} = \begin{pmatrix} x_D(y_p, D) \\ y_D(y_p, D) \\ D \end{pmatrix} \tag{107}$$

10.2 Tangent plane at point of contact

With the derivation according to y_p:

$$\overrightarrow{T1(y_p, D)} = \begin{pmatrix} \mathrm{d}\, x_D(y_p, D) \\ \mathrm{d}\, y_D(y_p, D) \\ 0 \end{pmatrix} \tag{108}$$

And $TD1$ the normalised vector is:

$$\overrightarrow{TD1(y_p, D)} = \frac{\overrightarrow{T1(y_p, D)}}{\left|\overrightarrow{T1(y_p, D)}\right|} \tag{109}$$

With the derivation according to D:

$$\mathrm{d}\, Dx_D(y_p, D) = \frac{p_{zu1}}{\cos(\delta_D(y_p, D)) \cdot y_x(y_p)} \tag{110}$$

$$\mathrm{d}\, Dy_D(y_p, D) = -\tan(\delta_D(y_p, D)) \tag{111}$$

$$\overrightarrow{T2(y_p, D)} = \begin{pmatrix} \mathrm{d}\, Dx_D(y_p, D) \\ \mathrm{d}\, Dy_D(y_p, D) \\ 1 \end{pmatrix} \tag{112}$$

And $TD2$, the normalised vector is:

$$\overrightarrow{TD2(y_p, D)} = \frac{\overrightarrow{T2(y_p, D)}}{\left|\overrightarrow{T2(y_p, D)}\right|} \tag{113}$$

10.3 Normal plane at point of contact

The unit normal vector to the point of contact: (orientation from the inside to the outside of the worm) is given by:

$$\overrightarrow{\mathrm{NORMAL}(y_p, D)} = \frac{\overrightarrow{TD2(y_p, D)} \times \overrightarrow{TD1(y_p, D)}}{\left|\overrightarrow{TD2(y_p, D)} \times \overrightarrow{TD1(y_p, D)}\right|} \tag{114}$$

$$nNxy(y_p, D) = \sqrt{(\mathrm{NORMAL}(y_p, D)_1)^2 + (\mathrm{NORMAL}(y_p, D)_2)^2} \tag{115}$$

$$\overrightarrow{\text{Normal}Nxy\left(y_p, D\right)} = \begin{pmatrix} \dfrac{\text{NORMAL}\left(y_p, D\right)_1}{nNxy\left(y_p, D\right)} \\ \dfrac{\text{NORMAL}\left(y_p, D\right)_2}{nNxy\left(y_p, D\right)} \\ 0 \end{pmatrix} \quad (116)$$

NOTE $\overrightarrow{\text{Normal}Nxy\left(y_p, D\right)}$ is the common normal vector to conjugate profiles at the point of contact.

10.4 Zone of contact

The zone of contact is limited in each offset plane by the active radius at the root of the worm and the tip radius of the worm or the cusp radius when there is limited conjugate contact.

In the longitudinal direction (along the face width of the worm wheel) the limitation is the face width of the worm wheel, or the tip radius of the worm for important values of face width or the cusp curve when there is limited conjugate contact. See Figure 31.

The zone of contact is the surface defined by all the path of contact in the different offset planes. It is limited by the tip cylinder of the worm and the external surface of the worm wheel defined by the external cylinder and external throat surface.

In the case of chamfering, those limits are respectively the addendum active cylinder of the worm and the active tip line at the tip of the worm wheel teeth.

In case of cusp in the gear mesh the zone of contact is limited by the cusp.

In each offset plane it can be defined:

— The start of active profile for the worm by the intersection of the path of contact with the external diameter of the worm wheel in this plane (either defined by the external cylinder or the throat diameter of the worm wheel). The result is that the radius of SAP of the worm is defined by the closest point to the axis of the worm of all offset planes. See Figure 30.

— The start of active profile for the worm wheel (SAP worm wheel) by either the intersection of the path of contact with the external diameter of the worm in this plane or by the point of tangency CUSP if there is a cusp (see Figure 29). The result is that for the worm wheel there is a distinct SAP in each offset planes.

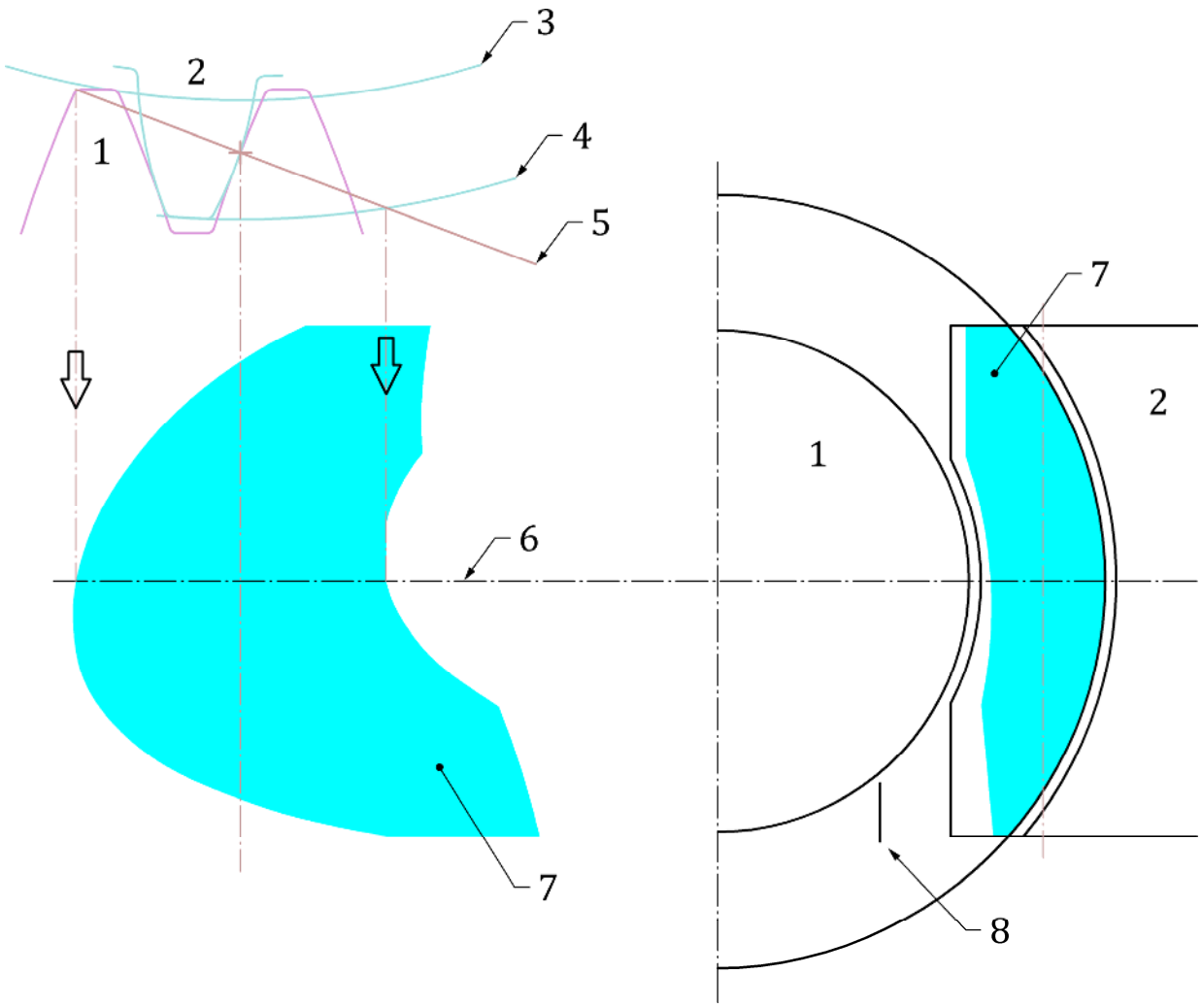

Key

1 worm
2 wheel
3 form circle
4 outside diameter
5 path contact
6 axis of worm
7 zone of contact
8 line of zero pressure angles

Figure 31 — Zone of contact

The lines of contact are moving on the surface limited by the zone of contact.

In each offset plane, the zone of contact (Figures 31, 34) is limited by the start of active profile (point A in Figure 23) and the end of active profile (point B in Figure 23) except if there is a cusp (point T of Figure 29). In the last case the zone of contact is truncated as in Figure 34.

This calculation has to be done for all offset planes. It is recommended to use between 30 and 80 offset planes uniformly distributed along the worm wheel face width.

Continuing from 6.8, the following algorithm can be executed **in each offset plane D_i:**

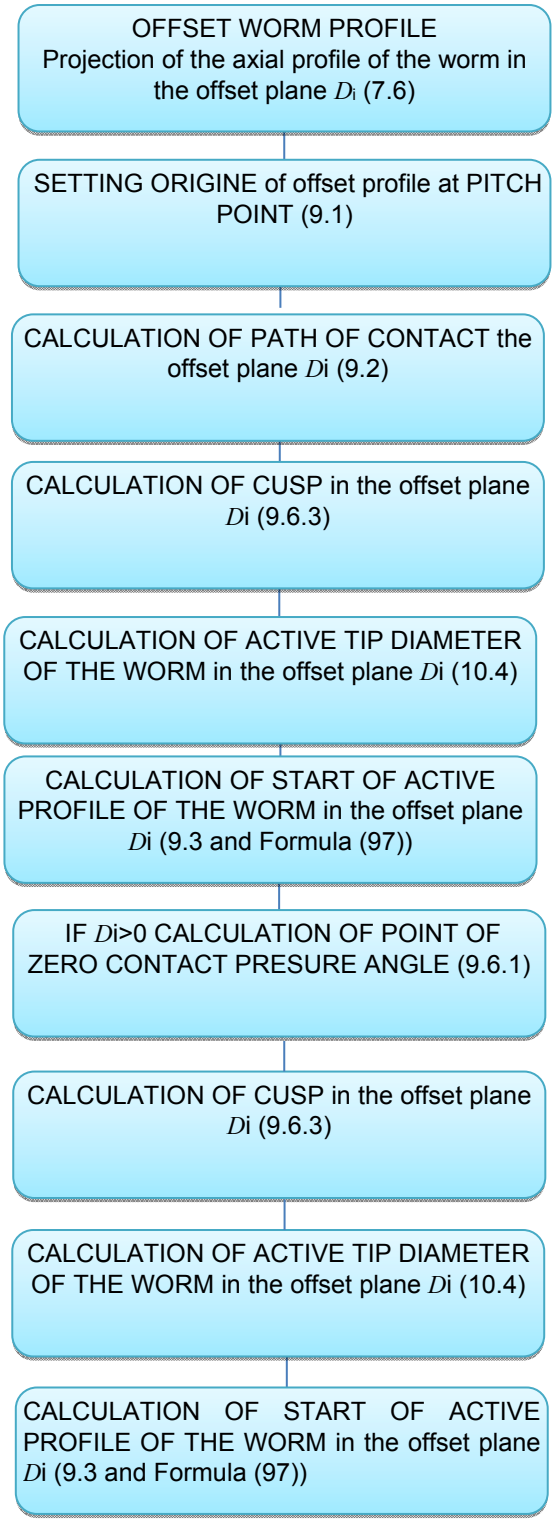

NOTE The zone of contact in an offset plane is delimited by the limit points as indicated in 10.4.

10.5 Lines of contact

A line of contact is composed of all the conjugate points between the flank of the worm and the conjugate flank of the worm wheel for a relative position of the worm gear set.

Several threads of the worm can be simultaneously in contact.

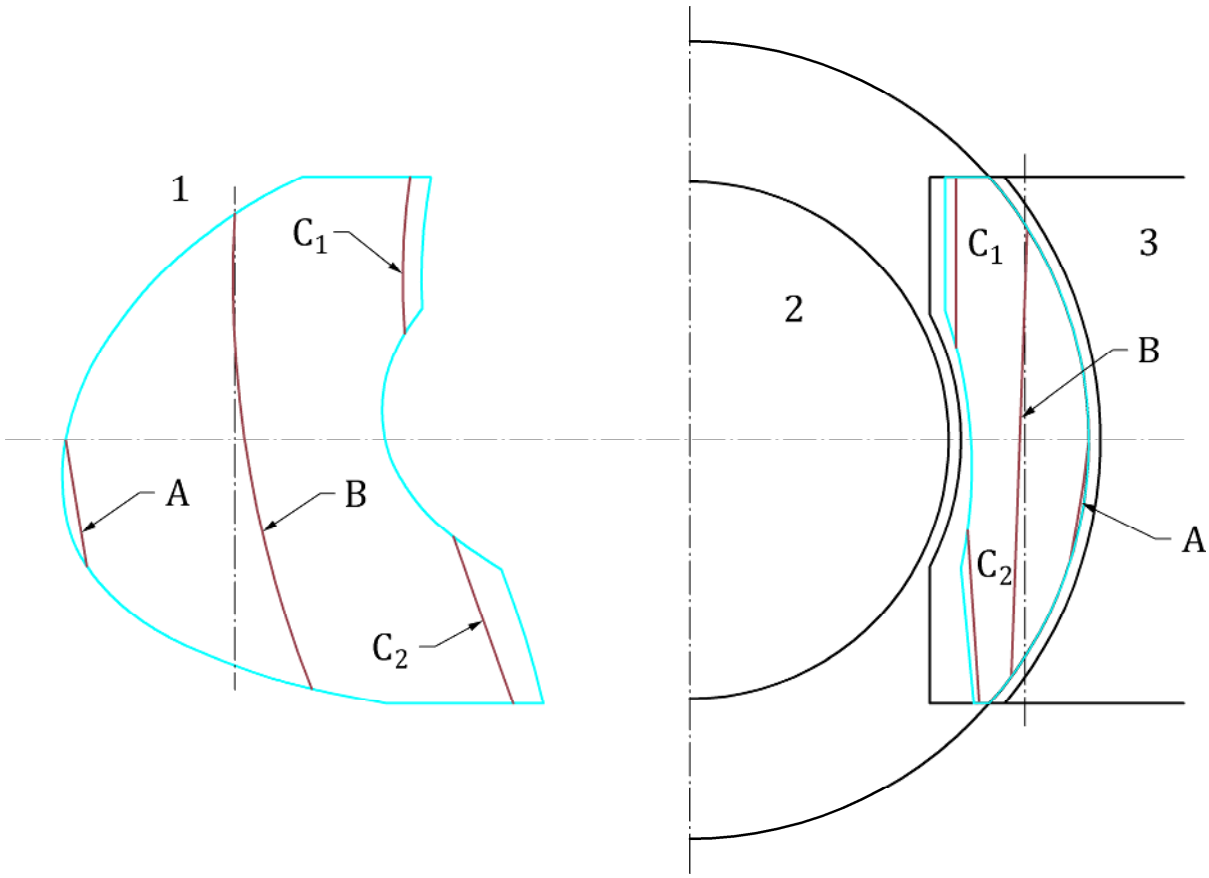

Key

A, B, C_1 and C_2 instantaneous lines of contact
1 zone of contact
2 worm
3 wheel

Figure 32 — Zone of contact and Lines of contact for one relative position of worm and worm wheel (here 3 threads are in contact for this relative position)

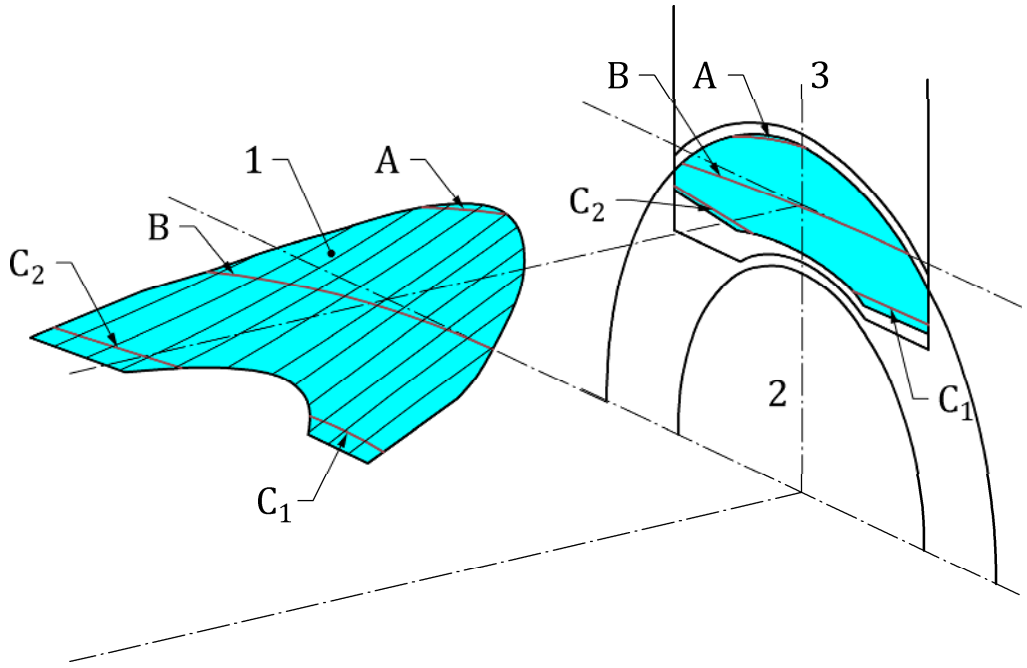

Key

A, B, C_1 and C_2 instantaneous lines of contact
1 zone of contact with path of contact in different offset planes
2 worm
3 worm wheel

Figure 33 — Path of contact, zone of contact and lines of contact for one relative position of worm and worm wheel

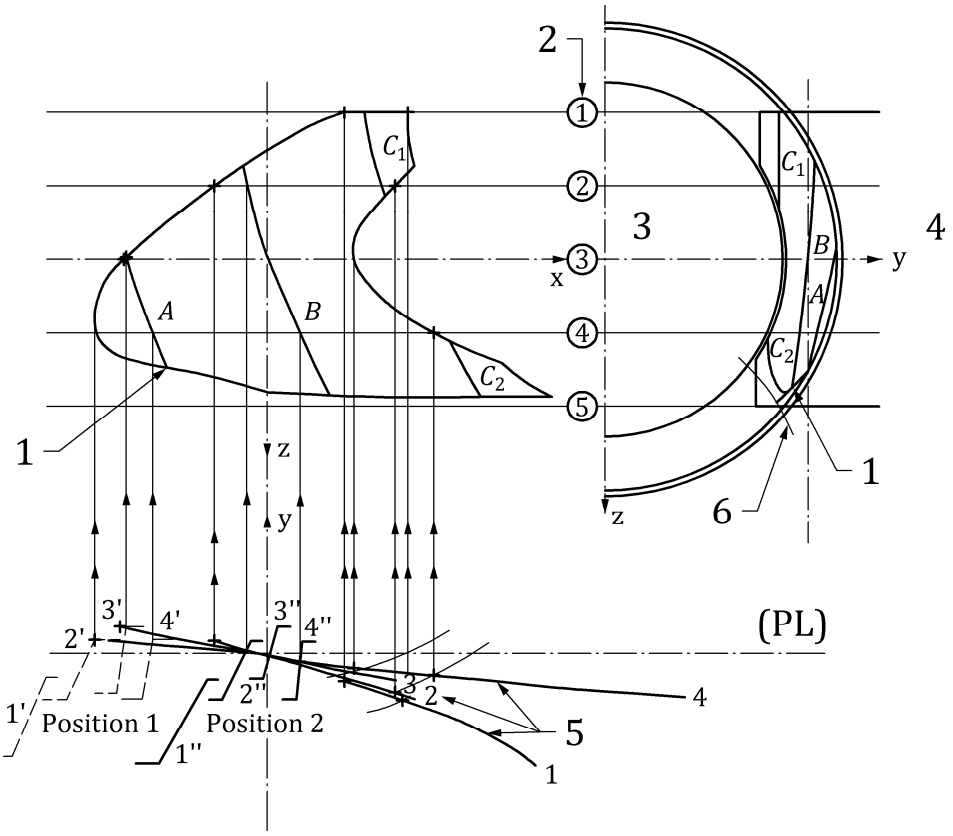

Key

A, B, C_1 and C_2 instantaneous line of contact
1 cusp
2 offset planes
3 worm
4 worm wheel
5 path of contact
6 line of zero pressure angles
(PL) pitch line

Figure 34 — Path of contact, zone of contact and lines of contact for one relative position of worm and worm wheel

The formula of the lines of contact $\text{Fcont}\left(y_p, D\right) = 0$ is given by:

$$\text{Fcont}\left(y_p, D\right) = x'_D\left(y_p, D\right) \cdot \tan\alpha_D\left(y_p, D\right) + y_D\left(y_p, D\right) - r_{w1} \tag{117}$$

Coordinate of a point of contact: For this we consider only the point along the path of contact (in fact for a relative position between the worm and the worm wheel there are 1 or 3 points of contact).

For the worm (0M):

$$\overrightarrow{M_1\left(y_p, D\right)} = \begin{pmatrix} x_{ID}\left(y_p, D\right) \\ y_D\left(y_p, D\right) \\ D \end{pmatrix} \tag{118}$$

For the worm wheel (0_2M):

$$\overrightarrow{M_2(y_p, D)} = \begin{pmatrix} x_{ID}(y_p, D) \\ -a_w + y_D(y_p, D) \\ D \end{pmatrix} \quad (119)$$

The determination of lines of contact is made by the determination of points of contact.

First of all the relative position of the worm is set up by the parameter $\Delta x_D(D)$ of Formula (89). This value is setup in order to obtain the first line of contact tangent to the zone of contact (see Figure 35), this is the initial value $\Delta x_{Dinit}(D)$.

To determine the 1st line of contact, the calculation is made in all the offset planes used to determine the zone of contact. In each offset plane, the initial value of y_p to calculate $Fcont(y_p, D) = 0$ is initialized between the values obtained for the start of active profile (point A in Figure 23) and the end of active profile (point B in Figure 23) or the cusp (point T of Figure 29). So the point of contact is obtained easily.

To obtain the next line of contact, the value of $\Delta x_{Dinit}(D)$ is decreased by the axial pitch p_{x1}, and all the points of contact are determined in each offset plane. Continue with this operation until the position of the worm for which there is no more contact points, it means points of contact out of the zone of contact.

To study a second relative position of the worm and the worm wheel the initial value $\Delta x_{Dinit}(D)$ is decreased by a portion of the axial pitch p_{x1}, p_{x1}/n where n is an integer corresponding to the number of relative positions to study. (e.g. for 10 relative positions to study n=10) and the process is started again with this new initial value.

10.6 Contact ratio

In a worm gear the contact ratio is obtained by the ratio of the distance between the 2 positions of the worm defined when the first line of contact is tangent to the zone of contact and the last line of contact is tangent to the zone of contact see Figure 35, divided by the axial pitch.

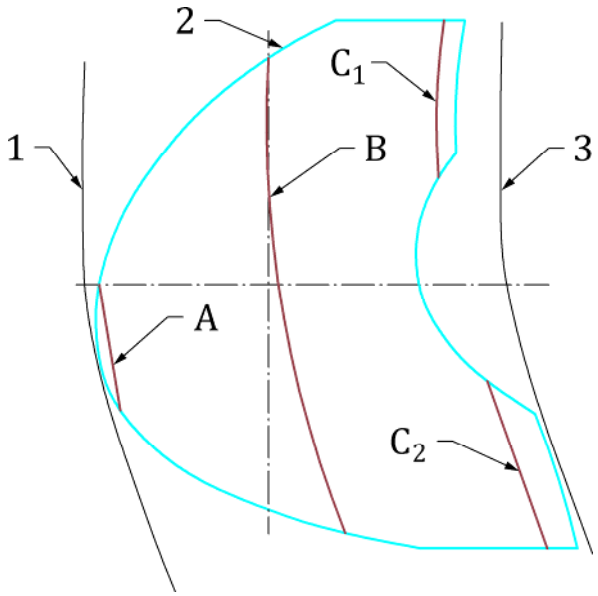

Key

A, B, C_1 and C_2 instantaneous line of contact
1 last line in contact
2 zone of contact
3 first line in contact

Figure 35 — Contact ratio

10.7 Tangent vector to the line of contact

To determine the vector tangent to the line of contact, we have to consider the formula of the lines of contact Fcont $(y_p, D) = 0$.

The derivatives of Fcont (y_p, D) have to be evaluated for the point the contact. It means that in the formulae $\mathrm{d}\,y\mathrm{Fcont}(y_p, D)$ and $\mathrm{d}\,D\mathrm{Fcont}(y_p, D)$, $x_D(y_p, D)$ has to be replaced by $x_{1D}(y_p, D)$ which satisfies the contact formula.

$$\mathrm{d}\,y\mathrm{Fcont}(y_p, D) = x_{1D}(y_p, D)\cdot \mathrm{d}\tan\alpha_D(y_p, D) + \mathrm{d}\,x_D(y_p, D)\cdot\tan\alpha_D(y_p, D) + \mathrm{d}\,y_D(y_p, D) \quad (120)$$

$$\mathrm{d}\,D\mathrm{Fcont}(y_p, D) = x_{1D}(y_p, D)\cdot \mathrm{d}\,D\tan\alpha_D(y_p, D) + \mathrm{d}\,Dx_D(y_p, D)\cdot\tan\alpha_D(y_p, D) + \mathrm{d}\,Dy_D(y_p, D) \quad (121)$$

With:

$$\mathrm{d}\,D\delta_D(y_p, D) = \frac{1}{y_x(y_p)\cdot\cos(\delta_D(y_p, D))} \quad (122)$$

$$\mathrm{d}\,D\delta_D(y_p, D) = -\sin(\delta_D(y_p, D))\cdot\tan\alpha_x(y_p)\cdot\mathrm{d}\,D\delta_D(y_p, D) - \frac{p_{zu1}}{y_x(y_p)^2} \quad (123)$$

This is obtained by considering the derivative of Fcont(y_p, D) at the point of contact, and it gives the relation between D and y_p along the line the contact as the relation of partial derivatives.

$$\mathrm{d}Dym\left(y_{\mathrm{p}},D\right)=\frac{-\mathrm{d}y\mathrm{Fcont}\left(y_{\mathrm{p}},D\right)}{\mathrm{d}D\mathrm{Fcont}\left(y_{\mathrm{p}},D\right)} \tag{124}$$

To obtain the tangent vector to the lines of contact we have to take the total derivative according to y_{p} (or D)

$$\overrightarrow{T\mathrm{cont}\left(y_{\mathrm{p}},D\right)}=\begin{pmatrix}\mathrm{d}x_{\mathrm{D}}\left(y_{\mathrm{p}},D\right)+\mathrm{d}Dx_{\mathrm{D}}\left(y_{\mathrm{p}},D\right)\cdot\mathrm{d}Dy\mathrm{m}\left(y_{\mathrm{p}},D\right)\\ \mathrm{d}y_{\mathrm{D}}\left(y_{\mathrm{p}},D\right)+\mathrm{d}Dy_{\mathrm{D}}\left(y_{\mathrm{p}},D\right)\cdot\mathrm{d}Dy\mathrm{m}\left(y_{\mathrm{p}},D\right)\\ \mathrm{d}Dy\mathrm{m}\left(y_{\mathrm{p}},D\right)\end{pmatrix} \tag{125}$$

And the unit vector is:

$$\overrightarrow{TN\ \mathrm{cont}\left(y_{\mathrm{p}},D\right)}=\frac{\overrightarrow{T\mathrm{cont}\left(y_{\mathrm{p}},D\right)}}{\left|\overrightarrow{T\mathrm{cont}\left(y_{\mathrm{p}},D\right)}\right|} \tag{126}$$

Or:

$$\overrightarrow{T\mathrm{cont1}\left(y_{\mathrm{p}},D\right)}=\begin{pmatrix}\mathrm{d}Dx_{\mathrm{D}}\left(y_{\mathrm{p}},D\right)+\dfrac{\mathrm{d}x_{\mathrm{D}}\left(y_{\mathrm{p}},D\right)}{\mathrm{d}Dy\mathrm{m}\left(y_{\mathrm{p}},D\right)}\\ \mathrm{d}Dy_{\mathrm{D}}\left(y_{\mathrm{p}},D\right)+\dfrac{\mathrm{d}y_{\mathrm{D}}\left(y_{\mathrm{p}},D\right)}{\mathrm{d}Dy\mathrm{m}\left(y_{\mathrm{p}},D\right)}\\ 1\end{pmatrix} \tag{127}$$

And the unit vector is:

$$\overrightarrow{TN1_{\mathrm{cont}}\left(y_{\mathrm{p}},D\right)}=\frac{\overrightarrow{T\mathrm{cont1}\left(y_{\mathrm{p}},D\right)}}{\left|\overrightarrow{T\mathrm{cont1}\left(y_{\mathrm{p}},D\right)}\right|} \tag{128}$$

NOTE $\vec{T}_{\mathrm{cont}}\left(y_{\mathrm{p}},D\right)$ and $\vec{T}\mathrm{cont1}\left(y_{\mathrm{p}},D\right)$ are identical.

10.8 Normal plane at point of contact

As the contact is linear along the lines of contact, according to EULER's theory on curvatures of surface, the direction tangent to line of contact is ONE of the principal directions of curvature.

The SECOND principal direction of curvature is normal to that ONE and can be obtain with the vector product between the tangent vector to the line of contact and the normal to the tangent plane of contact. Those 3 vectors [$\overrightarrow{TN_{\mathrm{cont}}\left(y_{\mathrm{p}},D\right)}$, $\overrightarrow{NORMAL\left(y_{\mathrm{p}},D\right)}$, $\overrightarrow{B\left(y_{\mathrm{p}},D\right)}$] defines the trihedral of DARBOUX RIBAUCOUR.

$$\overrightarrow{B\left(y_{\mathrm{p}},D\right)}=\overrightarrow{TN_{\mathrm{cont}}\left(y_{\mathrm{p}},D\right)}\times\overrightarrow{\mathrm{NORMAL}\left(y_{\mathrm{p}},D\right)} \tag{129}$$

10.9 Principal equivalent radius of curvature

For a point of contact, the equivalent of curvature reaches MIN and MAX values called PRINCIPAL RADIUS OF CURVATURE when we consider its projection in the MAIN PLANES.

In a point of contact, those MAIN PLANES are defined as follows:

— the MAX equivalent of curvature is always in the plane defined by the normal at the surface of the worm and the vector tangent to the instantaneous line of contact;

— the MIN equivalent of curvature is always in the plane defined by the normal at the surface of the worm and the vector normal to the instantaneous line of contact.

This equivalent radius of curvature in an offset plane (see 9.5) has to be projected in the 2 main planes of curvature, which are in this particular case

a) the plane normal to the instantaneous line of contact between the flanks of worm and worm wheel, crossing the studied point of contact,

b) the plane tangent to the instantaneous line of contact between the flanks of worm and worm wheel, crossing the studied point of contact, and

c) in this last plane the curvature is zero because the contact is locally linear.

At each point of contact we can define in an offset plane 3 vectors as follows:

— a tangent vector to the worm and worm wheel profile

$$\overrightarrow{t_{\mathrm{D}}\left(y_{\mathrm{p}}, D\right)} = \begin{pmatrix} \sin\alpha_{\mathrm{D}}\left(y_{\mathrm{p}}, D\right) \\ \cos\left(\arctan\left(\tan\alpha_{\mathrm{D}}\left(y_{\mathrm{p}}, D\right)\right)\right) \\ 0 \end{pmatrix} \tag{130}$$

— a normal vector to the worm and worm wheel profile

$$\overrightarrow{n_{\mathrm{D}}\left(y_{\mathrm{p}}, D\right)} = \begin{pmatrix} \cos\left(\arctan\left(\tan\alpha_{\mathrm{D}}\left(y_{\mathrm{p}}, D\right)\right)\right) \\ -\sin\alpha_{\mathrm{D}}\left(y_{\mathrm{p}}, D\right) \\ 0 \end{pmatrix} \tag{131}$$

— a vector normal to the offset plane

$$\overrightarrow{b_{\mathrm{D}}\left(y_{\mathrm{p}}, D\right)} = \begin{pmatrix} 0 \\ 0 \\ 1 \end{pmatrix} \tag{132}$$

The radius of curvature is projected along the normal to the point of contact contained in the offset plane.

First of all we have to determine the radius of curvature projected along the normal to the common tangent plane of conjugate flanks at the contact point.

The angle of projection is obtained by the scalar product between the 2 normal vectors.

$$\mathrm{Req1}\left(y_{\mathrm{p}}, D\right) = \frac{\mathrm{Req}xy\left(y_{\mathrm{p}}, D\right)}{\overrightarrow{\mathrm{NORMAL}\left(y_{\mathrm{p}}, D\right)} \cdot \overrightarrow{\mathrm{Normal}Nxy\left(y_{\mathrm{p}}, D\right)}} \tag{133}$$

EULER's formula on the radius of curvature of a surface is applicable. It gives the curvature C, as a function of the 2 principal curvatures C' and C'' and the angle ζ to direction of the curvature C' and the curvature C. The relation which classifies C' and C'' is: $C'' < C'$.

EULER's formula is: $C = C' \cdot \cos^2(\zeta) + C'' \cdot \sin^2(\zeta)$ (134)

In our case, because the profiles are conjugate we have always $C''=0$ (The contact is linear and the radius of curvature along the line the contact is infinite or the curvature equal to zero).

$$\mathrm{Re}\,q(y_p, D) = \mathrm{Re}\,q1(y_p, D) \cdot \left| \overrightarrow{t_D(y_p, D)} \cdot \overrightarrow{B(y_p, D)} \right|^2 \quad (135)$$

10.10 Calculation of path of contact and zone of contact

The following procedure has to be applied in each offset plane D

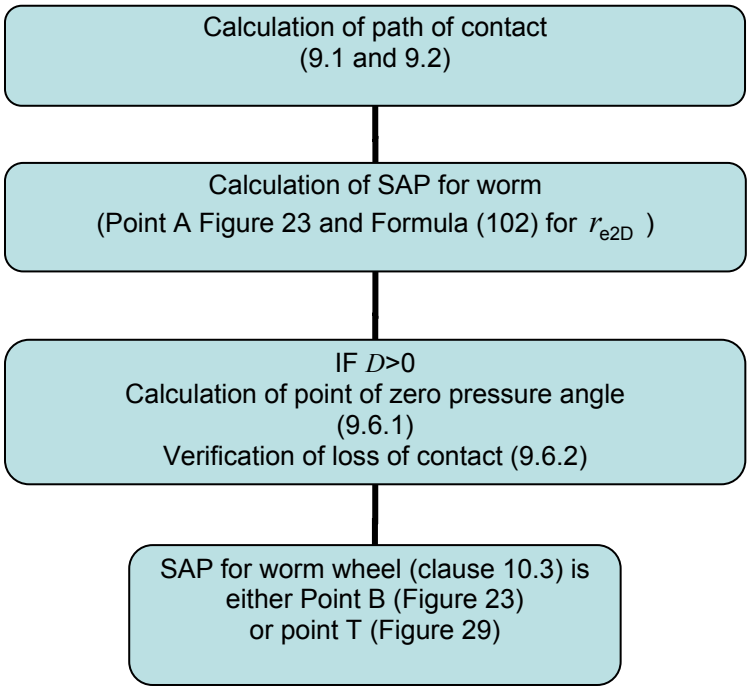

SAP points are the limit of the zone of contact.

For the worm it is possible to determine the minimum diameter for all SAP points (see 10.3).

10.11 Calculation of line of contact

For a given relative position of the worm and the worm wheel it is possible to determine the lines of contact between the flanks of threads and worm wheel teeth.

The relative positions are initialised by the parameter $\Delta x_{Dinit}(D)$ (see 10.4).

For the value $\Delta x_D(D)$ equal to $\Delta x_{Dinit}(D)$ in Formula (89) the contact is just beginning in ONE point of SAP points of worm (See Figure 35). Then the 1st line of contact is obtained for the next thread. This means that $\Delta x_{Dinit}(D)$ has to be increased by a value of axial pitch.

To determine the next line of contact $\Delta x_{\mathrm{Dinit}}(D)$ has to be again increased by a value of axial pitch p_{x1}. This process is carried out until the highest point of contact on a line of contact has reached the border of the zone of contact.

Then it is possible to re-initialise $\Delta x_{\mathrm{D}}(D)$ to $\Delta x_{\mathrm{Dinit}}(D)$, increased by a $0{,}1 \cdot p_{\mathrm{x1}}$ to set up a new relative initial position of the worm and the worm wheel and to restart the process.

In each point of contact the followings value have to be determined:

— tangent vector to the line of contact (see 10.6);

— principal equivalent of radius of curvature (see 10.7);

— Velocities at contact point (see Clause 11)

11 Velocities at contact point

11.1 Velocity of a point of worm

The angular velocity of the worm (*rd/s*) is given by:

$$\omega_{w1} = \pi \cdot \frac{n_1}{30} \tag{136}$$

The angular velocity vector of the worm (*rd/s*) is given by:

$$\overrightarrow{\omega_1} = \begin{pmatrix} \omega_{w1} \\ 0 \\ 0 \end{pmatrix} \tag{137}$$

Velocity of a point of the thread of the worm (in m/s):

$$\overrightarrow{V_1}(y_{\mathrm{p}}, D) = 10^{-3}\,\overrightarrow{\omega_1} \times \overrightarrow{M_1}(y_{\mathrm{p}}, D) \tag{138}$$

Velocity of a point of worm wheel.

The point of the worm wheel flank is given by:

$$\overrightarrow{M_2}(y_{\mathrm{p}}, D) = \begin{pmatrix} x_{1\mathrm{D}}(y_{\mathrm{p}}, D) \\ -\mathrm{a}_w + y_{\mathrm{D}}(y_{\mathrm{p}}, D) \\ D \end{pmatrix} \tag{139}$$

Velocitiy of a point of the tooth flank of the worm wheel (in m/s):

$$\overrightarrow{V_2}(y_{\mathrm{p}}, D) = 10^{-3}\,\overrightarrow{\omega_2} \times \overrightarrow{M_2}(y_{\mathrm{p}}, D) \tag{140}$$

11.2 Relative velocity between 2 conjugate flanks

The relative velocity between the 2 flanks (in m/s) (this is the sliding velocity):

$$\overrightarrow{V_s}\left(y_p, D\right) = \overrightarrow{V_1}\left(y_p, D\right) - \overrightarrow{V_2}\left(y_p, D\right) \tag{141}$$

This relative sliding velocity can be projected in the common tangent plane to the point of contact in 2 directions:

— one normal to the line of contact;

— the second tangent to the line of contact.

$$\overrightarrow{V_{1n}}\left(y_p, D\right) = \overrightarrow{V_1}\left(y_p, D\right) \cdot \vec{B}\left(y_p, D\right) \tag{142}$$

$$\overrightarrow{V_{2n}\left(y_p, D\right)} = \overrightarrow{V_2\left(y_p, D\right)} \cdot \overrightarrow{B\left(y_p, D\right)} \tag{143}$$

It results the projection of these velocities on the common normal at the point of contact are equal.

$$\overrightarrow{V_{Sn}\left(y_p, D\right)} = \overrightarrow{V_{1n}\left(y_p, D\right)} - \overrightarrow{V_{2n}\left(y_p, D\right)} = \overrightarrow{V_S\left(y_p, D\right)} \cdot \overrightarrow{TN1_{cont}\left(y_p, D\right)} \tag{144}$$

11.3 Tangent to the path of contact

The direction of the velocity of points of contact is obtained with the determination of the tangent vector to the path of contact in an offset plane:

$$\mathrm{d}\, y_{ID}\left(y_p, D\right) = \mathrm{d}\, y_{ID}\left(y_p, D\right) \tag{145}$$

$$\mathrm{d}\, x_{ID}\left(y_p, D\right) = \frac{-1}{\tan \alpha_D\left(y_p, D\right)^2} \cdot \left(\mathrm{d}\, y_{ID}\left(y_p, D\right) \cdot \tan \alpha_D\left(y_p, D\right) - y_{ID}\left(y_p, D\right) \cdot \mathrm{d} \tan \alpha_D\left(y_p, D\right)\right) \tag{146}$$

If $\varepsilon_D\left(y_p, D\right)$ is the angle between the direction of pitch line of worm and the tangent to the path of contact, then:

$$\tan \varepsilon_D\left(y_p, D\right) = \frac{\mathrm{d}\, y_{ID}\left(y_p, D\right)}{\mathrm{d}\, x_{ID}\left(y_p, D\right)} \tag{147}$$

$$\mathrm{d}\, xD\, \mathrm{d}\, yD\left(y_p, D\right) = \frac{1}{\tan \varepsilon_D\left(y_p, D\right)} \tag{148}$$

11.4 Velocity of the contact point along the path of contact

Velocity of the contact point along the path of contact in an offset plane:

$$\overrightarrow{V_{cD}\left(y_p, D\right)} = \frac{10^{-3} \cdot \omega_{w1} \cdot p_{z2}}{\tan \alpha_D\left(y_p, D\right) - \mathrm{d}\, xD\, \mathrm{d}\, yD\left(y_p, D\right)} \cdot \begin{pmatrix} \mathrm{d}\, xD\, \mathrm{d}\, yD\left(y_p, D\right) \\ 1 \\ 0 \end{pmatrix} \tag{149}$$

$$V_{cDn}\left(y_p, D\right) = \overrightarrow{V_{cD}\left(y_p, D\right)} \cdot \overrightarrow{B\left(y_p, D\right)} \tag{150}$$

11.5 Velocity at the point of contact

Velocity of the contact point on the worm:

$$\overrightarrow{V_{c1n}(y_p, D)} = \overrightarrow{V_{1n}(y_p, D)} - \overrightarrow{V_{cDn}(y_p, D)} \quad (151)$$

Velocity of the contact point on the worm wheel:

$$\overrightarrow{V_{c2n}(y_p, D)} = \overrightarrow{V_{2n}(y_p, D)} - \overrightarrow{V_{CDn}(y_p, D)} \quad (152)$$

$\overrightarrow{V_{Dn}(y_p, D)}$ is the projection along the normal to the line of contact in the common tangent plane at the contact point

$$V_{SUMn}(y_p, D) = \left| \overrightarrow{V_{c1n}(y_p, D)} + \overrightarrow{V_{c2n}(y_p, D)} \right| \quad (153)$$

Annex A
(informative)

Settings and derivatives of formulae for A, I, N profiles

A.1 Introduction

This annex contains the detailed for formula of profile in the axial plane of the worm ox X-Y plane according to the conventions of Figure 5.

A.2 Formulae of the profile in the X-Y plane for type A worms

See Figures 6 to 7 and A.1 for the setting of type A worms, where:

α_{0t} is the tool transverse pressure angle for A and I profiles;

α_{0n} is the tool normal pressure angle (see Formula (19));

γ_{m1} is the reference lead angle of worm.

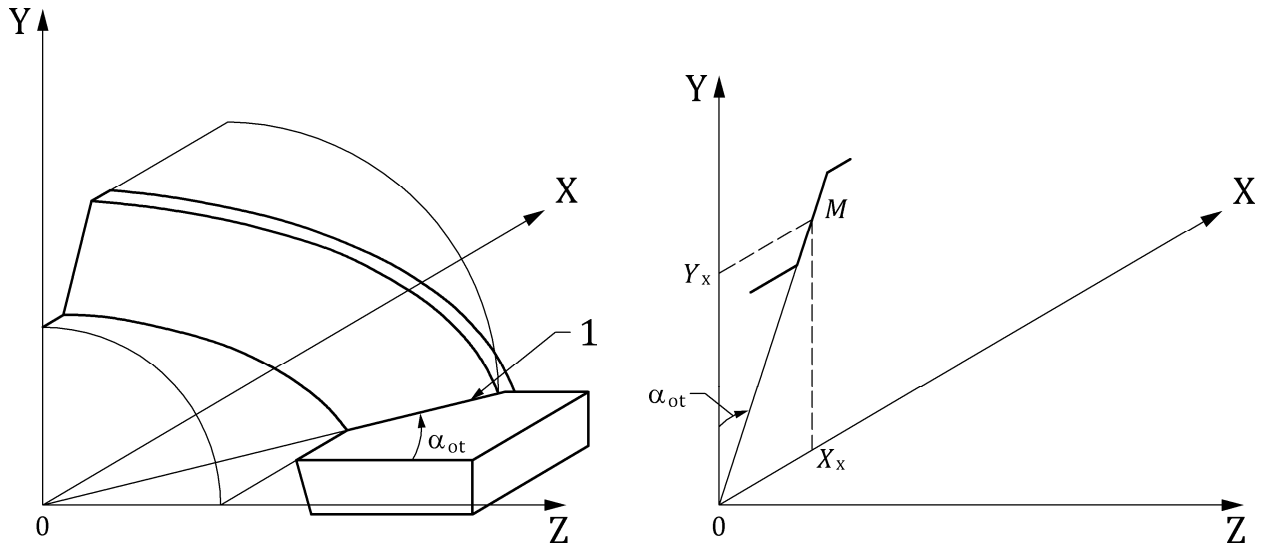

Key

1 generatrix

Figure A.1 — Generation of Type A profile

For a point (x_x, y_x) at a distance y_x from the worm axis:

$$x_x = y_x \cdot \tan(\alpha_{0t}) = y_x \cdot \tan(\alpha_{0n}) / \cos(\gamma_{m1}) \quad \text{(A.1)}$$

and

$$\alpha_x = \alpha_{0t} \tag{A.2}$$

A.3 Formulae of the profile in the X-Y plane for type I worms

See Figures 9 to 11 for the setting of type I worms, where

p_{z1} is the lead;

r_{b1} is the base radius of involute profile; (see Formula (22));

γ_{b1} is the base lead angle of worm thread; (see Formula (21)).

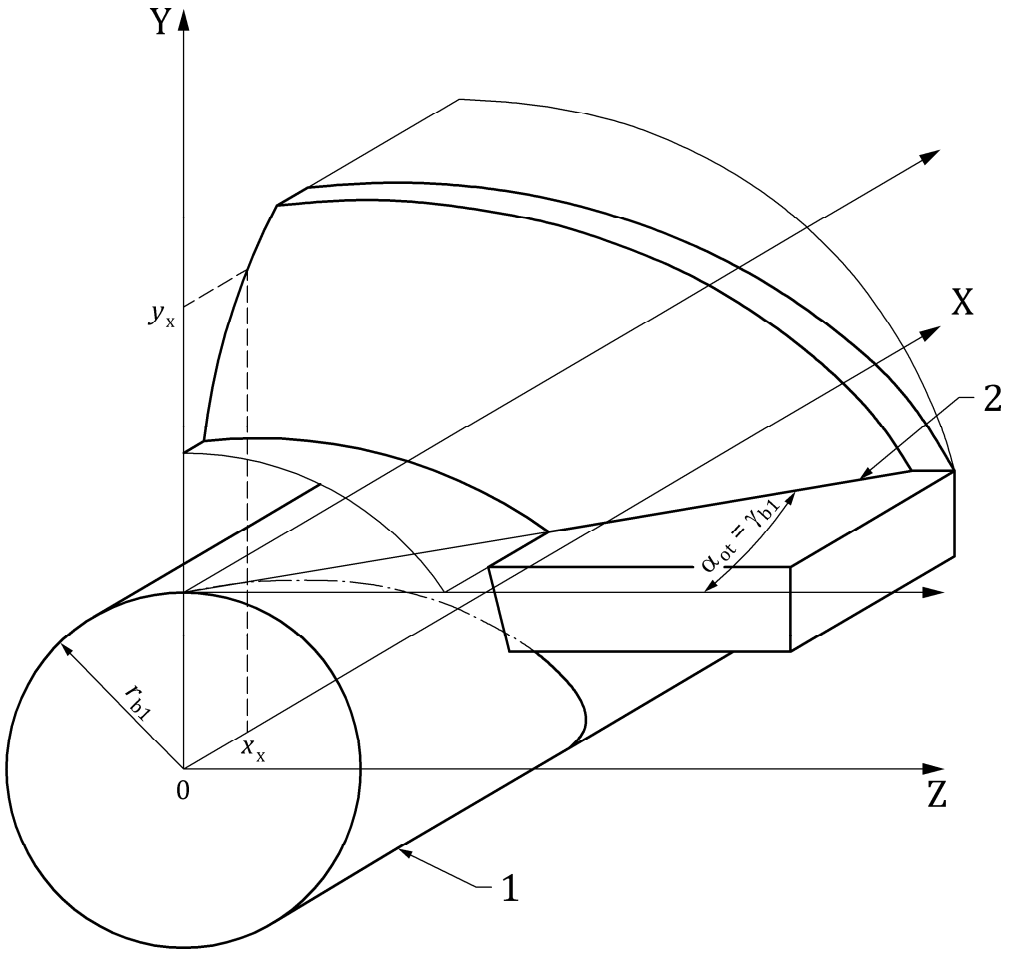

Key

1 base cylinder
2 generatrix

Figure A.2 — Generation of Type I profile

For a point (x_x, y_x) at a distance y_x from the worm axis:

$$x_x = -p_{zu1}\ \arctan\frac{\sqrt{y_x^2 - r_{b1}^2}}{r_{b1}} + \sqrt{y_x^2 - r_{b1}^2}.\tan(\gamma_{b1}) \tag{A.3}$$

$$\tan(\alpha_x) = \frac{\sqrt{y_x^2 - r_{b1}^2}}{r_{b1}} \cdot \frac{p_{zu1}}{y_x} \tag{A.4}$$

A.4 Formulae of the profiles in the X-Y plane for type N worms

See Figures 12 and 13 for the setting of type N worms, where

p_{x1} is the axial pitch;

p_{z1} is the lead (of worm);

r'_{b1} is the base radius of a notional base circle;

γ'_{b1} is the base lead angle of the notional base helix;

A is the distance from the worm axis to virtual point of the cutter (OO_1 on Figure A.4) (see ref.[1]);

γ_{m1} is the reference lead angle of worm;

α_{0n} is the normal pressure angle;

d_{m1} is the worm reference diameter.

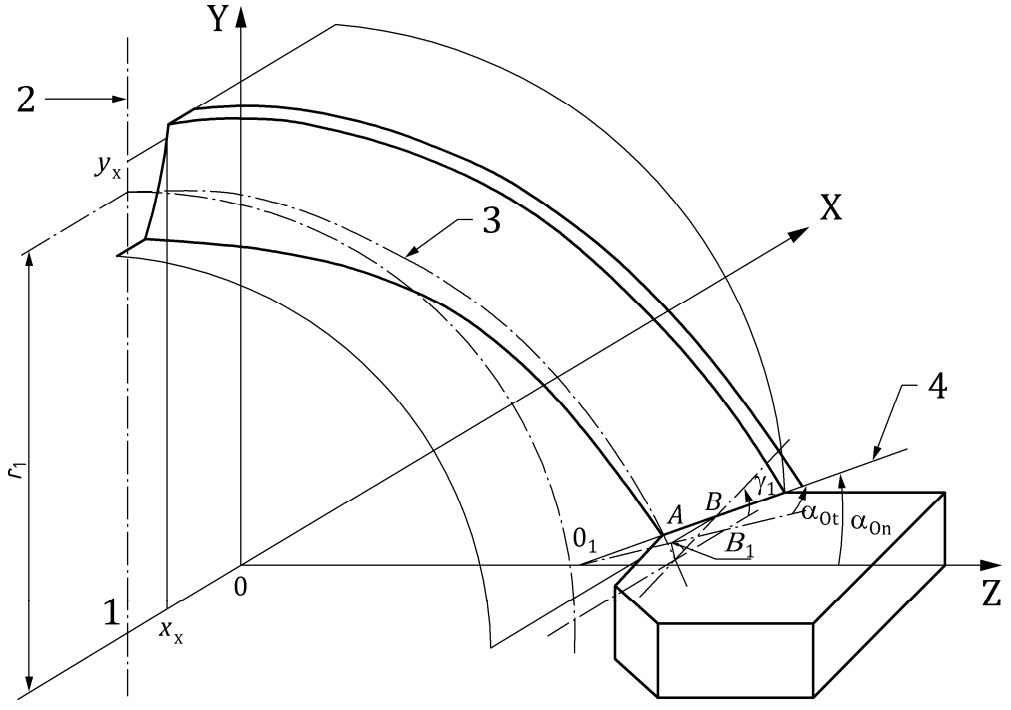

Key

1 axis of worm
2 axis of symmetry of the tooth space
3 reference helix
4 generatrix

Figure A.3 — Generation of Type N profile

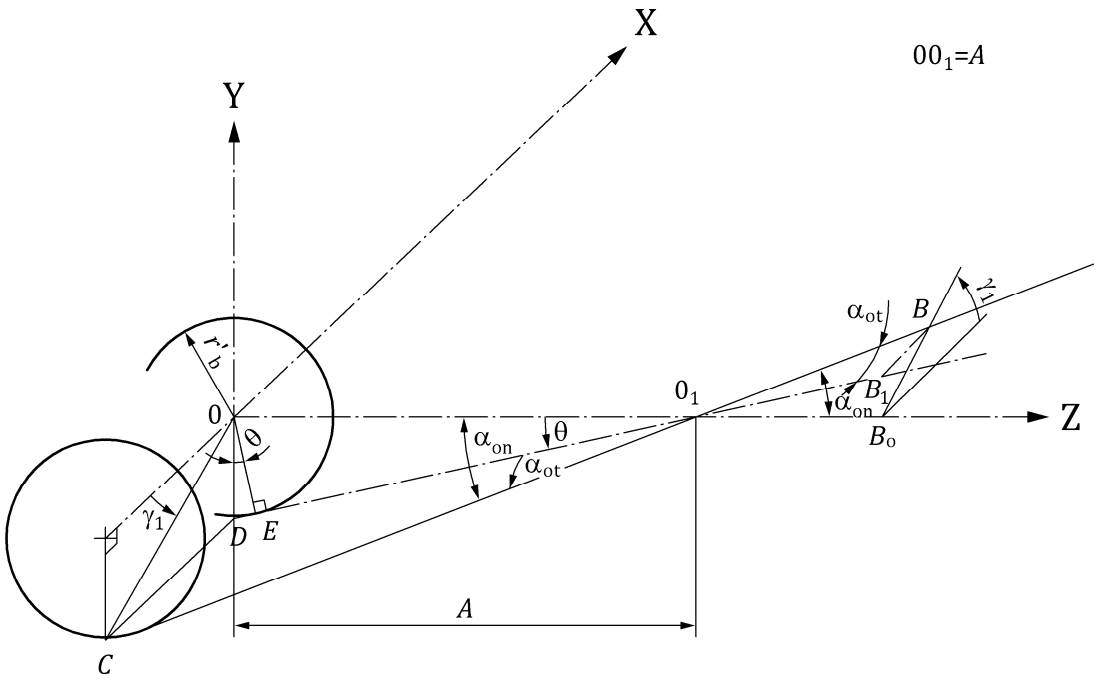

Figure A.4 — Profile N: Convention for formulae

For a point (x_X, y_X) at radial distance y_X from the worm axis:

$$x_X = p_{zu1} \cdot \left\{ \arctan\left(\frac{\sqrt{y_X^2 - r'^2_{b1}}}{r'_{b1}} \right) - \theta \right\} + \sqrt{y_X^2 - r'^2_{b1}} \cdot \tan(\gamma'_{b1}) \qquad \text{(A.5)}$$

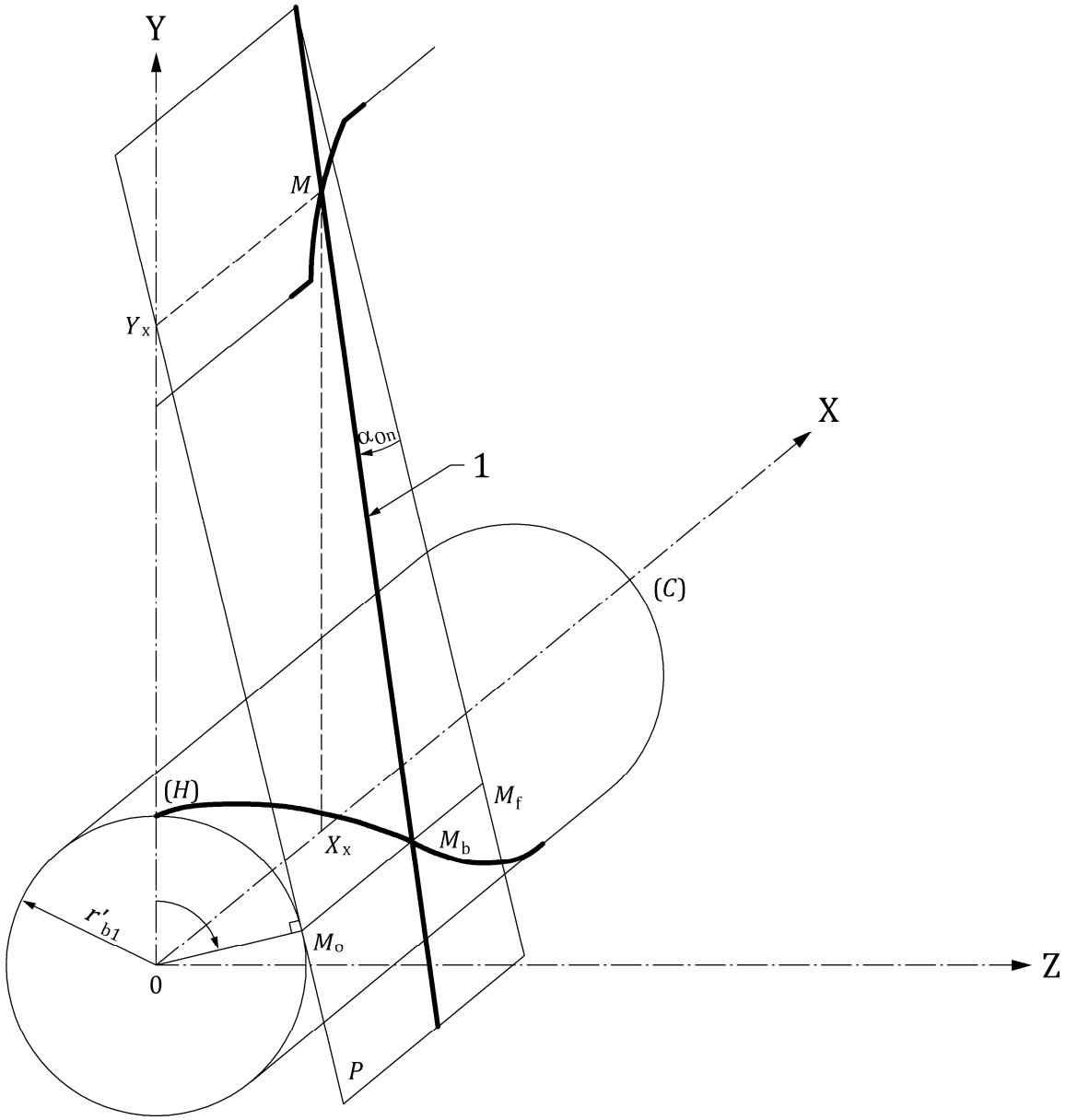

Key

1 generatrix

Figure A.5 — Profile N: Generatrix with pseudo base radius

With:

$$\theta = \arctan\left(\frac{\sqrt{A - r'^2_{b1}}}{r'_{b1}}\right) \tag{A.6}$$

$$\tan(\alpha_x) = \frac{p_{z1} \cdot r'_{b1} + 2 \cdot \pi \cdot y_x \cdot \tan(\gamma'_{b1})}{2 \cdot \pi \cdot y_x \sqrt{y_x^2 - r_{x1}^2}} \tag{A.7}$$

Where:

$$\tan(\gamma'_b) = \frac{r'_{b1}}{A \cdot \tan(\gamma_{m1})} \tag{A.8}$$

$$r'_{b1} = \frac{A \cdot \sin(\gamma_{m1}) \cdot \tan(\alpha_{0n})}{\sqrt{1 - (\sin(\gamma_{m1}) \cdot \tan(\alpha_{0n}))^2}} \tag{A.9}$$

$$A = \frac{1}{2} \cdot \left(d_1 - p_{z1} \cdot \frac{\cos(\gamma_{m1})}{2 \cdot \tan(\alpha_{0n})} \right) \tag{A.10}$$

A.5 Second derivative of axial profile formula

$$d2x_x(y_p) = \left[-a_1 \cdot a_2 \cdot \left[2 - \left(\frac{a_2}{y_p} \right)^2 \right] - a_3 \cdot {a_2}^2 \right] \cdot \frac{1}{\left({y_p}^2 - {a_2}^2 \right)^{\frac{3}{2}}} \tag{A.11}$$

$$d2y_x(y_p) = 0 \tag{A.12}$$

Annex B
(informative)

Settings and derivatives of formulae for K and C profiles

B.1 Formulae for K profile

Where

C	is the cutter spindle/worm centre distance;
γ_{m1}	is the reference lead angle of worm;
p_{z1}	is the lead;
$(y_G, x_G(y_G))$	are the coordinates of a point on the tool flank when the origin is at the point of intersection of the tool axis and the tool median plane, with the x-axis as the tool spindle axis and the abscissa on the trace of the median plane;
d_{m1}	worm reference diameter;
p_{x1}	axial pitch;
α_{0n}	normal pressure angle of the tool.

Formulae of the profile of a bi-conical grinding wheel (Figure 16)

Like type I profile, profile K is convex in axial planes.

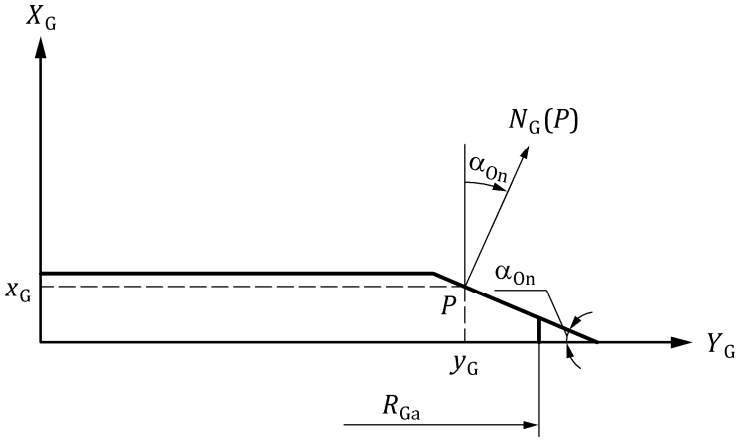

Figure B.1 — Profile K - Grinding wheel profile

One of the advantages of this type is that the two flanks of a thread space can be machined simultaneously.

A disadvantage is that the form of the thread flanks varies with tool diameter, so the reproductibility is approximated.

NOTE 1 The smaller the diameter of the tool, the more nearly the normal profiles of the thread spaces approach those of type N worms and the larger the tool diameter the more nearly the forms of the thread flanks approach those of type I worms.

NOTE 2 It is possible to machine type K worms with conical milling cutter. The flank surfaces have facets resulting of the cutting discontinuity caused by cutting tooth pitch.

$$x_{\mathrm{w}}(y_{\mathrm{G}}) = x_{\mathrm{ms}} - \tan(\alpha_{0\mathrm{n}}) \cdot (y_{\mathrm{G}} - R_{\mathrm{Ga}}) \tag{B.1}$$

$$\alpha_{\mathrm{G}}(y_{\mathrm{G}}) = \alpha_{0\mathrm{n}} \tag{B.2}$$

With:

y_{G} is the radius of grinding wheel which generates the point on the worm.

R_{p} is the radius of the circle of intersection of both conical surfaces of the grinding wheel flanks.

$$a_0 = R_{\mathrm{Ga}} + \frac{d_{\mathrm{f1}}}{2} \tag{B.3}$$

$$R_{\mathrm{w}} = a_0 - \frac{d_{\mathrm{m1}}}{2} \tag{B.4}$$

$$x_{\mathrm{ms}} = \frac{(\pi \cdot m_{\mathrm{x1}} - s_{\mathrm{x1}}) \cdot \cos(\gamma_{\mathrm{m1}})}{2} \tag{B.5}$$

B.2 Alternatives formulae for C profiles

Formulae enabling determination of the axial sections of worms

With the basic data of the tool indicated in Figure 17, the parameters y_{G}, x_{G} and α_{G} may be derived for any point G of the tool profile.

On the basis of these three parameters and with the formulae provided below, the coordinates x, r, of an axial profile and the angle α of the tangent may be determined for any point P of the profile of a worm.

Symbols:

a_0	is the worm/tool centre distance (length of the common perpendicular to the worm/tool axes);
p_{z1}	is the lead (of worm);
γ_{m1}	is the lead angle of worm;
$y_{\mathrm{Gm}} = R_{\mathrm{Gm}}$, x_{Gm}, $\alpha_{\mathrm{Gm}} = \alpha_{0\mathrm{n}}$	see Figure B.2;

Formula of the profile of the grinding wheel

$$\alpha_{\mathrm{G}}(y_{\mathrm{G}}) = \arcsin\left(\sin(\alpha_{0n}) - \frac{R_{\mathrm{Gm}} - y_{\mathrm{G}}}{\rho_{\mathrm{Gm}}}\right) \tag{B.6}$$

$$x_{\mathrm{G}}(y_{\mathrm{G}}) = x_{\mathrm{Gm}} + \rho_{\mathrm{Gm}} \cdot (\cos(\alpha_{\mathrm{G}}(y_{\mathrm{G}})) - \cos(\alpha_{0\mathrm{n}})) \tag{B.7}$$

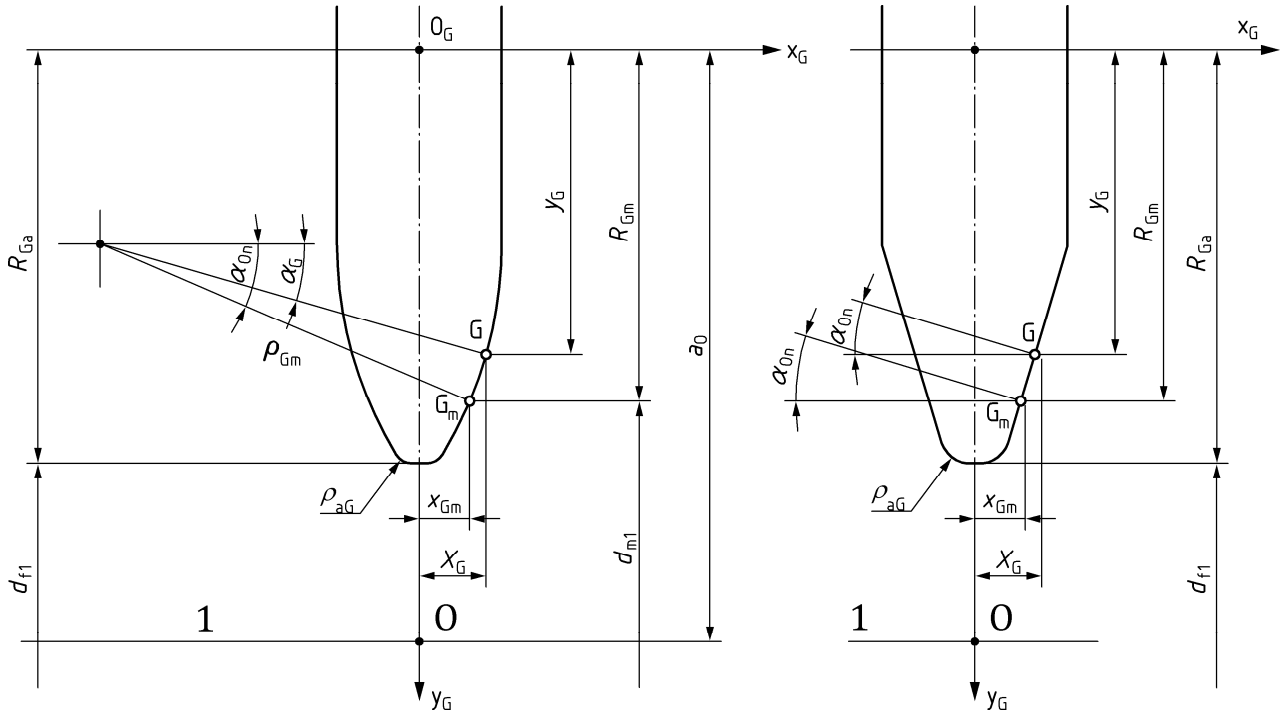

Key

1 axis of the grinding wheel

Figure B.2 — Profile C - Axial section of the tool

$$y_G(y_G) = y_G \tag{B.8}$$

With:

$$x_{Gm} = \frac{(\pi \cdot m_{x1} - s_{mx1}) \cdot \cos(\gamma_{m1})}{2} \tag{B.9}$$

$$a_0 = R_{Ga} + \frac{d_{f1}}{2} \tag{B.10}$$

$$R_{Gm} = a_0 - \frac{d_{m1}}{2} \tag{B.11}$$

B.3 Derivatives for K profile

B.3.1 First derivative of K profile formula

$$\mathrm{d}\alpha_G(y_G) = 0 \tag{B.12}$$

$$\mathrm{d}x_G(y_G) = -\tan(\alpha_{0n}) \tag{B.13}$$

B.3.2 Second derivative of K profile formula

$$\mathrm{d}2\alpha_{\mathrm{G}}(y_{\mathrm{G}}) = 0 \tag{B.14}$$

$$\mathrm{d}2x_{\mathrm{G}}(y_{\mathrm{G}}) = 0 \tag{B.15}$$

B.3.3 Third derivative of K profile formula

$$\mathrm{d}3\alpha_{\mathrm{G}}(y_{\mathrm{G}}) = 0 \tag{B.16}$$

$$\mathrm{d}3x_{\mathrm{G}}(y_{\mathrm{G}}) = 0 \tag{B.17}$$

B.4 Derivatives for C profile

B.4.1 First derivative of C profile formula

$$\mathrm{d}\alpha_{\mathrm{G}}(y_{\mathrm{G}}) = \frac{1}{\rho_{\mathrm{Gm}} \cdot \left[1 - \left(\sin(\alpha_{0\mathrm{n}}) - \frac{R_{\mathrm{Gm}} - y_{\mathrm{G}}}{\rho_{\mathrm{Gm}}}\right)^2\right]^{\frac{1}{2}}} \tag{B.18}$$

$$\mathrm{d}x_{\mathrm{G}}(y_{\mathrm{G}}) = -\rho_{\mathrm{Gm}} \cdot \sin(\alpha_{\mathrm{G}}(y_{\mathrm{G}})) \cdot \mathrm{d}\alpha_{\mathrm{G}}(y_{\mathrm{G}}) \tag{B.19}$$

B.4.2 Second derivative of C profile formula

$$\mathrm{d}2\alpha_{\mathrm{G}}(y_{\mathrm{G}}) = \frac{1}{{\rho_{\mathrm{Gm}}}^2 \cdot \left[1 - \left(\sin(\alpha_{0\mathrm{n}}) - \frac{R_{\mathrm{Gm}} - y_{\mathrm{G}}}{\rho_{\mathrm{Gm}}}\right)^2\right]^{\frac{3}{2}}} \cdot \left(\sin(\alpha_{0\mathrm{n}}) - \frac{R_{\mathrm{Gm}} - y_{\mathrm{G}}}{\rho_{\mathrm{Gm}}}\right) \tag{B.20}$$

$$\mathrm{d}2x_{\mathrm{G}}(y_{\mathrm{G}}) = \rho_{\mathrm{Gm}} \cdot \cos(\alpha_{\mathrm{G}}(y_{\mathrm{G}})) \cdot \mathrm{d}\alpha_{\mathrm{G}}(y_{\mathrm{G}})^2 - \rho_{\mathrm{Gm}} \cdot \sin(\alpha_{\mathrm{G}}(y_{\mathrm{G}})) \cdot \mathrm{d}2\alpha_{\mathrm{G}}(y_{\mathrm{G}}) \tag{B.21}$$

B.4.3 Third derivative of C profile formula

$$\mathrm{d}3\alpha_{\mathrm{G}}(y_{\mathrm{G}}) = \frac{3}{{\rho_{\mathrm{Gm}}}^3 \cdot \left[1 - \left(\sin(\alpha_{0\mathrm{n}}) - \frac{R_{\mathrm{Gm}} - y_{\mathrm{G}}}{\rho_{\mathrm{Gm}}}\right)^2\right]^{\frac{5}{2}}} \cdot \left(\sin(\alpha_{0\mathrm{n}}) - \frac{R_{\mathrm{Gm}} - y_{\mathrm{G}}}{\rho_{\mathrm{Gm}}}\right)^2 + \frac{1}{{\rho_{\mathrm{Gm}}}^3 \cdot \left[1 - \left(\sin(\alpha_{0\mathrm{n}}) - \frac{R_{\mathrm{Gm}} - y_{\mathrm{G}}}{\rho_{\mathrm{Gm}}}\right)^2\right]^{\frac{3}{2}}} \tag{B.22}$$

$$\begin{aligned} \mathrm{d}3x_{\mathrm{G}}(y_{\mathrm{G}}) = {} & \rho_{\mathrm{Gm}} \cdot \sin(\alpha_{\mathrm{G}}(y_{\mathrm{G}})) \cdot \mathrm{d}\alpha_{\mathrm{G}}(y_{\mathrm{G}})^3 \\ & -3\rho_{\mathrm{Gm}} \cdot \cos(\alpha_{\mathrm{G}}(y_{\mathrm{G}})) \cdot \mathrm{d}\alpha_{\mathrm{G}}(y_{\mathrm{G}}) \cdot \mathrm{d}2\alpha_{\mathrm{G}}(y_{\mathrm{G}}) \\ & -\rho_{\mathrm{Gm}} \cdot \sin(\alpha_{\mathrm{G}}(y_{\mathrm{G}})) \cdot \mathrm{d}3\alpha_{\mathrm{G}}(y_{\mathrm{G}}) \end{aligned} \tag{B.23}$$

B.5 Second derivative for K/C profile for $c2(y_{\mathrm{G}})$ et $c3(y_{\mathrm{G}})$

$$\mathrm{d}2c2(y_{\mathrm{G}}) = \left(\mathrm{d}2x_{\mathrm{G}}(y_{\mathrm{G}}) - \frac{2 \cdot \mathrm{d}2x_{\mathrm{G}}(y_{\mathrm{G}})}{\mathrm{d}x_{\mathrm{G}}(y_{\mathrm{G}})^2} + \frac{2 \cdot y_{\mathrm{G}}}{\mathrm{d}x_{\mathrm{G}}(y_{\mathrm{G}})^3} \cdot \mathrm{d}2x_{\mathrm{G}}(y_{\mathrm{G}})^2 - \frac{y_{\mathrm{G}}}{\mathrm{d}x_{\mathrm{G}}(y_{\mathrm{G}})^2} \cdot \mathrm{d}3x_{\mathrm{G}}(y_{\mathrm{G}}) \right) \cdot \sin(\gamma_{m1}) \tag{B.24}$$

$$\begin{aligned} \mathrm{d}2c3(y_{\mathrm{G}}) = {} & 2\left(\frac{a_0 \cdot \sin(\gamma_{\mathrm{m1}}) - p_{\mathrm{zu1}} \cdot \cos(\gamma_{\mathrm{m1}})}{\mathrm{d}x_{\mathrm{G}}(y_{\mathrm{G}})^3} \cdot \mathrm{d}2x_{\mathrm{G}}(y_{\mathrm{G}})^2 \right) \\ & - \frac{a_0 \cdot \sin(\gamma_{\mathrm{m1}}) - p_{\mathrm{zu1}} \cdot \cos(\gamma_{\mathrm{m1}})}{\mathrm{d}x_{\mathrm{G}}(y_{\mathrm{G}})^2} \cdot \mathrm{d}3x_{\mathrm{G}}(y_{\mathrm{G}}) \end{aligned} \tag{B.25}$$

B.6 Second derivative for K/C profile for $\varepsilon_{\mathrm{G}}(y_{\mathrm{G}})$

B.6.1 First derivation of the 1st term of $\mathrm{d}\varepsilon_{\mathrm{G}}(y_{\mathrm{G}})$

(See 6.7.2.1 and 6.7.2.3.2 for $\varepsilon_{\mathrm{w}}(y_{\mathrm{G}})$ and $\mathrm{d}\varepsilon_{\mathrm{w}}(y_{\mathrm{G}})$

$$\mathrm{d}A\varepsilon_{\mathrm{G}}(y_{\mathrm{G}}) = \frac{\mathrm{d}2c_3(y_{\mathrm{G}})}{\left(c_1{}^2 + c_2(y_{\mathrm{G}})^2 - c_3(y_{\mathrm{G}})^2\right)^{\frac{1}{2}}} - \frac{\mathrm{d}c_3(y_{\mathrm{G}}) \cdot (c_2(y_{\mathrm{G}}) \cdot \mathrm{d}c_2(y_{\mathrm{G}}) - c_3(y_{\mathrm{G}}) \cdot \mathrm{d}c_3(y_{\mathrm{G}}))}{\left(c_1{}^2 + c_2(y_{\mathrm{G}})^2 - c_3(y_{\mathrm{G}})^2\right)^{\frac{3}{2}}} \tag{B.26}$$

B.6.2 First derivation of the numerator of the 2nd term of $\mathrm{d}\varepsilon_{\mathrm{G}}(y_{\mathrm{G}})$

$$BN\varepsilon_{\mathrm{G}}(y_{\mathrm{G}}) = -c_3(y_{\mathrm{G}}) \cdot c_2(y_{\mathrm{G}}) \cdot \mathrm{d}c_2(y_{\mathrm{G}}) \tag{B.27}$$

and

$$\mathrm{d}BN\varepsilon_{\mathrm{G}}(y_{\mathrm{G}}) = -\mathrm{d}c_3(y_{\mathrm{G}}) \cdot c_2(y_{\mathrm{G}}) \cdot \mathrm{d}c_2(y_{\mathrm{G}}) - c_3(y_{\mathrm{G}}) \cdot \mathrm{d}c_2(y_{\mathrm{G}})^2 - c_3(y_{\mathrm{G}}) \cdot c_2(y_{\mathrm{G}}) \cdot \mathrm{d}2c_2(y_{\mathrm{G}}) \tag{B.28}$$

B.6.3 First derivation of the 3rd term of $\mathrm{d}\varepsilon_{\mathrm{G}}(y_{\mathrm{G}})$

$$\mathrm{d}C\varepsilon_{\mathrm{G}}(y_{\mathrm{G}}) = \left(-\mathrm{d}2c_2(y_{\mathrm{G}}) + \frac{2\,\mathrm{d}c_2(y_{\mathrm{G}})^2 \cdot c_2(y_{\mathrm{G}})}{c_1{}^2 + c_2(y_{\mathrm{G}})^2} \right) \cdot \frac{c_1}{c_1{}^2 + c_2(y_{\mathrm{G}})^2} \tag{B.29}$$

B.6.4 First derivation of the denominator of the 2nd term of $\mathrm{d}\varepsilon_{\mathrm{G}}(y_{\mathrm{G}})$

$$BD\varepsilon_{\mathrm{G}}(y_{\mathrm{G}}) = \left(c_1{}^2 + c_2(y_{\mathrm{G}})^2\right) \cdot \left(c_1{}^2 + c_2(y_{\mathrm{G}})^2 - c_3(y_{\mathrm{G}})^2\right)^{\frac{1}{2}} \tag{B.30}$$

$$\begin{aligned} \mathrm{d}BD\varepsilon_{\mathrm{G}}(y_{\mathrm{G}}) & 2c_2(y_{\mathrm{G}}) \cdot \mathrm{d}c_2(y_{\mathrm{G}}) \cdot \left(c_1{}^2 + c_2(y_{\mathrm{G}})^2 - c_3(y_{\mathrm{G}})^2\right)^{\frac{1}{2}} + \\ & \left(c_1{}^2 + c_2(y_{\mathrm{G}})^2\right) \cdot \left(c_1{}^2 + c_2(y_{\mathrm{G}})^2 - c_3(y_{\mathrm{G}})^2\right)^{\frac{-1}{2}} \cdot (c_2(y_{\mathrm{G}}) \cdot \mathrm{d}c_2(y_{\mathrm{G}}) - c_3(y_{\mathrm{G}}) \cdot \mathrm{d}c_3(y_{\mathrm{G}})) \end{aligned} \tag{B.31}$$

$$\mathrm{d}\,BD\varepsilon_{\mathrm{G}}(y_{\mathrm{G}}) = \frac{\mathrm{d}\,BN\varepsilon_{\mathrm{G}}(y_{\mathrm{G}}) \cdot BD\varepsilon_{\mathrm{G}}(y_{\mathrm{G}}) - \mathrm{d}\,BD\varepsilon_{\mathrm{G}}(y_{\mathrm{G}}) \cdot BN\varepsilon_{\mathrm{G}}(y_{\mathrm{G}})}{BD\varepsilon_{\mathrm{G}}(y_{\mathrm{G}})^2} \tag{B.32}$$

B.6.5 Second derivative for K/C profile for $\varepsilon_{\mathrm{G}}(y_{\mathrm{G}})$

$$\mathrm{d}2\varepsilon_{\mathrm{G}}(y_{\mathrm{G}}) = \mathrm{d}\,A\varepsilon_{\mathrm{G}}(y_{\mathrm{G}}) + \mathrm{d}\,BD\varepsilon_{\mathrm{G}}(y_{\mathrm{G}}) + \mathrm{d}\,C\varepsilon_{\mathrm{G}}(y_{\mathrm{G}}) \tag{B.33}$$

B.7 Second derivative of point generated by the grinding wheel

$$\begin{aligned}\mathrm{d}2xc_{\mathrm{uw}}(y_{\mathrm{G}}) = {} & \mathrm{d}\,2xc_{\mathrm{G}}(y_{\mathrm{G}}) \cdot \cos(\gamma_{\mathrm{m1}}) - \\ & (2\cos(\varepsilon_{\mathrm{w}}(y_{\mathrm{G}})) \cdot d\varepsilon_{\mathrm{w}}(y_{\mathrm{G}}) - y_{\mathrm{G}} \cdot \sin(\varepsilon_{\mathrm{w}}(y_{\mathrm{G}})) \cdot \mathrm{d}\,\varepsilon_{\mathrm{w}}(y_{\mathrm{G}})^2 + \\ & y_{\mathrm{G}} \cdot \cos(\varepsilon_{\mathrm{w}}(y_{\mathrm{G}})) \cdot \mathrm{d}\,2\varepsilon_{\mathrm{w}}(y_{\mathrm{G}})) \cdot \sin(\gamma_{\mathrm{m1}})\end{aligned} \tag{B.34}$$

$$\begin{aligned}\mathrm{d}2yc_{\mathrm{uw}}(y_{\mathrm{G}}) = {} & 2\sin(\varepsilon_{\mathrm{w}}(y_{\mathrm{G}})) \cdot \mathrm{d}\,\varepsilon_{\mathrm{w}}(y_{\mathrm{G}}) + \\ & y_{\mathrm{G}} \cdot \cos(\varepsilon_{\mathrm{w}}(y_{\mathrm{G}})) \cdot \mathrm{d}\,\varepsilon_{\mathrm{w}}(y_{\mathrm{G}})^2 + y_{\mathrm{G}} \cdot \sin(\varepsilon_{\mathrm{w}}(y_{\mathrm{G}})) \cdot \mathrm{d}\,2\varepsilon_{\mathrm{w}}(y_{\mathrm{G}}))\end{aligned} \tag{B.35}$$

$$\begin{aligned}\mathrm{d}2zc_{\mathrm{uw}}(y_{\mathrm{G}}) = {} & -\mathrm{d}\,2x_{\mathrm{G}}(y_{\mathrm{G}}) \cdot \sin(\gamma_{\mathrm{m1}}) - \\ & \left(2\cos(\varepsilon_{\mathrm{w}}(y_{\mathrm{G}})) \cdot \mathrm{d}\,\varepsilon_{\mathrm{w}}(y_{\mathrm{G}}) - y_{\mathrm{G}} \cdot \sin\left(\varepsilon_{\mathrm{w}}(y_{\mathrm{G}})\right) \cdot \mathrm{d}\,\varepsilon_{\mathrm{w}}(y_{\mathrm{G}})^2 + y_{\mathrm{G}} \cdot \cos(\varepsilon_{\mathrm{w}}(y_{\mathrm{G}})) \cdot \mathrm{d}\,2\varepsilon_{\mathrm{w}}(y_{\mathrm{G}})\right) \cdot \cos(\gamma_{\mathrm{m1}})\end{aligned} \tag{B.36}$$

B.8 Second derivative of point generated by the grinding wheel projected in the axial plane of worm

$$\begin{aligned}\mathrm{d}2\phi_{\mathrm{x}}(y_{\mathrm{G}}) = {} & \frac{\mathrm{d}\,2zc_{\mathrm{uw}}(y_{\mathrm{G}}) \cdot yc_{\mathrm{uw}}(y_{\mathrm{G}}) - zc_{\mathrm{uw}}(y_{\mathrm{G}}) \cdot \mathrm{d}\,2yc_{\mathrm{uw}}(y_{\mathrm{G}})}{yc_{\mathrm{uw}}(y_{\mathrm{G}})^2 + zc_{\mathrm{uw}}(y_{\mathrm{G}})^2} - \\ & 2(\mathrm{d}\,zc_{\mathrm{uw}}(y_{\mathrm{G}}) \cdot yc_{\mathrm{uw}}(y_{\mathrm{G}}) - zc_{\mathrm{uw}}(y_{\mathrm{G}}) \cdot \mathrm{d}\,yc_{\mathrm{uw}}(y_{\mathrm{G}})) \cdot \frac{yc_{\mathrm{uw}}(y_{\mathrm{G}}) \cdot \mathrm{d}\,yc_{\mathrm{uw}}\,yc_{\mathrm{uw}}(y_{\mathrm{G}}) + zc_{\mathrm{uw}}\,yc_{\mathrm{uw}}(y_{\mathrm{G}}) \cdot \mathrm{d}\,zc_{\mathrm{uw}}}{\left(yc_{\mathrm{uw}}(y_{\mathrm{G}})^2 + zc_{\mathrm{uw}}(y_{\mathrm{G}})^2\right)^2}\end{aligned} \tag{B.37}$$

$$\mathrm{d}\,2x_{\mathrm{x}}(y_{\mathrm{G}}) = \mathrm{d}\,2xc_{\mathrm{uw}}(y_{\mathrm{G}}) - p_{\mathrm{zu1}} \cdot \mathrm{d}\,2\phi_{\mathrm{x}}(y_{\mathrm{G}}) \tag{B.38}$$

$$\begin{aligned}d2y_x(y_{\mathrm{G}}) = {} & \frac{d2yc_{uw}(y_{\mathrm{G}})}{\cos(\phi_x(y_{\mathrm{G}}))} + \frac{2d2yc_{uw}(y_{\mathrm{G}})}{\cos(\phi_x(y_{\mathrm{G}}))^2} \cdot \sin(\phi_x(y_{\mathrm{G}})) \cdot d\phi_x(y_{\mathrm{G}}) + \\ & \left(\frac{2 \cdot \sin(\phi_x(y_{\mathrm{G}}))^2}{\cos(\phi_x(y_{\mathrm{G}}))^3} + \frac{1}{\cos(\phi_x(y_{\mathrm{G}}))}\right) \cdot yc_{uw}(y_{\mathrm{G}}) \cdot d\phi_x(y_{\mathrm{G}})^2 + \\ & \frac{yc_{uw}(y_{\mathrm{G}})}{\cos(\phi_x(y_{\mathrm{G}}))^2} \cdot \sin(\phi_x(y_{\mathrm{G}})) \cdot d2\phi_x(y_{\mathrm{G}})\end{aligned} \tag{B.39}$$

$$d\tan\alpha_c(y_{\mathrm{G}}) = \frac{d2x_x(y_{\mathrm{G}})}{dy_x(y_{\mathrm{G}})} - \frac{dx_x(y_{\mathrm{G}}) \cdot d2y_x(y_{\mathrm{G}})}{dy_x(y_{\mathrm{G}})^2} \tag{B.40}$$

Annex C
(informative)

Algorithm to determine the point of generations of worm and worm wheel

C.1 Algorithm to determine the point of the grinding wheel which generates a point of the axial profile

For C and K Profiles the algorithm to determine the radius grinding wheel which generates a point of the axial profile of the worm is the following:

$$
\begin{aligned}
R\text{grind}(R_G, m_{\text{xf1}}, r_{\text{worm}}) = \Big| \; & y\text{min} \leftarrow 0{,}2 \cdot R_{\text{G}} \\
& y\text{max} \leftarrow R_{\text{G}} + r_{\text{worm}} - m_{\text{x1}} \\
& \text{DO while } \left| y_{\text{x}}\left[0{,}5\left(y\,\text{min} + y\,\text{max}\right)\right] - r_{\text{worm}} \right| > 0{,}0000001 \\
& \quad \Big| \; y\text{min} \leftarrow 0{,}5 \cdot \left(y\text{min} + y\text{max}\right) \text{ if } \left[y_{\text{x}}\left[0{,}5\left(y\,\text{min} + y\,\text{max}\right)\right] - r_{\text{worm}}\right] > 0{,}0 \\
& \quad \Big| \; y\text{max} \leftarrow 0{,}5 \cdot \left(y\text{min} + y\text{max}\right) \text{ if } \left[y_{\text{x}}\left[0{,}5\left(y\,\text{min} + y\,\text{max}\right)\right] - r_{\text{worm}}\right] < 0{,}0 \\
& \quad \Big| \; R\text{grind} \leftarrow 0{,}5 \cdot \left(y\text{min} + y\text{max}\right) \\
& \text{END DO} \\
& \text{return } R\text{grind}
\end{aligned}
\tag{C.1}
$$

C.2 Algorithm to determine the point of generation of a worm wheel

For A, I, N Profiles the algorithm to determine the radius Rworm of the axial plane which generates a conjugate profile on the circle radius r_{Wheel} of the worm wheel is the following:

$$
\begin{aligned}
R\text{worm}\left(D, r_{\text{f1}}, r_{\text{a1}}, r_{\text{Wheel}}\right) = \Big| \; & y\text{min} \leftarrow r_{\text{f1}} \\
& y\text{max} \leftarrow r_{\text{a1}} \\
& \text{DO while } \left| r_{\text{M2D}}\left[0{,}5 \cdot \left(y\text{min} + y\text{max}\right), D\right] - r_{\text{Wheel}} \right| > 0{,}0000001 \\
& \quad \Big| \; y\text{min} \leftarrow 0{,}5 \cdot \left(y\text{min} + y\text{max}\right) \text{if } \left[r_{\text{M2D}}\left[0{,}5 \cdot \left(y\text{min} + y\text{max}\right), D\right] - r_{\text{Wheel}}\right] > 0{,}0 \\
& \quad \Big| \; y\text{max} \leftarrow r_{\text{a1}} \leftarrow 0{,}5 \text{ if } \left[r_{\text{M2D}}\left[0 \cdot \left(y\text{min} + y\text{max}\right), D\right] - r_{\text{Wheel}}\right] < 0{,}0 \\
& \quad \Big| \; R\text{worm} \leftarrow 0{,}5 \cdot \left(y\text{min} + y\text{max}\right) \\
& \text{END DO} \\
& \text{return } R\text{worm}
\end{aligned}
\tag{C.2}
$$

For C and K Profiles the algorithm to determine the radius grinding wheel which generates a conjugate profile on the circle radius r_{Wheel} of the worm wheel is the following:

$$
Rworm\left(D, r_{f1}, r_{a1}, r_{Wheel}\right) = \left|\begin{array}{l}
\\
ymin \leftarrow r_{f1} \\
ymax \leftarrow r_{a1} \\
Rgrind \leftarrow 0{,}5 \cdot \left(ymin + ymax\right) \\
\text{DO while } \left|r_{M2D}\left(Rgrind, D - r_{e2D}\right)\right| > 0{,}000001 \\
\quad \left|ymin \leftarrow Rgrind \text{ if} \left(r_{M2D}\left(Rgrind, D\right) - r_{Wheel}\right) > 0{,}0\right. \\
\quad \left|ymax \leftarrow Rgrind \text{ if} \left(r_{M2D}\left(Rgrind, D\right) - r_{Wheel}\right) < 0{,}0\right. \\
\quad \left|Rgrind \leftarrow 0{,}5 \cdot \left(ymin + ymax\right)\right. \\
\text{END DO} \\
\text{return } Rworm
\end{array}\right. \tag{C.3}
$$

The active root radius of worm can be calculated according to the outside radius of the worm wheel:

$$
y.p_{ACT}\left(D\right) = Rworm\left(D, r_{f1}, r_{al}, r_{.e2D}\left(D\right)\right) \tag{C.4}
$$

Annex D
(informative)

Comparison of different worm profiles

The goal of this annex is to show the geometric difference between the five profiles A, I, N, K and C.

For this evaluation, the data from example 1 from ISO/TR 14521, Annex J have been used and are reproduced below.

example number	**1**	**2**	**3**	**3b**	**4**
Assumption: ha1*=ha2*=1 hf1*=hf2*=1.2 he2*=0.5					
Type of flank ZA ZK ZI ZC ZI ZC	**ZA**	**ZK**	**ZI**	**ZN**	**ZC**
number of threads z1	2	2	2	2	2
axial module mx1 mm	4	4	4	4	4
diameter factor q1 -	9	9	9	9	9
normal pressure angle αn °	20	20	20	20	20
reference lead angle of worm γm1 ° 12,53 11,01	12.5288077	12.5288077	12.5288077	12.5288077	12.5288077
worm reference diameter dm1 mm	36	36	36	36	36
worm root diameter df1 mm	26.4	26.4	26.4	26.4	26.4
worm tip diameter da1 mm	44	44	44	44	44
number of teeth z2	41	41	41	41	41
worm wheel profile shift coefficient x2	0	0	0	0	0
worm wheel reference diameter dm2 mm	164	164	164	164	164
worm wheel root diameter df2 mm	154.4	154.4	154.4	154.4	154.4
worm wheel tip diameter da2 mm	172	172	172	172	172
worm wheel outside diameter de2 mm	176	176	176	176	176
effective wheel facewidth b2H mm	30	30	30	30	30
wheel rim width b2R mm	30	30	30	30	30
outside diameter of the grinding disk dgr mm		309.6			309.6
profile radius of grinding disk ρ mm					24
centre distance a mm	100	100	100	100	100

For a better understanding, the comparison has been conducted in an axial plane with

- in Figure D.1, the superposition of all profiles, and
- in Figure D.2, the difference between each profiles according to the A profile, because the A profile is a straight line.

Convention for the representation:

- abscissa represent the radius of worm,
- the identification of thread is below the curves

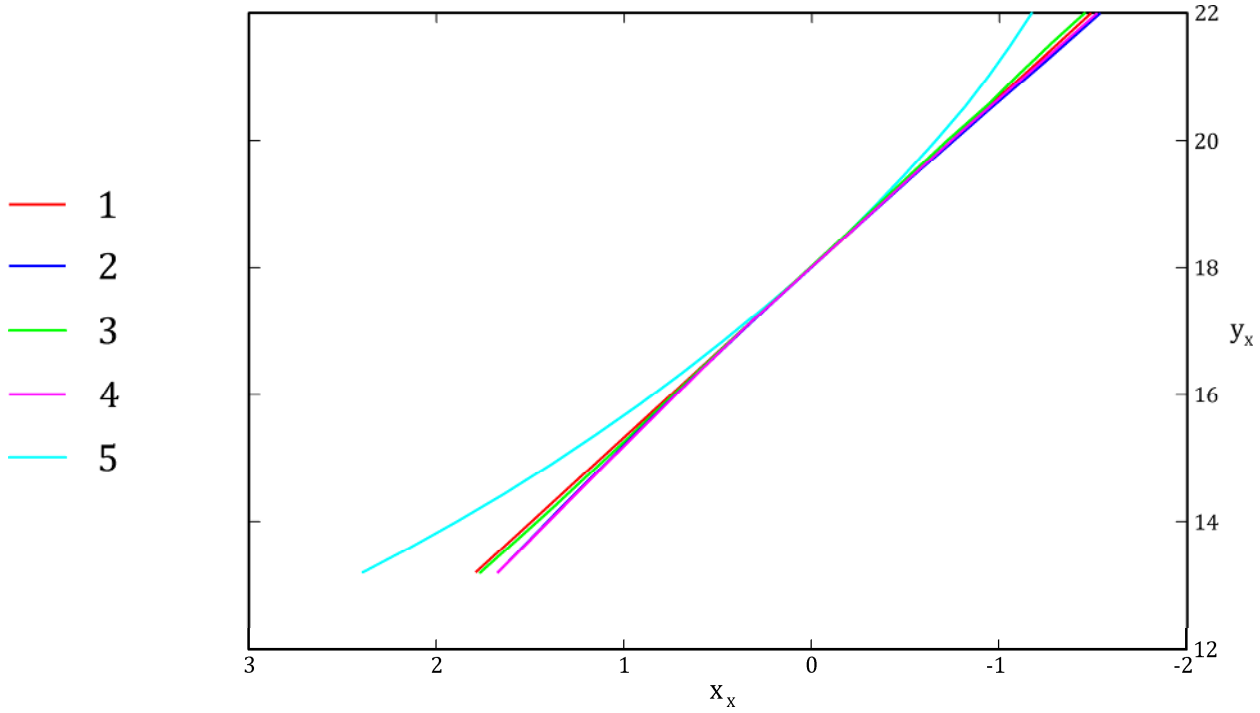

Key

1 A profile
2 I profile
3 N profile
4 K profile
5 C profile

Figure D.1 — Superposition of all right flank axial profiles

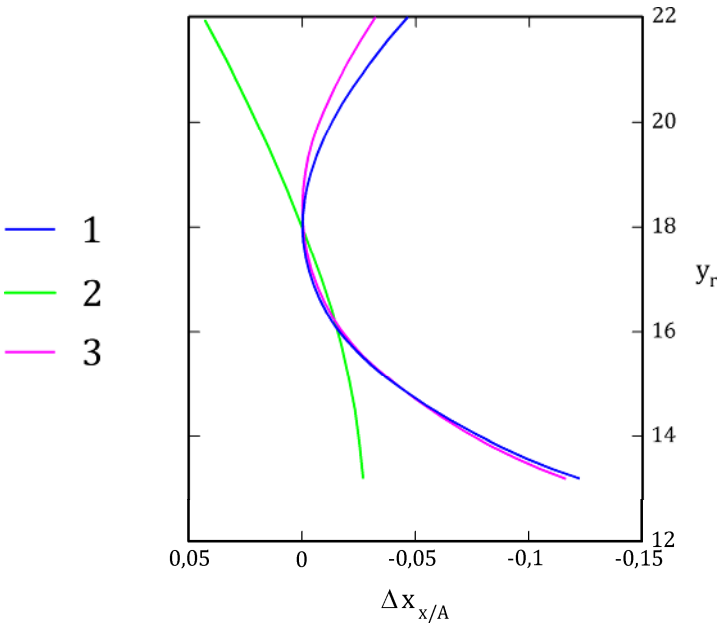

Key

1 I profile/ A profile
2 N profile/ A profile
3 K profile/ A profile

Figure D.2 — Difference between I,N,K profiles according to A profile

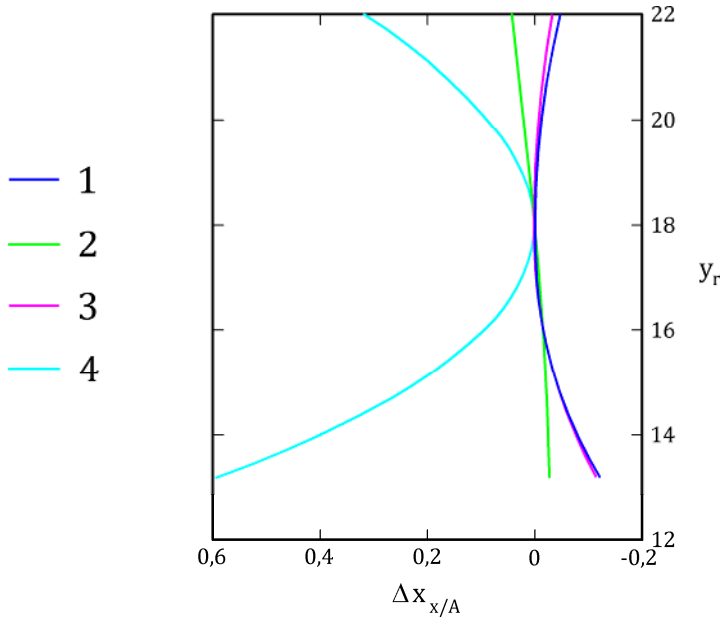

Key

1 I profile/ A profile
2 N profile/ A profile
3 K profile/ A profile
4 C profile/ A profile

Figure D.3— Difference between I,N,K and C profiles according to A profile

Remarks: I and K profiles are convex and very close, N and C profiles are concave.

N is very close to A**.** The curvature of C is important noticeably different than the other profiles.

In general the differences between profiles are larger when lead angle of worm increases.

Annex E
(informative)

Comparison of singularities for different worm profiles

In this annex the same examples as in Annex D are used.

E.1 Line of zero pressure angle

The following representation is a projection in a plane perpendicular to the worm axis.

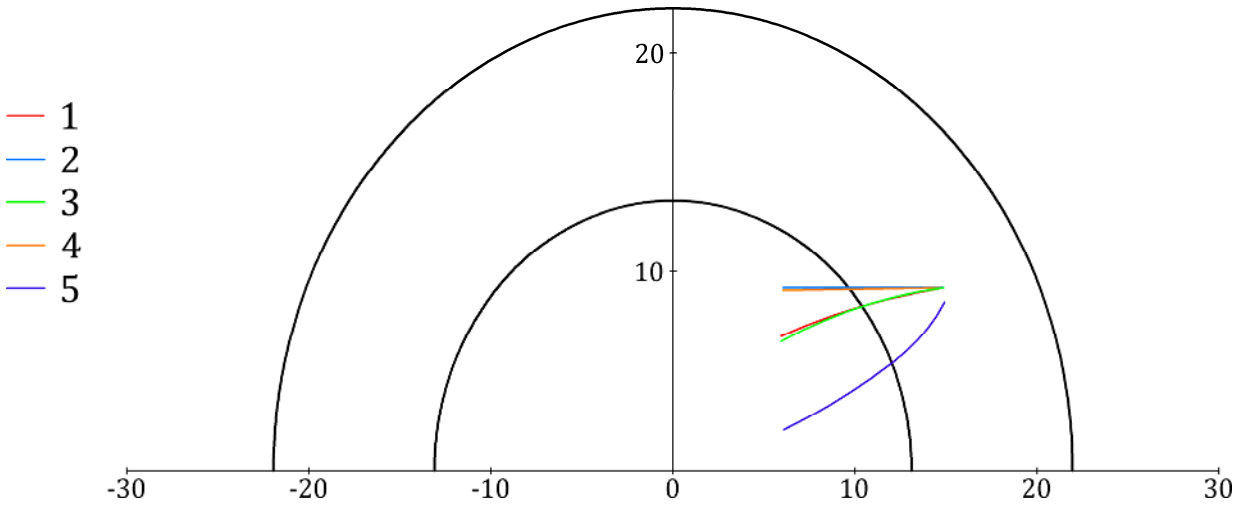

Key

1 A profile
2 I profile
3 N profile
4 K profile
5 C profile

Figure E.1 — Lines of zero pressure angle for A,I,N,K and C profiles

Remarks:

- for profile I this line is tangent to the base circle of the worm;
- it is quite the same for K profile;
- it is recommended to keep this line farway from lines of contact area.

NOTE For C profile (investigation are in process for the validity of this curve).

E.2 Cusp Line and root active radius line of the worm

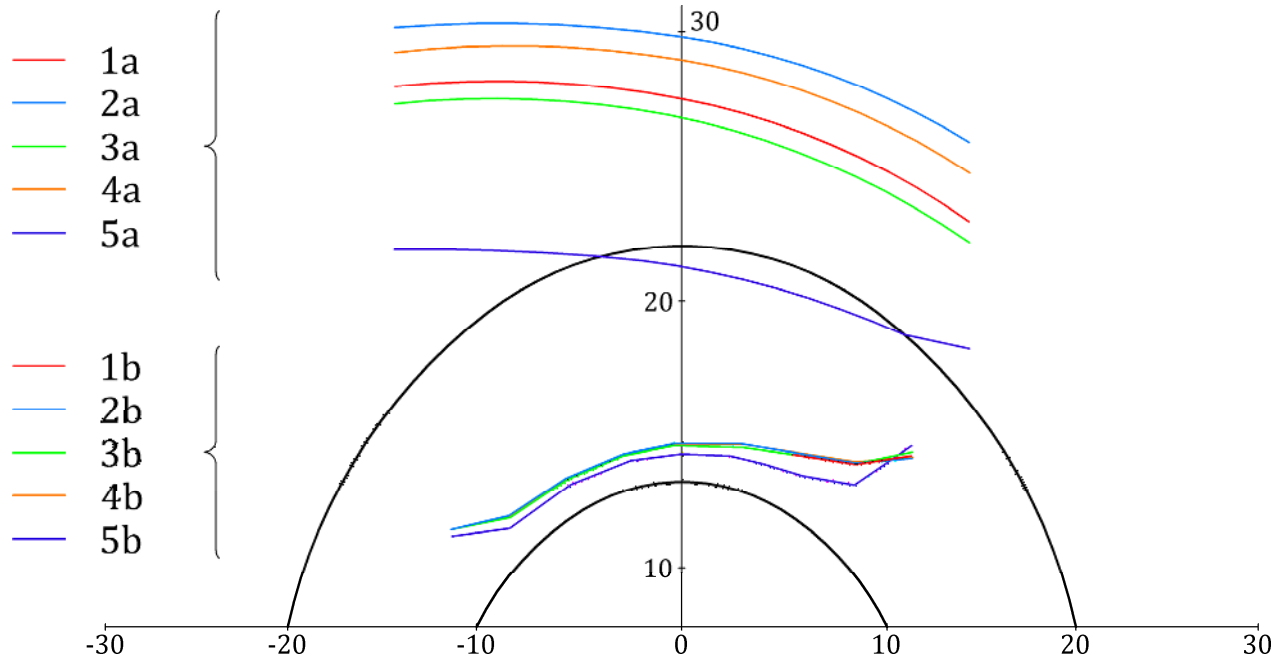

Key

1a cusp line for A profile
2a cusp line for I profile
3a cusp line for N profile
4a cusp line for K profile
5a cusp line for C profile
1b root active line for A profile
2b root active line for I profile
3b root active line for N profile
4b root active line for K profile
5b root active line for C profile

Figure E.2 — Cusp lines and root active radius of the worm angle for A, I, N, K and C profiles

The root active radius lines are represented by the colour lines in the middle of the figure. The root active radius of the worm is changing in each offset planes.

The cusp lines are those at the top of the figure:

- it is recommended to keep this line outside from tip cylinder of worm otherwise;
- for A, I, N and K profiles, this line is above the tip cylinder of the worm. For C profile the cusp line is (in that case of parameters) crossing the tip cylinder of the worm. It means that the contact lines could not exist above this line and consequently the contact ratio is limited in such case;
- C profile seems more sensitive than others profiles on this aspect.

The lower is the root active diameter line, higher is the potential of contact which is limited by this curve and the active tip cylinder of the worm if there is no cusp interference.

A, I, N and K profiles have a similar potential of contact – C profile has a higher potential of contact but is very sensitive to cusp effect as the example in Figure E.2.

Annex F
(informative)

Comparison of gear mesh for different worm profiles

The same data as in Annex D are used in this annex.

Example 1: ZA

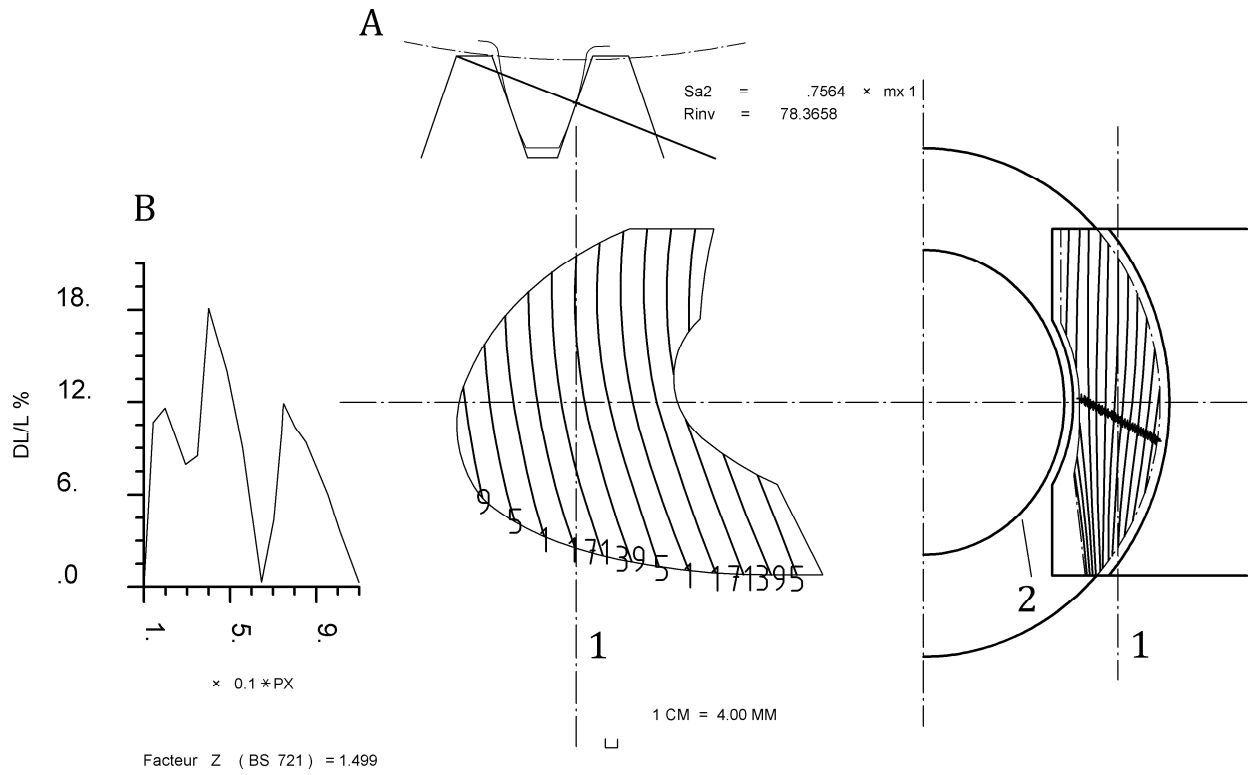

Key

A	gear mesh in median plane of gear wheel
B	relative variation of length of contact lines during 1 axial pitch
1	pitch line
2	line of zero pressure angle

Figure F.1 a — Lines of contacts

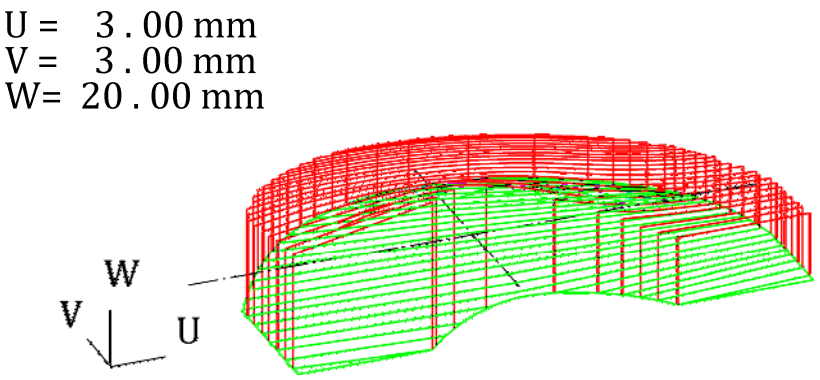

Figure F.1 b — Equivalent radius of curvature in projection on worm wheel flank

Example 2 – ZK

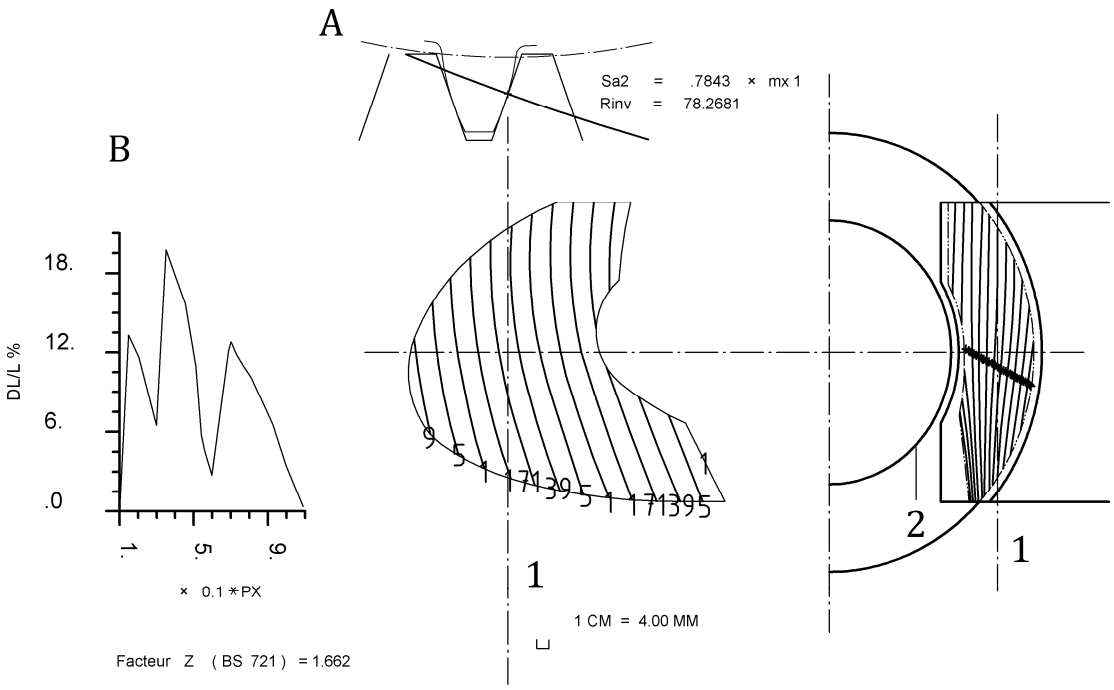

Key

A	gear mesh in median plane of gear wheel
B	relative variation of length of contact lines during 1 axial pitch
1	pitch line
2	line of zero pressure angle

Figure F.2 a — Lines of contacts

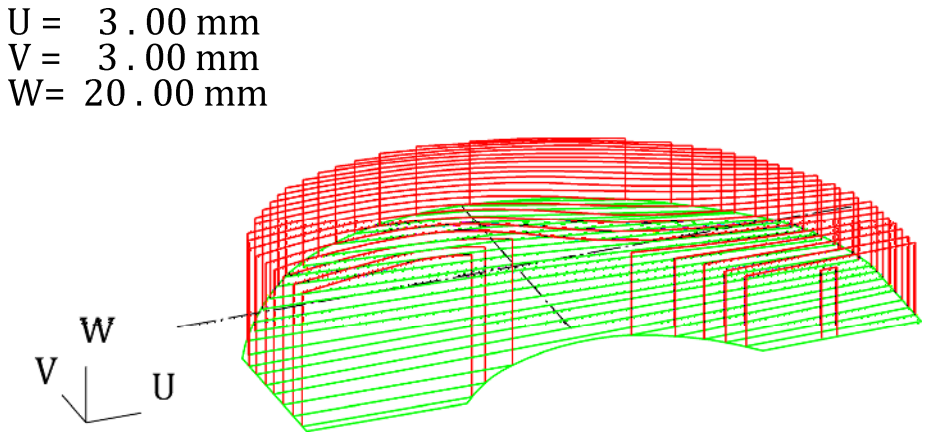

Figure F.2 b — Equivalent radius of curvature in projection on worm wheel flank

Example 3 – ZI

NOTE Geometry based on example number 5.

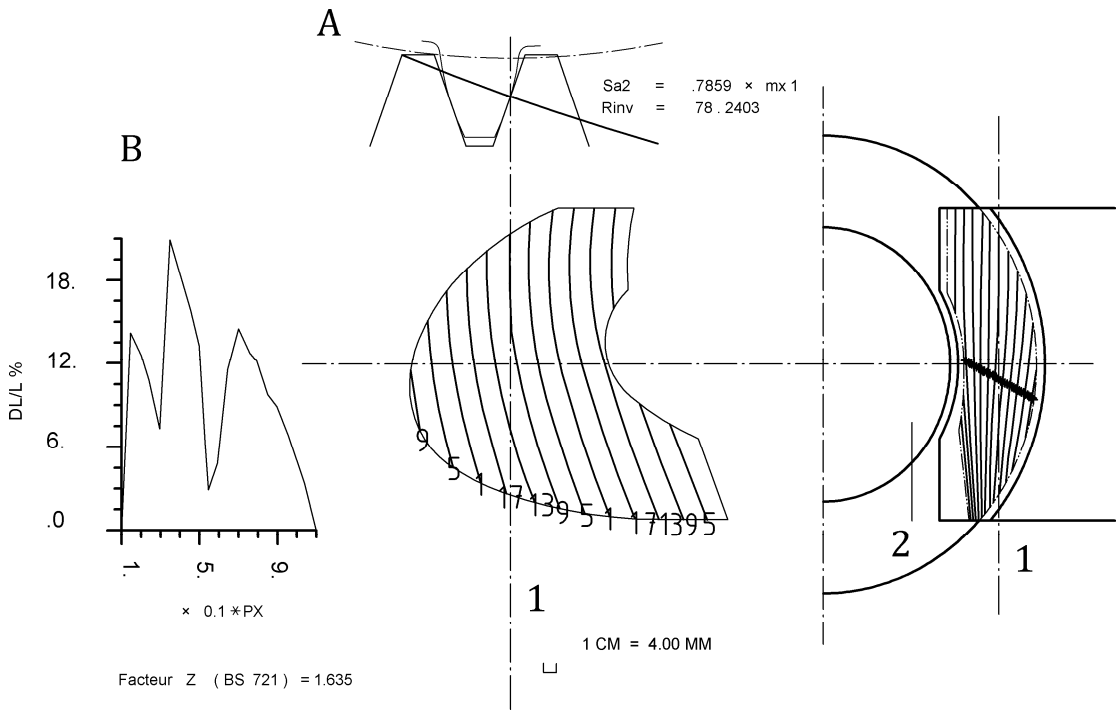

Key

A	gear mesh in median plane of gear wheel
B	relative variation of length of contact lines during 1 axial pitch
1	pitch line
2	line of zero pressure angle

Figure F.3 a — Lines of contacts

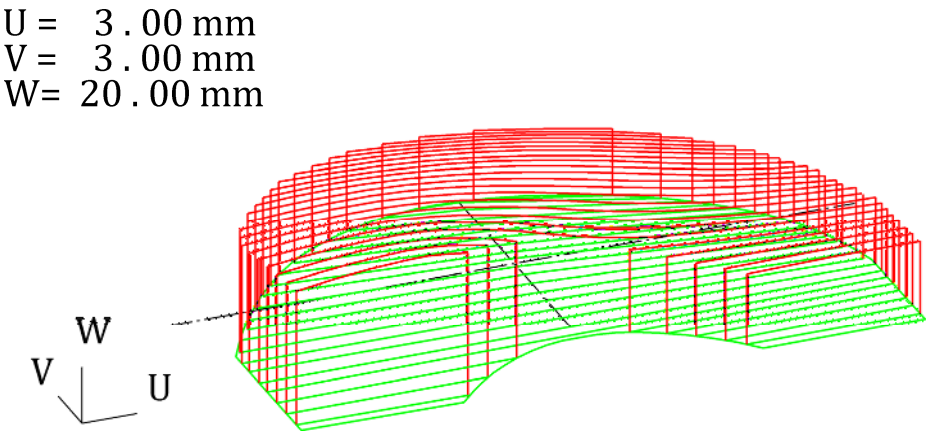

Figure F.3 b — Equivalent radius of curvature in projection on worm wheel flank

Example 4 – ZC

NOTE Geometry based on example number 6.

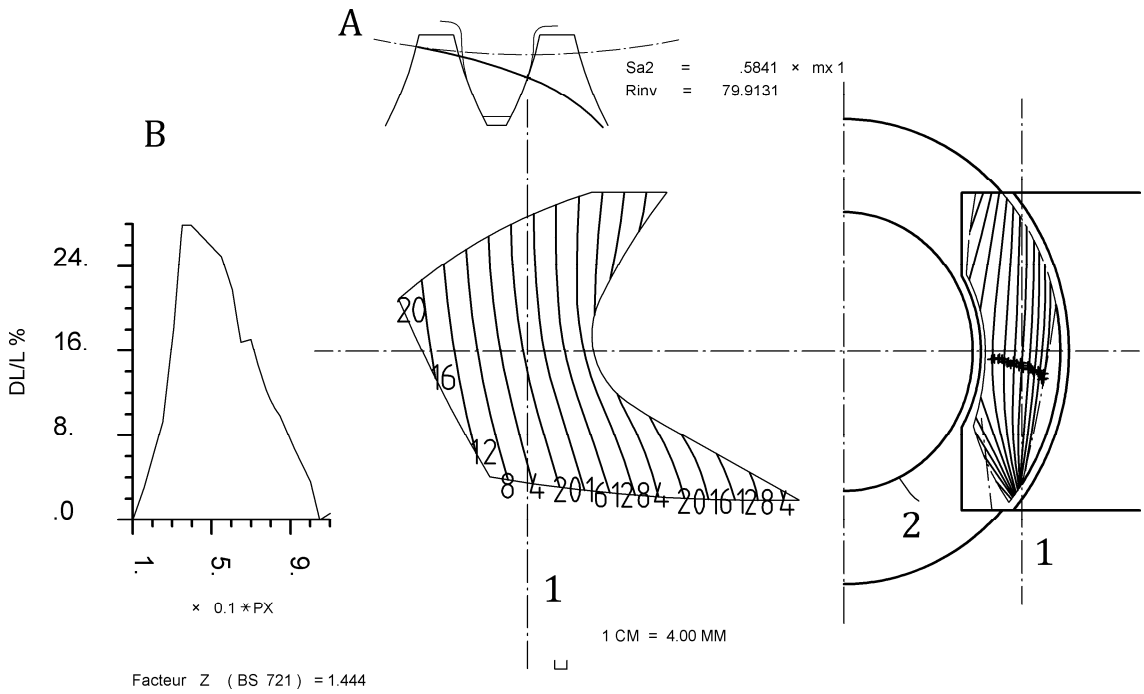

Key

A	gear mesh in median plane of gear wheel
B	relative variation of length of contact lines during 1 axial pitch
1	pitch line
2	line of zero pressure angle

Figure F.4 a — Lines of contacts

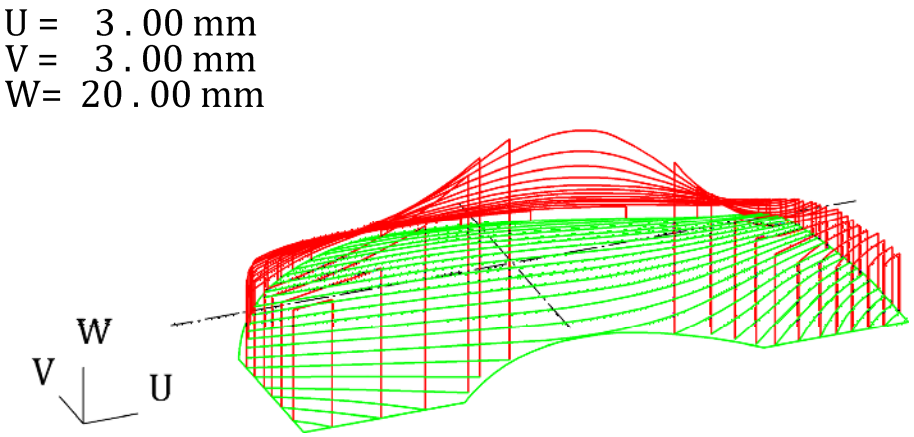

Figure F.4 b — Equivalent radius of curvature in projection on worm wheel flank

In order to be able to make the comparison between profile 2 extra examples have been added to avoid the cusp interference obtained with C profile.

example number	**5**	**6**
Assumption: ha1*=ha2*=1 hf1*=hf2*=1.2 he2*=0.5		
Type of flank ZA ZK ZI ZC ZI ZC	**ZI**	**ZC**
number of threads z1	2	2
axial module mx1 mm	4	4
diameter factor q1 -	10.28	10.28
normal pressure angle αn °	20	20
reference lead angle of worm γm1 ° 12,53 11,01	11.0095079	11.0095079
worm reference diameter dm1 mm	41.12	41.12
worm root diameter df1 mm	31.52	31.52
worm tip diameter da1 mm	49.12	49.12
number of teeth z2	39	39
worm wheel profile shift coefficient x2	0.36	0.36
worm wheel reference diameter dm2 mm	158.88	158.88
worm wheel root diameter df2 mm	149.28	149.28
worm wheel tip diameter da2 mm	166.88	166.88
worm wheel outside diameter de2 mm	170.88	170.88
effective wheel facewidth b2H mm	30	30
wheel rim width b2R mm	30	30
outside diameter of the grinding disk dgr mm		309.6
profile radius of grinding disk ρ mm		24
centre distance a mm	100	100

Example 5 – ZI optimised

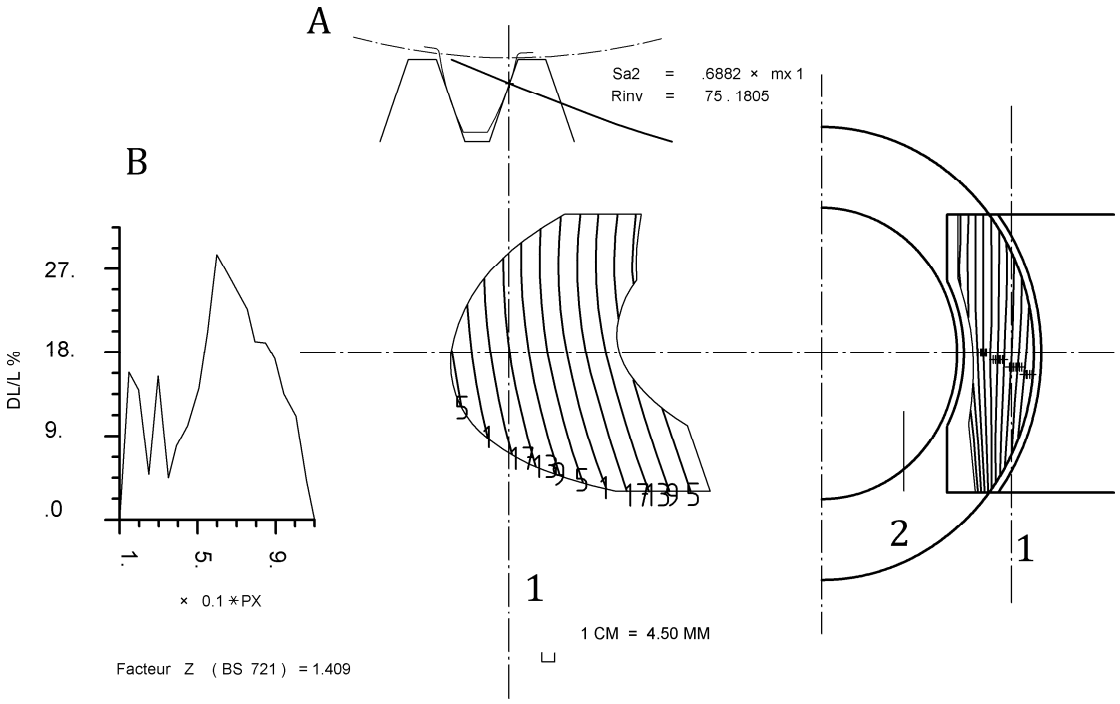

Key

A	gear mesh in median plane of gear wheel
B	relative variation of length of contact lines during 1 axial pitch
1	pitch line
2	line of zero pressure angle

Figure F.5 a — Lines of contacts

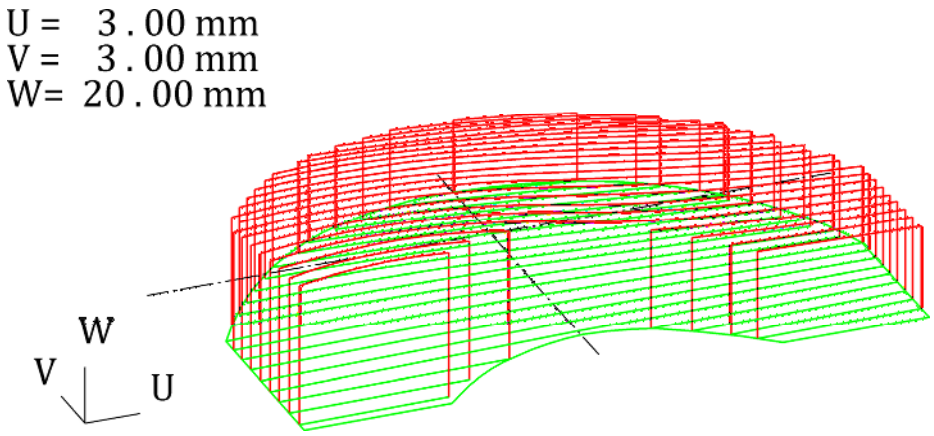

Figure F.5 b — Equivalent radius of curvature in projection on worm wheel flank

Example 6 – ZC optimised

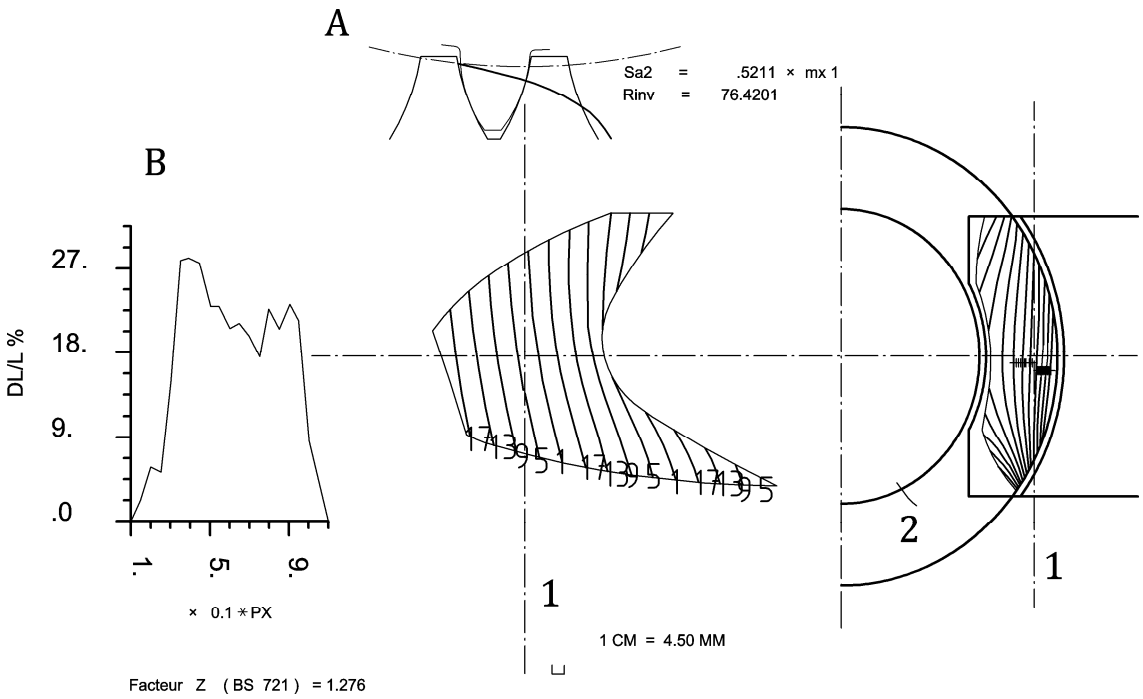

Key

A	gear mesh in median plane of gear wheel
B	relative variation of length of contact lines during 1 axial pitch
1	pitch line
2	line of zero pressure angle

Figure F.6 a — Lines of contacts

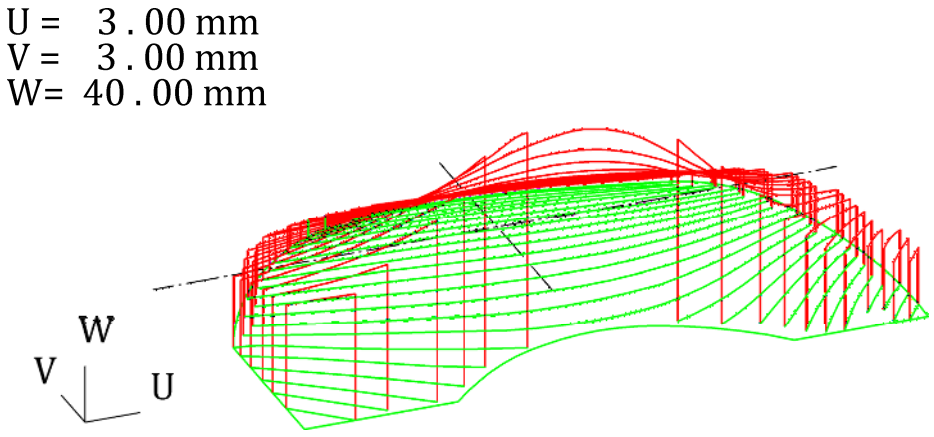

Figure F.6 b — Equivalent radius of curvature in projection on worm wheel flank

Annex G
(informative)

The utilisation of existing tooling for machining of worm wheel teeth

It is usual for the designer, knowing the ratio required in terms of the number of threads in the worm z_1 and the number of teeth in the worm wheel z_2 and the centre distance a, to establish the diameter factor q_1 prior to the module m_{x1}. This is due to the influence of q_1 on the reference diameter of the worm and its proportions relative to the required stiffness and diameters to each side of the threads.

When a satisfactory q_1 value is established the module can be determined from:

$$m_{x1} \approx \frac{2 \cdot a}{z_2 + q_1} \tag{G.1}$$

This would complete the proposed designation: $z_1/z_2/q_1/m_{x1}$.

There are occasions where the gear manufacturer can have a stock of hobs or cutters which are available for utilisation in the machining of worm wheels for which they were not originally produced and yet may be suitable for use in other centre distances and ratios.

This is sometimes possible where the diameter factor and module of a hob approximate to those of the worm, the number of threads, hand and pressure angle, and with a modification to the reference diameter of the worm wheel the number of teeth required can be accommodated within the new centre distance.

In BS 721-2 there is guidance in checking the z_1, q_1, m_{x1}, values of the hob against the limits of the resulting modification. This is contained in 6.1 and 6.7 of [2] which provide methods of obtaining the allowable a_{max0} - a_{min0} and m_{max0} - m_{min0} values respectively.

Using the new z_2 value with the hob z_1, q_0, and m_{x0} values enables a check to be made that, the new centre distance falls within the established tolerance, or the limiting values of axial module encompass the existing m_{x0} of the hob.

The method proposed is as follows:

— Limiting values of centre distance for given values of a, z_1, z_2, and q_0 are as follows:

$$a_{max0} = 0{,}5 \cdot m_{x0} \cdot \left(z_2 + q_0 + 2 \cdot x_{2max}\right) \tag{G.2}$$

where x_{2max} is as given in Figure G.1;

$$a_{min0} = 0{,}5 \cdot m_{x0} \cdot \left(z_2 + q_0 - 2 \cdot x_{2min}\right) \tag{G.3}$$

where x_{2min} is as given in Figure G.2.

— Limiting values of axial module for given values of a, z_1, z_2, and q_0 are as follows:

$$m_{max0} = \frac{2 \cdot a}{z_2 + q_0 - 2 \cdot x_{2min}} \tag{G.4}$$

$$m_{min0} = \frac{2 \cdot a}{z_2 + q_0 + 2 \cdot x_{2max}} \quad \text{(G.5)}$$

In order to use Figures G.1 and G.2 it is necessary to obtain the lead angle of the hob which can be found from:

$$\tan\gamma_1 = \frac{z_1}{q_0} \quad \text{(G.6)}$$

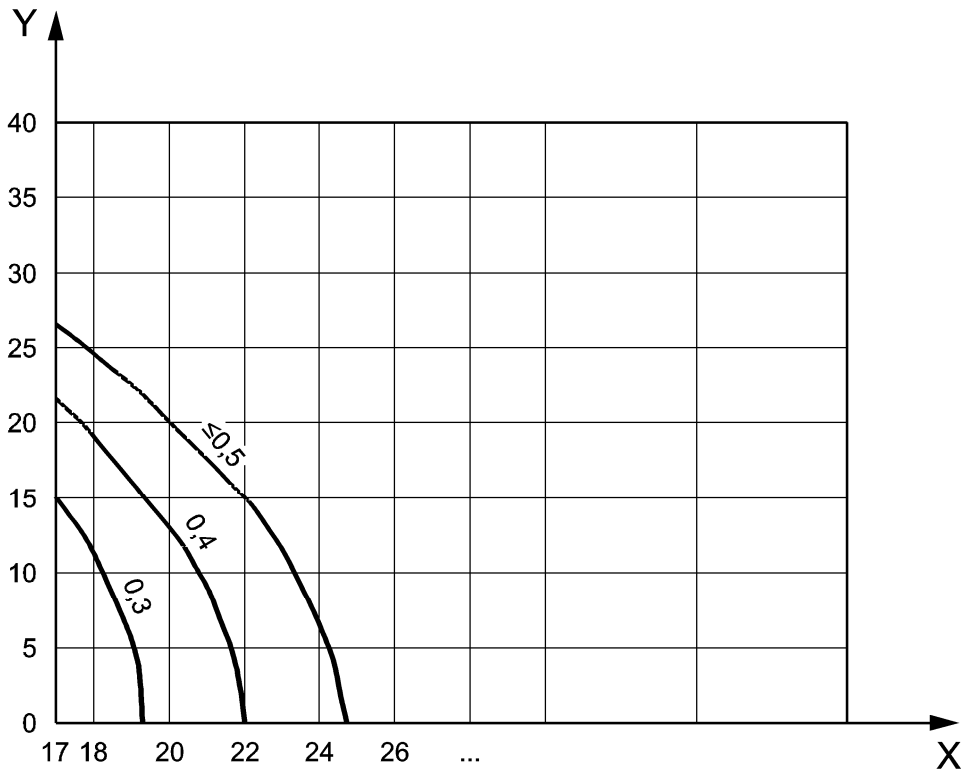

Key

X number of teeth z_2
Y lead angle γ_1 in degree

Figure A.1 — Maximum value of addendum modification coefficient (x_{2max})

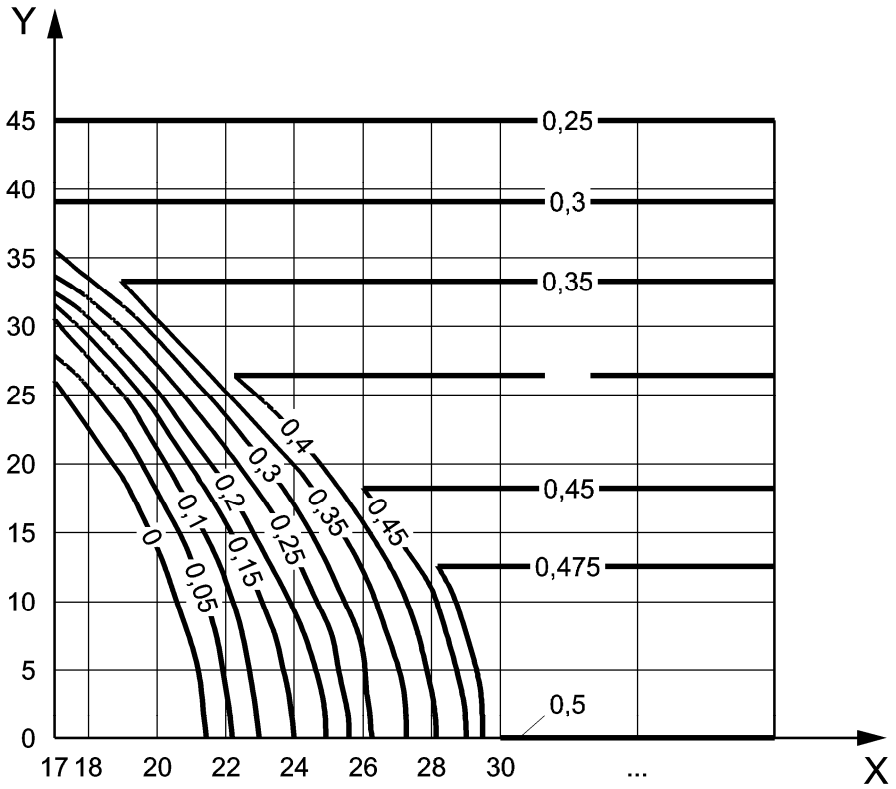

Key

X number of teeth z_2
Y lead angle γ_1 in degree

Figure A.2 — Minimum value of addendum modification coefficient (x_{2min})

If the required centre distance has a value which lies between a_{max} - a_{min} and the module m_{x0} has a value which lies between and m_{max0} - m_{min0} the cutter can be utilised. The values q_0 and m_{x0} then can be taken as q_1 and m_{x1} for the gears.

Bibliography

[1] M. DENIS and M. OCTRUE, Note technique CETIM n°22, Cylindrical worm gear geometry, Ed. CETIM - Senlis - FRANCE – 1982

[2] BS 721-2:1983, *Specification for worm gearing — Metric units*

ICS 21.200
Price based on 95 pages

This page deliberately left blank

British Standards Institution (BSI)

BSI is the national body responsible for preparing British Standards and other standards-related publications, information and services.

BSI is incorporated by Royal Charter. British Standards and other standardization products are published by BSI Standards Limited.

About us

We bring together business, industry, government, consumers, innovators and others to shape their combined experience and expertise into standards -based solutions.

The knowledge embodied in our standards has been carefully assembled in a dependable format and refined through our open consultation process. Organizations of all sizes and across all sectors choose standards to help them achieve their goals.

Information on standards

We can provide you with the knowledge that your organization needs to succeed. Find out more about British Standards by visiting our website at bsigroup.com/standards or contacting our Customer Services team or Knowledge Centre.

Buying standards

You can buy and download PDF versions of BSI publications, including British and adopted European and international standards, through our website at bsigroup.com/shop, where hard copies can also be purchased.

If you need international and foreign standards from other Standards Development Organizations, hard copies can be ordered from our Customer Services team.

Subscriptions

Our range of subscription services are designed to make using standards easier for you. For further information on our subscription products go to bsigroup.com/subscriptions.

With **British Standards Online (BSOL)** you'll have instant access to over 55,000 British and adopted European and international standards from your desktop. It's available 24/7 and is refreshed daily so you'll always be up to date.

You can keep in touch with standards developments and receive substantial discounts on the purchase price of standards, both in single copy and subscription format, by becoming a **BSI Subscribing Member**.

PLUS is an updating service exclusive to BSI Subscribing Members. You will automatically receive the latest hard copy of your standards when they're revised or replaced.

To find out more about becoming a BSI Subscribing Member and the benefits of membership, please visit bsigroup.com/shop.

With a **Multi-User Network Licence (MUNL)** you are able to host standards publications on your intranet. Licences can cover as few or as many users as you wish. With updates supplied as soon as they're available, you can be sure your documentation is current. For further information, email bsmusales@bsigroup.com.

BSI Group Headquarters

389 Chiswick High Road London W4 4AL UK

Revisions

Our British Standards and other publications are updated by amendment or revision.

We continually improve the quality of our products and services to benefit your business. If you find an inaccuracy or ambiguity within a British Standard or other BSI publication please inform the Knowledge Centre.

Copyright

Useful Contacts:

Customer Services
Tel: +44 845 086 9001
Email (orders): orders@bsigroup.com
Email (enquiries): cservices@bsigroup.com

Subscriptions
Tel: +44 845 086 9001
Email: subscriptions@bsigroup.com

Knowledge Centre
Tel: +44 20 8996 7004
Email: knowledgecentre@bsigroup.com

Copyright & Licensing
Tel: +44 20 8996 7070
Email: copyright@bsigroup.com

bsi.

...making excellence a habit.™